



PB96-165162



U.S. Department
of Transportation

**Federal Highway
Administration**

Publication No. FHWA-RD-95-079
December 1995

Ruggedness Testing of the Dynamic Shear Rheometer and the Bending Beam Rheometer Test Procedures

Research and Development
Turner-Fairbank Highway Research Center
6300 Georgetown Pike
McLean, Virginia 22101-2296

REPRODUCED BY: **NTIS**
U.S. Department of Commerce
National Technical Information Service
Springfield, Virginia 22161

FOREWORD

This report presents the findings of an inter-laboratory study of the procedures to test asphalt binders by the SUPERPAVE binder specification tests. The inter-laboratory tests were performed according to ASTM C1067, in which the ruggedness of the procedures are tested. This work is a prelude to a round-robin study to determine the precision and bias for these tests. This work will be useful to State highway agencies, asphalt producers, pavement construction contractors, and other agencies involved in grading asphalt according to the SUPERPAVE performance (PG-) grading.



Charles J. Nemmers, Director
Office of Engineering and Highway
Operations Research and Development

NOTICE

This document is disseminated under the sponsorship of the Department of Transportation in the interest of information exchange. The United States Government assumes no liability for its contents or use thereof. This report does not constitute a standard, specification, or regulation.

The United States Government does not endorse products or manufacturers. Trade and manufacturers' names appear in this report only because they are considered essential to the object of the document.

PB96-165162



1. Report No. FHWA-RD-95-079		3. Recipient's Catalog No.	
4. Title and Subtitle RUGGEDNESS TESTING OF THE DYNAMIC SHEAR RHEOMETER AND THE BENDING BEAM RHEOMETER TEST PROCEDURES		5. Report Date December 1995	
7. Author(s) N. Shashidhar and Brian H. Chollar		6. Performing Organization Code HNR-30	
9. Performing Organization Name and Address Office of Engineering and Highway Operations R&D Federal Highway Administration 6300 Georgetown Pike, McLean, VA 22101-2296		8. Performing Organization Report No.	
12. Sponsoring Agency Name and Address Office of Engineering and Highway Operations R&D Federal Highway Administration 6300 Georgetown Pike, McLean, VA 22101-2296		10. Work Unit No. (TRAIS) 2E1B	
		11. Contract or Grant No. Inhouse Report	
		13. Type of Report and Period Covered Final Report Sept. 1992 - Dec. 1994	
		14. Sponsoring Agency Code	
15. Supplementary Notes Project Manager: Brian H. Chollar, HNR-30			
16. Abstract Ruggedness testing of the bending beam rheometer (BBR) and the dynamic shear rheometer (DSR) was performed. Four laboratories participated in this effort. Three materials were used for BBR ruggedness testing and four materials were used for DSR ruggedness testing. Measurement of the creep stiffness and m -value at 60 s with the BBR was found to be fairly repeatable. Of the factors studied, the mold used for casting the beams had a significant effect. Different beam thickness by the two molding techniques was found to be a factor that caused this variation. Other unknown factor(s) also seemed to contribute to this effect. The test temperature also had a significant effect and should be controlled to $\pm 0.1^\circ\text{C}$. Measurement of the complex shear modulus (G^*) and the phase angle (δ) with the DSR was very repeatable. The measurement of G^* with 8-mm parallel plates had more variation than the measurement of G^* with 25-mm parallel plates. The measurement of δ with both 8- and 25-mm plates had lesser variation than the G^* measurement. Test temperature was the primary factor that affected the test results for both 8-mm and 25-mm parallel plates, requiring $\pm 0.1^\circ\text{C}$ control. For G^* measurements with 8-mm parallel plates, it seemed to make a difference whether asphalt was directly applied to the plates or if it was transferred in the form of a pellet. This effect can probably be accounted for by different thermal history imparted to the pellet. Inconclusive, but definite, effects were observed due to overhang in the case of the 8-mm parallel plates.			
17. Key Words Ruggedness testing, bending beam rheometer, dynamic shear rheometer, complex shear modulus, creep stiffness, rheological properties, inter-laboratory study		18. Distribution Statement No Restrictions. This document is available to the public through the National Technical Information Service, Springfield, Virginia 22161.	
19. Security Classif. (of this report) Unclassified	20. Security Classif. (of this page) Unclassified	21. No. of Pages 73	22. Price

SI* (MODERN METRIC) CONVERSION FACTORS

APPROXIMATE CONVERSIONS TO SI UNITS					APPROXIMATE CONVERSIONS FROM SI UNITS				
Symbol	When You Know	Multiply By	To Find	Symbol	Symbol	When You Know	Multiply By	To Find	Symbol
LENGTH					LENGTH				
in	inches	25.4	millimeters	mm	mm	millimeters	0.039	inches	in
ft	feet	0.305	meters	m	m	meters	3.28	feet	ft
yd	yards	0.914	meters	m	m	meters	1.09	yards	yd
mi	miles	1.61	kilometers	km	km	kilometers	0.621	miles	mi
AREA					AREA				
in ²	square inches	645.2	square millimeters	mm ²	mm ²	square millimeters	0.0016	square inches	in ²
ft ²	square feet	0.093	square meters	m ²	m ²	square meters	10.764	square feet	ft ²
yd ²	square yards	0.836	square meters	m ²	m ²	square meters	1.195	square yards	yd ²
ac	acres	0.405	hectares	ha	ha	hectares	2.47	acres	ac
mi ²	square miles	2.59	square kilometers	km ²	km ²	square kilometers	0.386	square miles	mi ²
VOLUME					VOLUME				
fl oz	fluid ounces	29.57	milliliters	mL	mL	milliliters	0.034	fluid ounces	fl oz
gal	gallons	3.785	liters	L	L	liters	0.264	gallons	gal
ft ³	cubic feet	0.028	cubic meters	m ³	m ³	cubic meters	35.71	cubic feet	ft ³
yd ³	cubic yards	0.765	cubic meters	m ³	m ³	cubic meters	1.307	cubic yards	yd ³
MASS					MASS				
oz	ounces	28.35	grams	g	g	grams	0.035	ounces	oz
lb	pounds	0.454	kilograms	kg	kg	kilograms	2.202	pounds	lb
T	short tons (2000 lb)	0.907	megagrams (or "metric ton")	Mg (or "t")	Mg (or "t")	megagrams (or "metric ton")	1.103	short tons (2000 lb)	T
TEMPERATURE (exact)					TEMPERATURE (exact)				
°F	Fahrenheit temperature	5(F-32)/9 or (F-32)/1.8	Celcius temperature	°C	°C	Celcius temperature	1.8C + 32	Fahrenheit temperature	°F
ILLUMINATION					ILLUMINATION				
fc	foot-candles	10.76	lux	lx	lx	lux	0.0929	foot-candles	fc
fl	foot-Lamberts	3.426	candela/m ²	cd/m ²	cd/m ²	candela/m ²	0.2919	foot-Lamberts	fl
FORCE and PRESSURE or STRESS					FORCE and PRESSURE or STRESS				
lbf	poundforce	4.45	newtons	N	N	newtons	0.225	poundforce	lbf
lbf/in ²	poundforce per square inch	6.89	kilopascals	kPa	kPa	kilopascals	0.145	poundforce per square inch	lbf/in ²

* SI is the symbol for the International System of Units. Appropriate rounding should be made to comply with Section 4 of ASTM E380.

TABLE OF CONTENTS

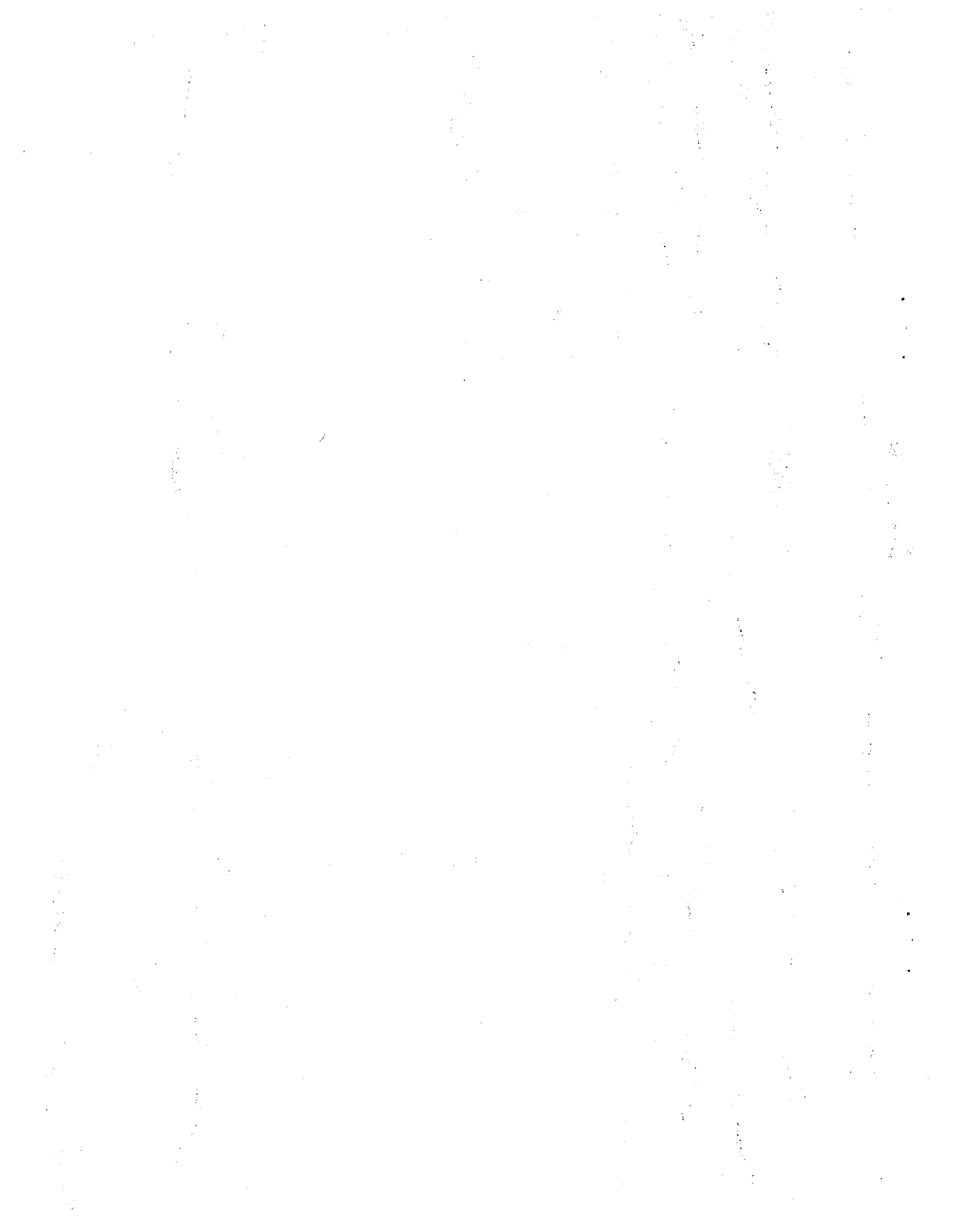
INTRODUCTION	1
Objectives	2
EXPERIMENTAL PROCEDURES	3
Asphalts	3
Labeling	3
Testing	3
Equipment Used	4
Miscellaneous	4
Statistical Analysis	4
RESULTS AND DISCUSSION	7
Bending Beam Rheometer	7
Analysis of the Standardized Residuals	7
Data Overview	8
Ruggedness Testing Analysis	9
Precision and Bias Estimates	19
Dynamic Shear Rheometer	21
Analysis of Standardized Residuals	21
Data Overview	21
Ruggedness Testing Analysis	32
Precision and Bias Estimates	38
APPENDIX 1. TESTING PROCEDURES	41
Introduction	41
Samples	42
Pre-Testing Requirements	43
Sources for Molds	44
Note	44
1. BENDING BEAM RHEOMETER	45
2. DYNAMIC SHEAR RHEOMETER	51
3. PRESSURE AGING VESSEL	56
APPENDIX 2. CHANGES TO PROCEDURES	61
Bending Beam Rheometer	61
Dynamic Shear Rheometer	61
Pressure Aging Vessel	62
Pressure Release Rate	63
REFERENCES	67

LIST OF FIGURES

1	Standardized residuals in $S(60)$ measurements: (a) grouped by laboratory and material, and (b) distribution of all standardized residuals.	11
2	Standardized residuals in $m(60)$ measurements: (a) grouped by laboratory and material, and (b) distribution of all standardized residuals.	12
3	Creep Stiffness measurements averaged by laboratory and material.	13
4	Coefficient of variation in creep stiffness measurements averaged by material and laboratory.	13
5	m -value measurements averaged by material and laboratory.	14
6	Coefficient of variation in m -value measurements averaged by material and laboratory.	14
7	Standardized residuals in G^* measurements with 8-mm parallel plates: (a) grouped by material and laboratory, and (b) distribution of all standardized residuals.	24
8	Standardized residuals in phase angle measurements with 8-mm parallel plates: (a) grouped by material and laboratory, and (b) distribution of all standardized residuals.	25
9	Standardized residuals in G^* measurements with 25-mm parallel plates: (a) grouped by material and laboratory, and (b) distribution of all standardized residuals.	26
10	Standardized residuals in phase angle measurements with 25-mm parallel plates: (a) grouped by laboratory and materials, and (b) distribution of all standardized residuals.	27
11	Complex shear modulus measurements with 8-mm parallel plates averaged by material and laboratory.	28
12	Coefficient of variation in G^* measurements with 8-mm parallel plates averaged by material and laboratory.	28
13	Phase angle measurements with 8-mm parallel plates averaged by material and laboratory.	29
14	Coefficient of variation in phase angle measurements with 8-mm parallel plates averaged by material and laboratory.	29
15	Complex shear modulus measurements with 25-mm plates averaged by material and laboratory.	30
16	Coefficient of variation in G^* measurements with 25-mm parallel plates averaged by material and laboratory.	30
17	Phase angle measurements with 25-mm parallel plates averaged by material and laboratory.	31
18	Coefficient of variation in phase angle measurements with 25-mm parallel plates averaged by material and laboratory.	31
19	The thermistor embedded in silicone rubber for DSR temperature calibration.	43
20	Schematic diagram of an aluminum mold.	45
21	Schematic diagram of a silicone rubber mold.	46
22	Three-point flexural testing setup for measuring the low-temperature properties of asphalt.	47
23	Pressure in a PAV as a function of time when released at different valve settings.	63
24	Relationship between pressure release rate constant and the vernier setting on the valve.	63

LIST OF TABLES

1	Asphalts used in BBR ruggedness testing.	3
2	Asphalts used in DSR ruggedness testing.	4
3	Uniformity of samples distributed to the laboratories.	4
4	Repeatability of measurements with the BBR and the DSR by various laboratories.	5
5	Flexural creep stiffnesses measured by the bending beam rheometer.	7
6	m -values determined by the bending beam rheometer.	8
7	Average $S(60)$ and $m(60)$ measurements with the bending beam rheometer.	9
8	F-values and percent effects for $S(60)$ measurements.	10
9	F-values and percent effects for $m(60)$ measurements.	10
10	Average percent effects for $S(60)$ and $m(60)$ measurements.	15
11	Thickness of beams cast in aluminum and silicone rubber molds.	15
12	Ruggedness analysis after correcting for beam thickness.	16
13	Effect of correcting thickness on ruggedness results.	17
14	Effect of leaving cast beams at room temperature.	17
15	Between- and within-laboratory coefficient of variation.	19
16	Complex shear modulus (in kPa) measured with 8-mm parallel plates.	21
17	Phase angles (in degrees) measured with 8-mm parallel plates.	22
18	Complex modulus (in Pa) measured with 25-mm parallel plates.	23
19	Phase angles (in degrees) measured with 25-mm parallel plates.	32
20	Average G^* and d measured with 8-mm parallel plates.	33
21	F-values and percent effects for G^* measurements with 8-mm parallel plates.	34
22	F-values and percent effects for d measurements with 8-mm parallel plates.	35
23	Average percent effects for G^* and d measurements with 8-mm parallel plates.	35
24	F-values and percent effects for d measurements with 25-mm parallel plates.	36
25	F-values and percent effects for G^* measurements with 25-mm parallel plates.	37
26	Average percent effects for G^* and d measurements with 25-mm parallel plates.	37
27	Between- and within-laboratory coefficient of variation for G^* and d measurements.	38
28	Fractional factorial design for BBR ruggedness testing.	47
29	Recommended sequence of experiments for BBR ruggedness testing.	49
30	Fractional factorial design for DSR ruggedness testing.	53
31	Recommended sequence of experiments for DSR ruggedness testing.	54
32	Fractional factorial design for PAV ruggedness testing.	57
33	Recommended sequence of experiments for PAV ruggedness testing.	58
34	Temperatures and strains to perform DSR ruggedness testing.	62
35	Modified sequence of experiments for PAV ruggedness testing.	64
36	Instantaneous release rates at different pressures.	65
37	Calibration of the pressure release valve.	65



INTRODUCTION

The Strategic Highway Research Program (SHRP) introduced three new testing techniques and one new conditioning procedure for predicting the performance of binders—the dynamic shear rheometer (DSR), bending beam rheometer (BBR), direct tension (DT), and the pressure aging vessel (PAV), respectively. The properties measured using these methods and aging treatments are used to define a climatic temperature range within which the asphalt can be used. These constitute the performance grading (PG) of asphalts. The results of the ruggedness testing of the bending beam rheometer and the dynamic shear rheometer will be described in this report.

The bending beam rheometer (BBR) is a flexural creep testing device that is used to measure the low-temperature viscoelastic properties of asphalts. The creep stiffness (S) and the slope of the log stiffness-log time curve (m), at 60 s loading time, are determined at specification temperatures of 0, -6, -12, -18, -24, -30, and -36°C.⁽¹⁾

The dynamic shear rheometer (DSR), also known as the dynamic mechanical analyzer, is an instrument that determines the shear properties of a material under oscillating stresses or strains. When the strain is imparted to the sample and the development of torque is measured, the instrument is called a strain-controlled rheometer. When a torque is induced in the sample and the displacement is measured as strain, the instrument is a stress-controlled rheometer. Both these rheometers exist and have their respective advantages and disadvantages. For the purposes of SHRP testing of asphalt binders, the differences in the property measurement between the two instruments are considered negligible.

For asphalt cement, the complex modulus (G^*) and the phase angle (δ) at different temperatures are measured as described in American Association of State Highway and Transportation Officials (AASHTO) provisional specifications.⁽²⁾ $G^*/\sin(\delta)$ is then used to predict the rutting characteristics of pavement binders and $G^* \cdot \sin(\delta)$ is used to predict the fatigue cracking of pavements.

Ruggedness testing is a screening test for "...detecting and reducing sources of variation in a test method early in its development and prior to an inter-laboratory study..." for precision and bias.⁽³⁾ In this procedure, a few laboratories introduce known variations in pertinent variables related to testing techniques and environment in order to judge the magnitude of their effect on the test results. This information is used to determine the controls necessary for these variables in the test method. Starting with a valid, well-written test method, the ruggedness testing process identifies pertinent variables that cause variation in the test results. It is the goal of this screening process to reduce the variability of test results to a minimum through the detection and control of pertinent variables.

Objectives

The objectives of this study are to:

- Study the ruggedness of the test procedure for the bending beam rheometer and dynamic shear rheometer by:
 - Identifying those factors in the test procedure that cause variation in the measurements.
 - Setting limits on these factors with the goal of achieving repeatable measurements when tested by various operators and laboratories.
 - Verifying that the limits chosen will ensure acceptable variability when the factors are controlled within these limits.
- Obtain a preliminary estimate of the precision and bias from the data obtained for ruggedness testing.

EXPERIMENTAL PROCEDURES

Asphalts

The asphalts selected for testing were from the SHRP reference library. Though it was not essential for ruggedness testing, it was decided that all participating laboratories would test the same asphalts so that the results could be compared with each other for reproducibility. For this purpose, asphalts were prepared at the Federal Highway Administration (FHWA) and sent to the participating laboratories. Four materials were used for DSR tests, two of which were thin film oven residues of the other two. The three materials used for BBR tests were thin film oven and pressure vessel aged residues. The asphalts used are summarized in Tables 1 and 2. In order to ensure homogeneity, the samples prepared were heated in a single container, stirred well, and poured into more than 100 30-mL containers and labeled. Additionally, G^* at 50°C was measured for 8 samples chosen at random from those 100 30-mL containers. The mean and coefficient of variation for each of the materials are listed in Table 3.

Labeling

The 30-mL containers were labeled with the coded material identification as given in Tables 1 and 2. In addition, each container had a unique serial number that could be tracked. The containers were distributed to various laboratories.

Table 1. Asphalts used in BBR ruggedness testing.

CODE	SHRP CODE	TEST TEMP	GLASS TRANS. TEMP ¹	SOURCE
BBR-A	AAM-1	-18°C	-4.1°C	West Texas Intermediate
BBR-B	AAK-1	-12°C	-16.5°C	Boscan
BBR-C	AAC-1	-24°C	-9.9°C	Redwater

¹Glass transition temperatures were measured at the Pennsylvania Transportation Institute and reported in the SHRP report. These were reported for unaged asphalts.

Testing

The testing was performed according to the procedures summarized in Appendix 1. As the ruggedness testing was started before formal procedures were available, testing procedures were written and finalized through a process of iterative revision by the laboratories. These procedures were written for these tests in four versions, with each successive version being approved by the participating laboratories and other players, such as SHRP and Asphalt Materials Reference Laboratory (AMRL). The final version had further changes that were announced to the participants through memos (attached as Appendix 2).

Table 2. Asphalts used in DSR ruggedness testing.

CODE	SHRP CODE	TEMP TEST (°C)		SOURCE
		25 mm	8 mm	
DSR-A	AAG-1	45	20	California Valley (thin film residue)
DSR-B	AAM-1	60	15	West Texas Intermediate
DSR-C	AAM-1	70	35	West Texas Intermediate (thin film residue)
DSR-D	AAG-1	55	10	California Valley

participants through memos (attached as Appendix 2).

Equipment Used

All the laboratories used a Cannon bending beam rheometer. Laboratories I and III used the constant-strain Rheometrics asphalt analyzer, while laboratories II and IV used a Bohlin CS-10 controlled-stress rheometer operating in the strain-controlled mode.

Miscellaneous

The variables that were most likely to affect the test results were identified and the upper and lower limits were selected by the participants in a meeting. The specific asphalts that were used in the testing were also identified in that meeting. The decisions were based on prior laboratory experience with the tests and best guesses as to the effects of the variables. The repeatability of each laboratory in performing the DSR and BBR tests was documented. Each laboratory conducted the DSR and BBR tests in six replications on a randomly selected asphalt. The mean and the coefficient of variation of these measurements, as given in Table 4, indicate the testing to be repeatable.

Statistical Analysis

The experimental design for ruggedness analysis is based on fractional factorial experiments, also called Youden squares, as described in American Society for Testing and Materials (ASTM) C1067. For our analysis, a statistical software package, Statistical Analysis System (SAS), was used. The model for the ruggedness testing is as follows:

Table 3. Uniformity of samples distributed to the laboratories.

MATERIAL	G* (kPa)	tan(δ)	Asphalt
BBR-A	3.23	0.361	AAM-1
BBR-B	7.43	0.436	AAK-1
BBR-C	1.25	0.617	AAC-1
DSR-A	2.66	1.948	AAG-1/TF
DSR-B	5.21	1.694	AAM-1
DSR-C	4.81	1.145	AAM-1/TF
DSR-D	1.62	2.668	AAG-1

$$Z = \beta_0 + \beta_1 X_1 + \beta_2 X_2 + \beta_3 X_3 + \beta_4 X_4 + \beta_5 X_5 + \beta_6 X_6 + \beta_7 X_7 + \beta_8 X_8 + e$$

Table 4. Repeatability of measurements with the BBR and the DSR by various laboratories.

LAB	Dynamic Shear Rheometer								Bending Beam Rheometer			
	8-mm parallel plate				25-mm parallel plate				S(60) (MPa)	CV	m	CV
	G* (MPa)	CV ¹	tan(δ) or δ	CV	G* (kPa)	CV	tan(δ) or δ	CV				
I	2.54	3.6	1.40	1.5	32.66	1.3	4.17	0.6	176.25	5.0	0.41	2.4
II	3.61	2.3	1.06	1.3	4.84	0.8	5.24	1.7				
III	2.34	4.2	60.40	0.4	2.73	2.6	85.00	0.4	196.12	8.3	0.32	3.1
IV	9.06	2.8	44.82	0.7	2.66	5.1	84.61	0.2				

¹CV = Coefficient of variation.

where X_i are the seven main effects and a repetition effect, and β_i are unknown coefficients, and e is the random error.

In this study, the complete set of experiments was randomized so that the replication, while important in providing the information needed for the estimation of the within-laboratory component of variance, did not allow for the removal of a one degree-of-freedom effect from the experimental error. Thus, the replication factor was not included in the model for the analysis. Analysis of the data was done to estimate the coefficients β_i , or the "effects" and the F-values (F-values are the statistics used to compare means using the standard F-test). The effects are reported as percent effects and indicate the percent change that ensues when the associated factor is increased by one coded unit. In our case, all factors (except the mold) are coded to either increase by one unit or decrease by one unit. The percent effects for such factors may be regarded as the maximum effect that will occur when one variable is off the target by the maximum allowable amount. The qualitative factors, such as mold type for making the BBR beams, have been coded -1 for silicone rubber mold and +1 for aluminum mold. There is no target value midway between the two materials. Thus, the reported percent effect is one-half the observed difference accounted for by the two materials.

From the F-values and percent effects, decisions were made as to the acceptability of the observed effects of each factor by applying the following criteria:

- **Magnitude of the effect:** An estimated percent effect of less than 1 percent due to a factor was arbitrarily chosen as representing an acceptable control for that factor.
- **Consistency of the effect:** The limits selected for a factor were considered to have an unacceptable effect when the percent effect for 3 or more of the 16 material-laboratories had estimated effects greater than 1 percent for that factor.
- **Consistency of F-values:** The critical F-values for testing the significance (at the 0.05 level) of an observed effect in this experiment was 5.59. Since there are 16 material-

laboratories¹ to be considered when evaluating any one of the factors, chance would often give one or two significant results even when there was no real effect. Thus, only those factors that had 3 or more of the 16 material-laboratories showing significant F-values (i.e., greater than 5.59) were regarded as clearly significant factor effects. In this sense, the experiment was providing a certain validation of the observed effects by means of the consistency of the observed effects over material-laboratory combinations.

In determining the importance of a factor, the results of the statistical analyses were examined on the basis of all three criteria listed above. In addition, the physical reason why a factor may have an effect on the measurement was also taken into account.

Precision and bias were calculated from the data by an analysis of variance. Consider the model

$$Z = \beta_0 + \text{LAB} + \beta_1 X_1 + \beta_2 X_2 + \beta_3 X_3 + \beta_4 X_4 + \beta_5 X_5 + e$$

In this model, three factors that were shown not to have an important effect on the measured value (based on ruggedness testing results) were omitted and a factor for laboratory was added. When an analysis of variance was performed, the standard deviation of the factor for the laboratory provided information regarding the variability introduced by the laboratory. The standard deviation for the error, e , provided the pooled estimate of the within-laboratory error for this test.

¹ A material-laboratory is the results from testing one material by one laboratory. Four laboratories testing three materials each would yield results from 12 material-laboratories.

RESULTS AND DISCUSSION

The results and discussions for the BBR and DSR ruggedness testing will be done separately. For each of the tests, the standardized residuals were analyzed, the average mean and coefficient of variation of the measurements were studied, and the results of factorial experiments were analyzed.

Bending Beam Rheometer

Analysis of the Standardized Residuals

It is important to examine the standardized residuals after carrying out a regression analysis. The actual residuals are the difference between the observed values and the values predicted by the regression function. The standardized residuals are these residuals divided by their standard deviation. These residuals should generally have values between ± 3 , with approximately 95 percent of them between ± 2 . Standardized residuals that exceed 2.5 should call our attention to data points that may have been recorded incorrectly or may have been the result of some problem during the experiment. This is one of the convenient methods available to analyze the data with the presence of such outliers.

Figure 1 illustrates the standardized residuals for the 196 measurements of S(60) in this experiment. From Figure 1(a), one can see that there are no trends in the standardized residuals. No one laboratory or material consistently showed higher or lower standardized residuals. The

Table 5. Flexural creep stiffnesses measured by the bending beam rheometer.

	FIRST REPLICATION								SECOND REPLICATION							
	1	2	3	4	5	6	7	8	1	2	3	4	5	6	7	8
LAB I																
A	311	411	408	394	314	268	306	339	370	367	377	347	308	278	312	297
B	123	175	144	154	140	121	133	139	154	159	171	153	143	121	130	131
C	635	587	769	649	560	530	551	560	629	676	598	658	549	516	510	531
LAB II																
A	233	294	304	327	237	252	230	253	233	264	307	283	227	226	308	249
B	98	116	136	121	85	97	90	102	111	100	127	106	86	86	103	103
C	535	609	594	554	577	483	478	498	511	635	610	592	472	376	485	507
LAB III																
A	319	323	337	329	282	272	268	302	315	317	341	322	276	283	276	361
B	139	146	137	130	138	132	136	144	138	137	142	137	123	144	143	155
C	496	583	591	592	522	475	486	448	479	598	585	597	534	414	463	490
LAB IV																
A	325	317	355	350	245	242	261	250	302	333	343	313	248	239	238	264
B	152	162	147	145	116	96	107	117	149	169	145	142	116	108	117	122
C	616	569	559	582	434	428	460	478	604	575	562	570	477	479	442	469

histogram of the residuals is shown in Figure 1(b). The standardized residuals are symmetrically distributed around 0, with five measurements over 2.0 and five measurements under -2.0. This indicates that the data obtained were of good quality. Such observations can also be made for $m(60)$ in Figure 2. There is no indication of any unreasonable residuals. We did not eliminate any data points as a result of this residual analysis.

Data Overview

Tables 5 and 6 display the raw data showing the creep stiffness and m -value at 60 s, respectively. These tables list the properties for three materials (A, B, and C) and eight experiments (1 through 8). The eight experiments test seven variables according to the Youden square experimental design as described in Table 28 in Appendix 1. The materials used in this study, along with their glass transition temperatures, are listed in Table 1.

Table 6. m -values determined by the bending beam rheometer.

	FIRST REPLICATION								SECOND REPLICATION							
	1	2	3	4	5	6	7	8	1	2	3	4	5	6	7	8
LAB I																
A	0.25	0.25	0.26	0.25	0.26	0.27	0.24	0.25	0.24	0.26	0.26	0.26	0.25	0.26	0.24	0.26
B	0.34	0.37	0.38	0.39	0.34	0.38	0.38	0.35	0.38	0.32	0.37	0.37	0.35	0.37	0.37	0.36
C	0.21	0.21	0.22	0.22	0.21	0.22	0.20	0.20	0.21	0.21	0.21	0.22	0.21	0.24	0.21	0.21
LAB II																
A	0.38	0.36	0.36	0.39	0.37	0.37	0.38	0.37	0.37	0.37	0.37	0.39	0.37	0.38	0.38	0.37
B	0.21	0.21	0.21	0.20	0.21	0.22	0.20	0.23	0.21	0.21	0.22	0.21	0.22	0.22	0.22	0.22
C	0.22	0.23	0.24	0.23	0.24	0.24	0.24	0.24	0.24	0.24	0.23	0.23	0.23	0.25	0.24	0.24
LAB III																
A	0.19	0.21	0.19	0.23	0.23	0.23	0.23	0.21	0.21	0.22	0.22	0.23	0.22	0.21	0.22	0.23
B	0.25	0.24	0.26	0.25	0.26	0.26	0.25	0.25	0.25	0.25	0.26	0.25	0.26	0.25	0.24	0.25
C	0.33	0.33	0.35	0.35	0.33	0.36	0.35	0.33	0.34	0.34	0.36	0.35	0.35	0.34	0.35	0.34
LAB IV																
A	0.27	0.25	0.26	0.27	0.26	0.27	0.24	0.26	0.26	0.25	0.27	0.27	0.26	0.27	0.26	0.29
B	0.36	0.36	0.38	0.37	0.37	0.36	0.35	0.35	0.35	0.35	0.38	0.38	0.36	0.36	0.35	0.35
C	0.19	0.19	0.19	0.19	0.19	0.20	0.20	0.21	0.20	0.20	0.19	0.20	0.20	0.20	0.20	0.19

Table 7 shows an overall view of the data, averaged by laboratory and material. It is helpful to view the averaged $S(60)$ and $m(60)$ values (Figures 3 and 5) and the averaged coefficient of variation (CV) (Figures 4 and 6) for $S(60)$ and $m(60)$ from different laboratories and materials. The following observations can be made from these data:

- There are considerable differences between the laboratories in the measurement of $S(60)$. Lab I consistently measured higher values of average $S(60)$ than other laboratories, while Lab III tended to be the lowest. This aspect will be discussed later in this report.

- The CVs for $S(60)$ range from 9.9 percent through 3.2 percent, with Lab III showing the highest average CV and Lab IV showing the lowest.
- The $m(60)$, on the other hand, does not vary significantly between laboratories. The range of $m(60)$ among laboratories was within 0.2 percent.
- The CVs for $m(60)$ were lower than for $S(60)$ by a factor of nearly 2. Lab II showed the highest average CV and Lab I showed the lowest average CV.
- $S(60)$ and $m(60)$ showed good repeatability within a laboratory, while the differences among the laboratory averages for $S(60)$ were a cause for concern.

Ruggedness Testing Analysis

Ruggedness data was analyzed by SAS as explained previously. The results from these analyses in the form of F-values and percent effects for $S(60)$ and $m(60)$ are tabulated in Tables 8 and 9, respectively.

The percent effects are the change in the measured parameter (e.g., $S(60)$) when the factor varied is changed from the mid-value to the high value. For instance, in the case of temperature, which was varied $T \pm 0.2^\circ\text{C}$, the effects listed in Table 8 are the percent the $S(60)$ will increase when the temperature is changed from T to $T + 0.2^\circ\text{C}$. The effects are further averaged by material as shown in Table 10.

Since the software used for the bending beam rheometer calculated m -values to two significant figures, the m -values were calculated manually to three significant figures in a Microsoft Excel® spreadsheet program according to the guidelines in AASHTO TP1. The creep stiffness at 8, 15, 30, 60, 120, and 240 s were used for this purpose.

In the following paragraphs, the significance of each of the factors will be considered separately.

Table 7. Average $S(60)$ and $m(60)$ measurements with the bending beam rheometer.

	CREEP STIFFNESS (MPa)			m -VALUE		
	MEAN	STD DEV	CV	MEAN	STD DEV	CV
LAB I						
A	337.9	25.6	7.6	0.248	0.007	2.6
B	143.2	11.3	7.9	0.365	0.005	1.4
C	594.3	50.1	8.4	0.316	0.006	2.8
			8.0			2.3
LAB II						
A	307.7	15.5	5.0	0.252	0.012	4.5
B	138.8	6.6	4.7	0.353	0.019	5.3
C	522.1	20.5	3.9	0.209	0.005	2.4
			4.5			4.1
LAB III						
A	264.2	24.6	9.3	0.244	0.003	1.0
B	104.2	8.0	7.7	0.351	0.007	1.9
C	532.3	40.0	7.5	0.206	0.007	3.4
			8.2			2.1
LAB IV						
A	289.1	13.8	4.8	0.244	0.006	2.3
B	131.9	4.6	3.5	0.351	0.011	3.2
C	519.0	18.0	3.5	0.208	0.004	2.1
			4.0			2.5

Aluminum vs. Silicone Rubber Molds

The specimen preparation method had the most significant effect of all. Samples molded from aluminum molds showed higher stiffness than samples made from silicone rubber molds. It is clear from examining Table 8 that this mold effect is real and consistent for all materials and laboratories and is very large.

Table 8. F-values and percent effects for S(60) measurements.

VARIABLE	LAB I			LAB II			LAB III			LAB IV		
	A	B	C	A	B	C	A	B	C	A	B	C
F-VALUES												
Molds	30.1	15.1	19.9	7.1	26.0	22.8	21.0	0.1	70.5	139.4	286.3	181.4
Time at RT	2.2	0.2	0.5	9.0	11.6	0.6	5.8	1.1	3.4	5.0	2.0	0.7
Temp demold	0.0	0.1	0.2	0.5	0.0	0.0	2.4	1.2	0.3	0.0	0.4	0.0
Time demold	0.0	0.0	0.6	1.0	0.4	0.0	0.4	4.4	10.6	0.7	18.8	2.9
Time in bath	1.2	3.4	0.0	1.3	2.8	3.3	4.9	2.4	23.4	0.1	4.3	1.4
Load	0.2	0.1	0.0	2.1	1.8	0.0	2.1	0.2	0.2	0.3	0.2	4.7
Test temp	5.3	6.3	0.6	0.2	1.8	9.3	6.3	0.8	18.1	2.4	17.9	0.7
PERCENT EFFECTS												
Molds	-10.4	-7.6	-9.4	-6.2	-9.8	-9.0	-5.7	0.4	-8.2	-14.1	-14.8	-11.7
Time at RT	2.8	0.8	1.5	7.0	6.5	1.4	3.0	1.2	1.8	2.7	-1.2	-0.7
Temp demold	0.1	-0.7	1.0	-1.6	0.3	0.1	-1.9	-1.3	-0.5	0.2	-0.6	0.0
Time demold	0.4	-0.1	-1.6	-2.3	-1.3	0.0	0.8	2.5	-3.2	-1.0	3.8	1.5
Time in bath	2.1	3.6	-0.3	2.7	-3.2	3.4	-2.8	-1.8	4.8	-0.3	1.8	-1.0
Load	-0.9	-0.7	0.4	-3.4	-2.6	-0.3	1.8	-0.6	-0.4	-0.7	0.4	1.9
Test temp	-4.3	-4.9	-1.6	-1.0	-2.6	-5.7	-3.1	-1.0	-4.2	-1.8	-3.7	0.7

The shaded area indicates F-values that are not significant at 95 percent confidence level.

Table 9. F-values and percent effects for m(60) measurements.

VARIABLE	LAB I			LAB II			LAB III			LAB IV		
	A	B	C	A	B	C	A	B	C	A	B	C
F-VALUES												
Molds	0.1	0.0	0.0	0.1	0.2	1.0	1.0	7.0	0.5	9.8	0.2	16.3
Time at RT	1.3	4.0	0.7	0.4	2.1	0.0	1.0	1.3	0.0	0.2	0.2	0.3
Temp demold	7.0	4.0	0.0	1.2	0.0	0.0	1.0	1.3	2.0	0.2	0.0	0.3
Time demold	0.1	4.0	0.0	0.4	0.4	0.0	81.0	24.1	8.0	1.8	1.8	0.3
Time in bath	0.1	4.0	0.7	2.3	0.2	4.0	1.0	0.1	0.0	0.2	0.0	0.3
Load	3.6	0.0	0.0	1.2	0.9	1.0	1.0	0.1	4.5	5.0	3.2	0.3
Test temp	3.6	16.0	0.7	0.4	2.1	1.0	1.0	1.3	0.5	0.2	0.8	0.3
PERCENT EFFECTS												
Molds	0.0	0.0	0.0	0.2	-0.5	0.6	-0.3	-1.2	0.6	1.8	-0.4	2.1
Time at RT	-1.0	0.7	0.6	0.7	1.9	0.0	-0.3	0.5	0.0	0.3	0.4	-3.0
Temp demold	-2.0	-0.7	0.0	-1.2	0.2	0.0	-0.3	0.5	-1.2	-0.3	0.0	0.3
Time demold	0.0	-0.7	0.0	-0.7	-0.9	0.0	-2.3	-2.3	-2.4	-0.8	-1.1	0.3
Time in bath	0.0	0.7	0.6	-1.7	-0.5	-1.2	-0.3	-0.2	0.0	-0.3	0.0	-1.5
Load	-1.0	0.0	0.0	1.2	-1.2	0.6	0.3	-0.2	-1.8	-1.3	-1.4	0.3
Test temp	-1.0	1.4	0.6	-0.7	1.9	-0.6	-0.3	-0.5	0.6	0.3	0.7	0.3

The shaded area indicates F-values that are not significant at 95 percent confidence level.

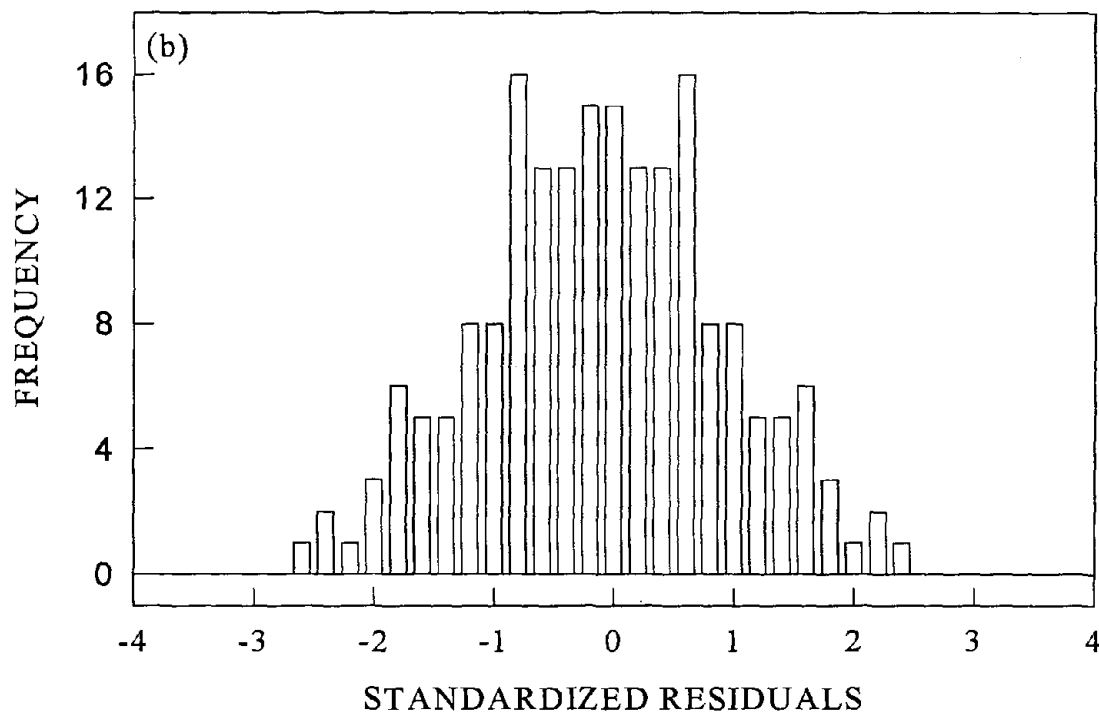
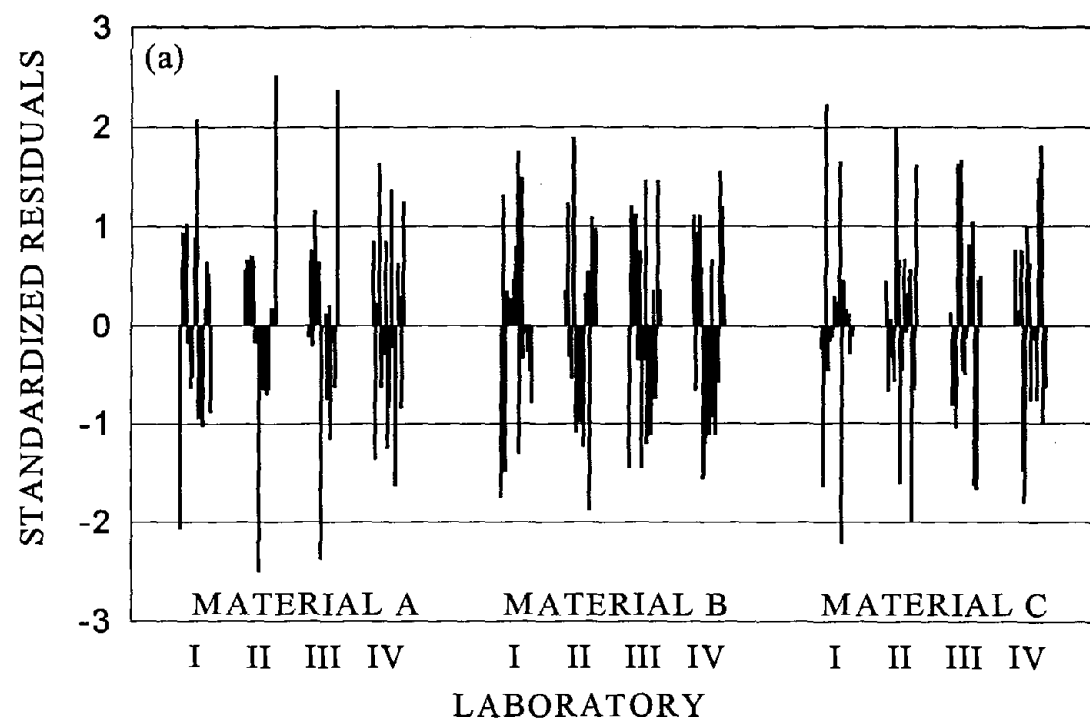


Figure 1. Standardized residuals in $S(60)$ measurements: (a) grouped by laboratory and material, and (b) distribution of all standardized residuals.

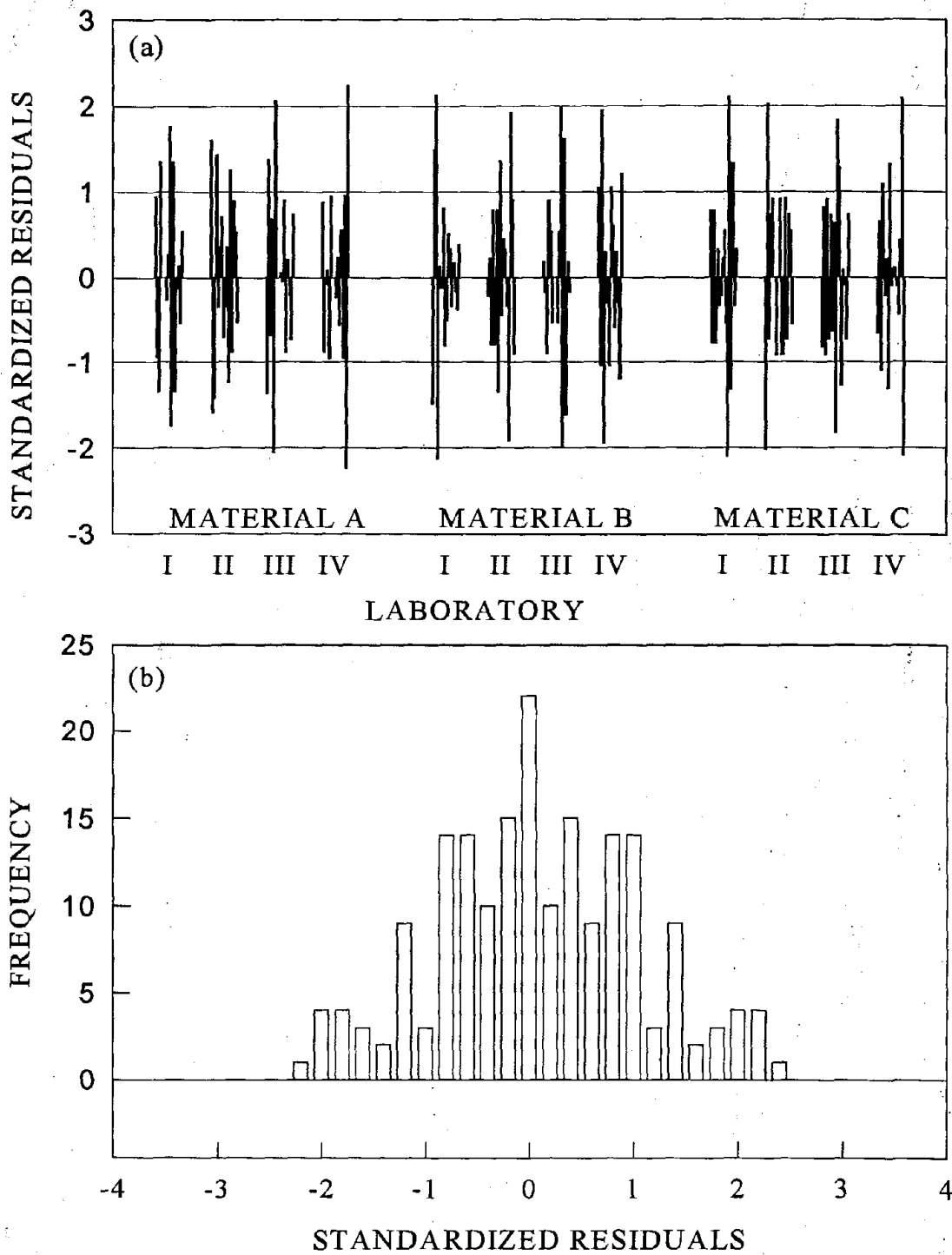


Figure 2. Standardized residuals in $m(60)$ measurements: (a) grouped by laboratory and material, and (b) distribution of all standardized residuals.

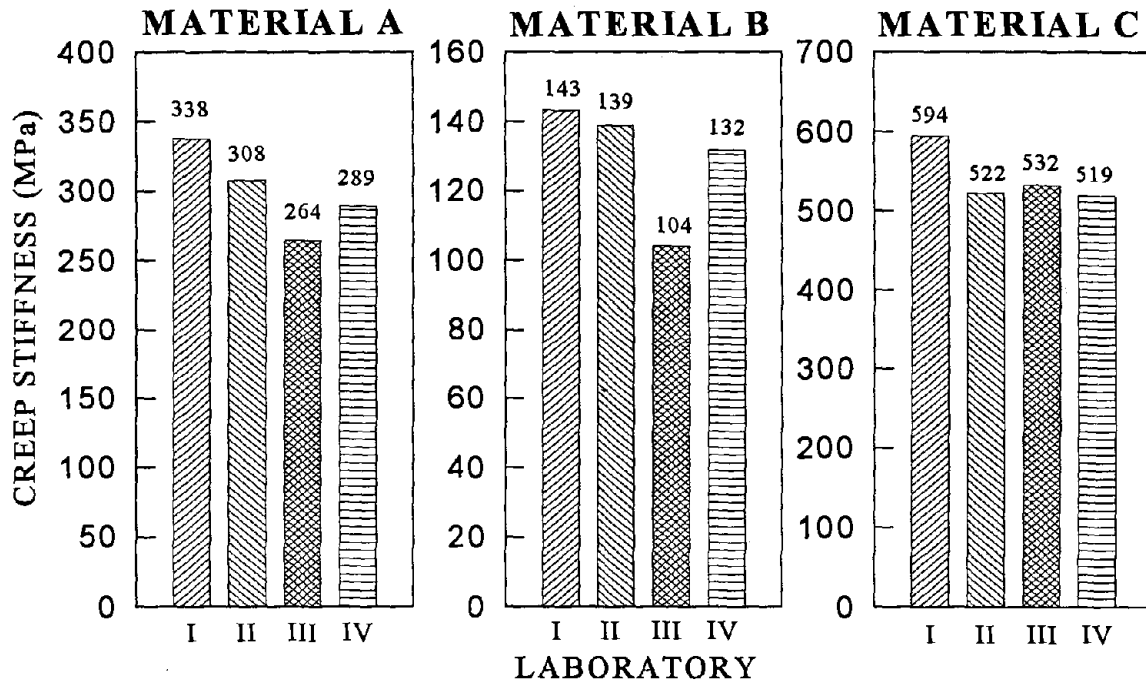


Figure 3. Creep stiffness measurements averaged by laboratory and material.

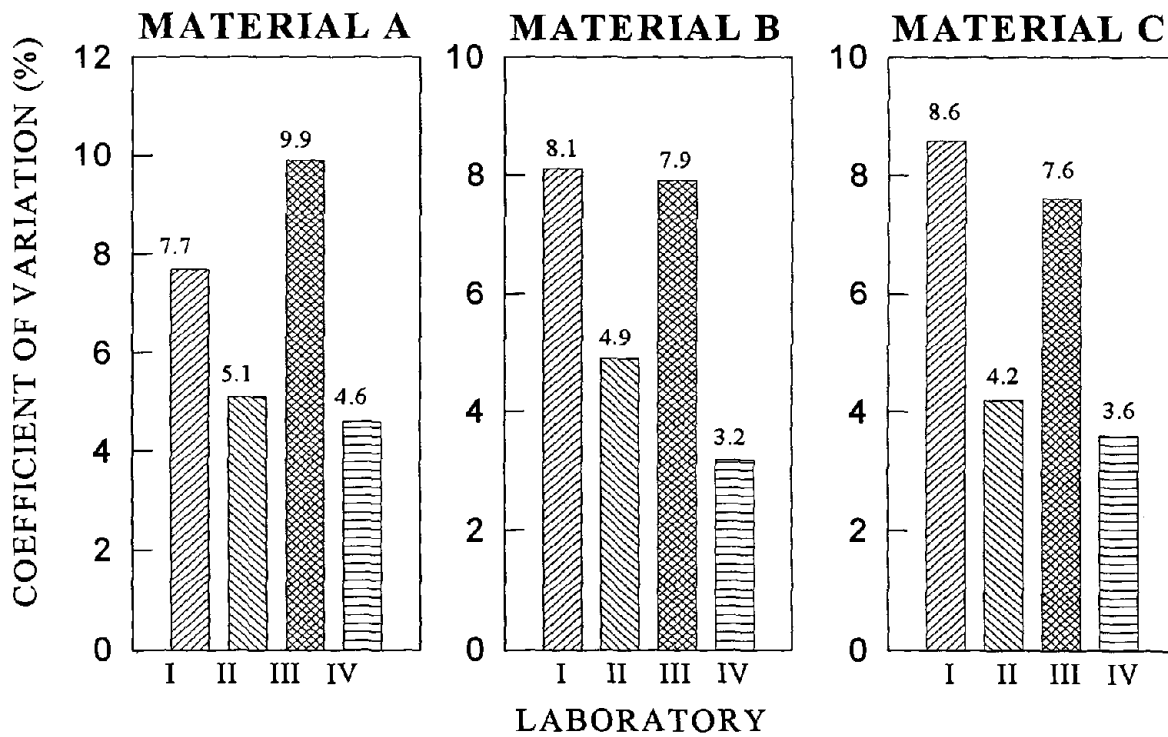


Figure 4. Coefficient of variation in creep stiffness measurements averaged by material and laboratory.

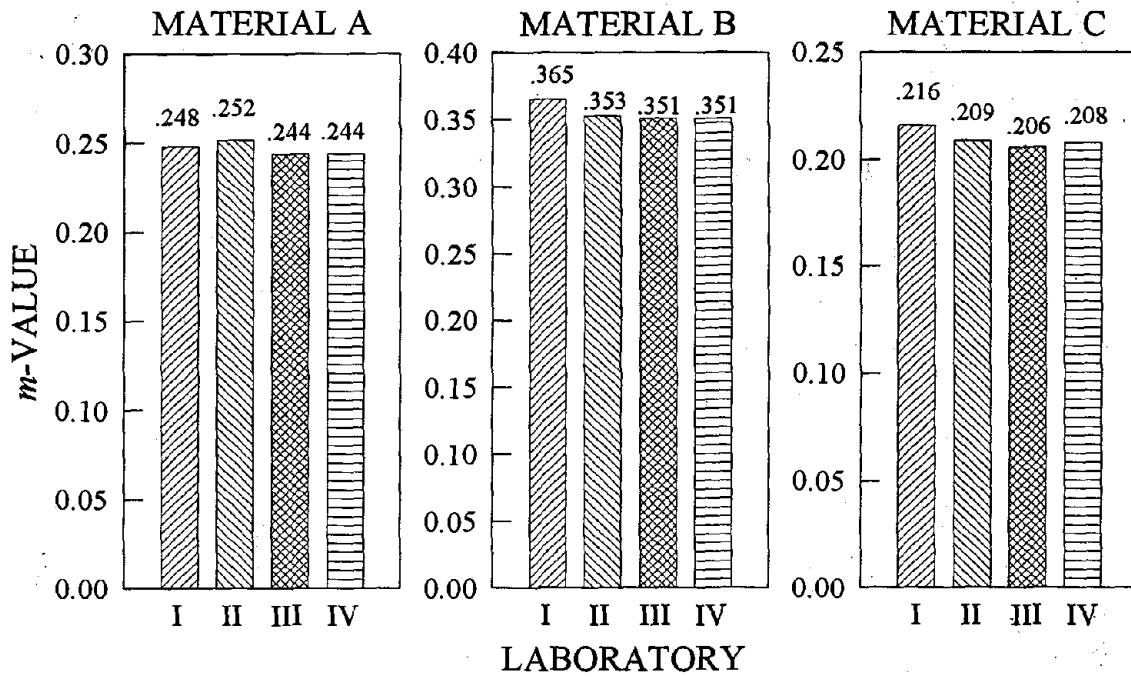


Figure 5. *m*-value measurements averaged by material and laboratory.

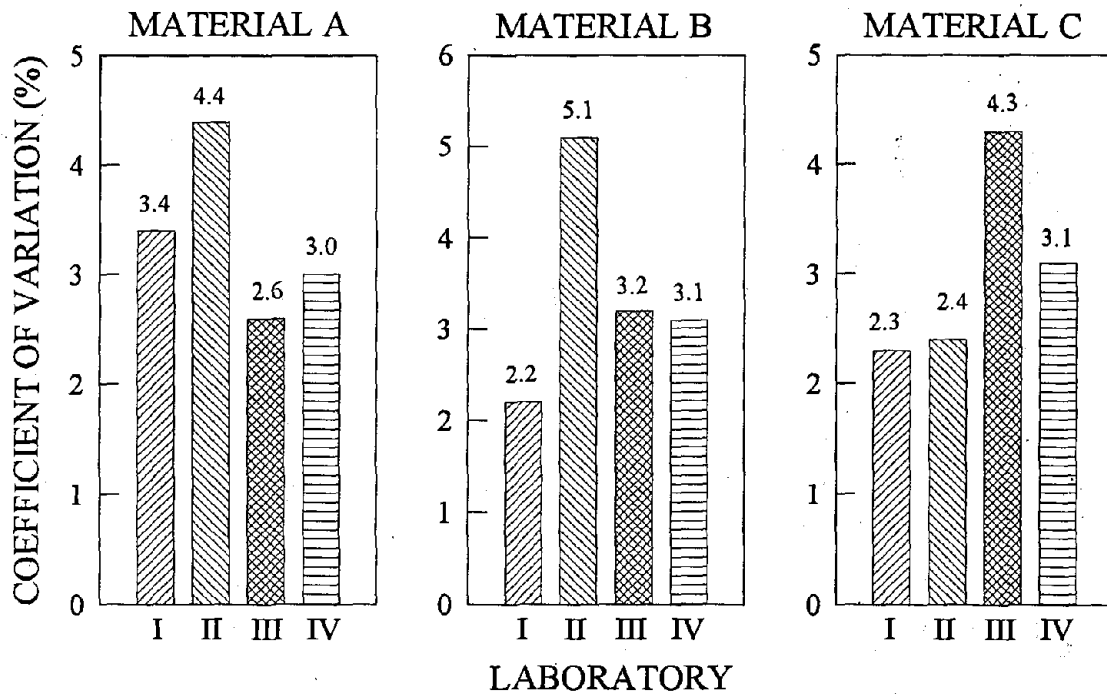


Figure 6. Coefficient of variation *m*-value measurements averaged by material and laboratory.

Table 10. Average percent effects for S(60) and m(60) measurements.

VARIABLES	RANGE	S(60)				m(60)			
		A	B	C	AVG.	A	B	C	AVG.
Aluminum vs. silicone rubber molds		-9.11	-7.95	-9.58	-8.88	2.75	1.84	4.46	3.02
Time left at room temp after trimming	20 vs. 300 min	3.87	1.84	1.00	2.24	0.73	1.90	0.25	0.96
Temperature before demolding	0 vs. -10°C	-0.82	-0.56	0.16	-0.41	2.35	1.33	0.58	1.42
Time in freezer before demolding	10 vs. 30 min	-0.54	1.22	-0.83	-0.05	20.84	7.60	2.08	10.17
Time in test bath	55 vs. 65 min	0.40	0.10	1.70	0.74	0.92	1.08	1.25	1.08
Load on the beam	95 vs. 105 g	-0.78	-0.88	0.38	-0.43	2.69	1.05	1.46	1.73
Test temperature	T+0.2 vs. T-0.2	-2.59	-3.06	-2.70	-2.78	1.30	5.05	0.63	2.33

In order to find the cause of such variation, Lab I conducted an experiment in which six bars each were cast with the two molds and the thickness was measured with a micrometer. Also, Lab IV measured the thickness of some specimens that were used for the ruggedness experiments. The data is tabulated in Table 11. The following observations can be made:

- The thickness of beams made with silicone rubber molds was smaller than that of the beams made with aluminum molds in both laboratories.
- All the thicknesses were not within the specification value of 6.35 ± 0.05 mm.
- The S(60) of beams cast with aluminum molds measured higher than that of beams cast with silicon rubber molds.

The patterns used for making the silicone rubber mold and the aluminum mold will be within specifications at room temperature. Any beam cast in this mold will be within specification at room temperature, but will contract when cooled to the test temperature.

The flexural creep stiffness (S(t)) is calculated by the formula:

$$S(t) = \frac{PL^3}{4bh^3\delta(t)} \quad (1)$$

where P is the load, L is the distance between the bottom supports, b is the width of the beam, h is the thickness of the beam, and $\delta(t)$ is the deflection. The parameters b, h, and L are input by the user, while the instrument measures P and $\delta(t)$ and calculates S(t).

Table 11. Thickness of beams cast in aluminum and silicone rubber molds.

	Aluminum Mold			Silicone Rubber Mold		
	n	μ	σ	n	μ	σ
ASPHALT						
LAB I	6	6.554	0.144	6	6.079	0.052
LAB IV	12	6.172	0.132	12	5.893	0.121
EPOXY						
LAB I	5	6.285	0.003	6	6.212	0.002
LAB III	6	6.336	0.000	6	6.191	0.002
LAB IV				4	6.104	0.002
WAX						
LAB I				6	6.039	0.003
LAB II	6	6.326	0.014	6	6.160	0.036

S(60) and m(60) measured on asphalt beams

	μ	σ	μ	σ
S(60)	326	16	289	20
m(60)	0.262	0.01	0.25	0.01

When a certain value is input for the thickness in the software, and the actual value turns out to be smaller than the input value, the machine will calculate a stiffness smaller than it actually is. This is because the machine uses the wrong value for thickness since it is not required that the thickness be measured at the test temperature. The smaller the thickness, the lower the $S(t)$. Even though the width of the beam has a similar effect on $S(t)$, the magnitude is much less than for thickness, because $S(t)$ depends on the cube of the thickness. Table 11 does show smaller $S(60)$ values for beams cast with silicone rubber molds.

Table 12. Ruggedness analysis after correcting for beam thickness.

	F-VALUES						PERCENT EFFECTS							
	LAB I			LAB IV			LAB I			LAB IV			Average	
	A	B	C	A	B	C	A	B	C	A	B	C	Lab I	Lab IV
Molds	0.21	4.12	0.92	38.67	74.41	26.65	0.8	3.6	1.8	-7.2	-8.0	-4.8	1.8	-6.7
Time at RT	2.66	0.19	0.48	5.13	1.04	0.43	2.9	0.8	1.3	2.6	-0.9	-0.6	1.7	0.4
Temp demold	0.04	0.01	0.26	0.03	0.24	0.00	0.3	-0.2	1.0	0.2	-0.5	-0.0	0.4	-0.1
Time demold	0.16	0.00	0.54	0.48	16.21	2.40	0.7	-0.1	-1.4	-0.8	3.7	1.4	-0.3	1.5
Time in bath	1.39	4.12	0.01	0.07	3.62	1.22	2.1	3.6	-0.2	-0.3	1.8	-1.0	1.8	0.1
Load	0.05	0.02	0.08	0.25	0.57	3.98	-0.4	-0.3	0.5	-0.6	0.7	1.9	-0.0	0.7
Test temp	5.80	7.59	0.74	2.43	16.21	0.38	-4.3	-4.9	-1.7	-1.8	-3.7	0.6	-3.6	-1.7

The shaded area indicates F-values that are not significant at 95 percent confidence level.

Table 11 shows the thickness measurements from two laboratories, I and IV. In both cases, the beams cast in silicone rubber molds were thinner than the beams cast in aluminum molds. If the $S(60)$ values for these beams are measured, the beams cast in silicone rubber mold should have lower $S(60)$ values than the beams cast in aluminum molds. This is indeed what was found when the beams for which the thicknesses are given in Table 11 were tested.

This is consistent with the results in Table 8 that indicate that the beams cast with aluminum molds were stiffer than the beams cast with silicone rubber molds. The effect of the differing beam thicknesses can be corrected for by using the actual beam thickness in the formula and calculating the $S(60)$. When the corrected $S(60)$ values were used in the statistical model, the results shown in Table 12 were obtained. The F-values and the percent effects drop significantly when the stiffness is corrected for thickness. But the F-values and percent effects still show a significant mold effect.

In order to understand the thickness effect further, beams of wax and epoxy were cast and the thicknesses were measured (Table 11). The beams cast in the aluminum molds were within specifications (6.35 ± 0.5 mm). Not only were the thicknesses of the beams cast in the silicone rubber molds less than the specification, but they also varied from 6.04 to 6.21 mm. This would (theoretically) underestimate the thickness by 14 percent and 7 percent, respectively. Furthermore, the thicknesses of the asphalt beams were less than those measured for the epoxy beams. It was noted that the thermal contraction of the asphalt beam at low temperatures was not the sole cause of this difference. Taking the coefficient of thermal expansion of asphalt to be $1.73 \times 10^{-4}/^{\circ}\text{C}$,⁽⁴⁾ the asphalt beams from Lab I and Lab IV had to be cooled by 200°C and 123°C , respectively, to yield this thickness difference. This is highly unreasonable. This is reflected in the fact that the mold effect did not vanish entirely when the thickness was corrected for and it suggests that there may be some other factors contributing to the mold effect.

Table 13. Effect of correcting thickness on ruggedness results.

	FIRST REPLICATION								SECOND REPLICATION							
	1	2	3	4	5	6	7	8	1	2	3	4	5	6	7	8
BEFORE THICKNESS CORRECTION																
LAB I																
A	311	411	408	394	314	268	306	339	370	367	377	347	308	278	312	297
B	123	175	144	154	140	121	133	139	154	159	171	153	143	121	130	131
C	635	587	769	649	560	530	551	560	629	676	598	658	549	516	510	531
LAB IV																
A	325	317	355	350	245	242	261	250	302	333	343	313	248	239	238	264
B	152	162	147	145	116	96	107	117	149	169	145	142	116	108	117	122
C	616	569	559	582	434	428	460	478	604	575	562	570	477	479	442	469
AFTER THICKNESS CORRECTION																
LAB I																
A	283	374	371	358	358	305	349	386	337	334	343	316	351	317	356	339
B	112	159	131	140	160	138	152	158	140	145	156	139	163	138	148	149
C	578	534	699	590	638	604	628	638	572	615	544	598	626	588	581	605
LAB IV																
A	354	345	387	381	307	303	327	313	329	363	374	341	310	299	298	330
B	166	176	160	158	145	120	134	146	162	184	158	155	145	135	146	153
C	671	620	609	634	543	535	576	598	658	626	612	621	597	599	553	587

Time Left at Room Temperature after Trimming

After the beams (in aluminum molds) were trimmed, they were left at room temperature for 20 and 300 min before they were chilled and demolded. Asphalt beams cast in silicone rubber molds did not need trimming and, hence, were left in the mold for an equivalent amount of time. F-values (Table 8) indicated that 3 of the 12 material-laboratories showed a significant effect. The percent effects showed positive values, indicating that the asphalt became stiff at the test temperature when left standing at room temperature for 300 min prior to testing. Even though only three material-laboratories showed significant F-values, nine material-laboratories showed effects greater than 1 percent and all values were negative. None of the F-values for the $m(60)$ showed significant effects (Table 9). The percent effects also varied randomly, indicating little effect on the $m(60)$ measurement.

In order to understand how $S(60)$ changed with time while left at room temperature, an experiment was performed in which beams of PAV-aged AAM-1 asphalt were left at room temperature for 20, 100, 315, and 1440 min.

Table 14. Effect of leaving cast beams at room temperature.

No. beams	Time at room temperature (min)			
	20	100	315	1440
$S(60)$				
8	337	328	347	336
8	22	18	12	12
$m(60)$				
8	0.251	0.263	0.253	0.256
8	0.007	0.012	0.007	0.005

These results are shown in Table 14. The data do not show any trends and, hence, are inconclusive.

Physically, there are known mechanisms, such as steric hardening and physical hardening, by which asphalt can stiffen when left at room temperature. The ruggedness data showed that by increasing the time the bars are left in the mold at room temperature from 140 min to 300 min, $S(60)$ increased 2.24 percent. The maximum time the bars can be left at room temperature according to the criteria selected is 130 min. The m -values showed no significant effect due to this factor.

Temperature to Which Beams Were Chilled Before Demolding

The two levels tested were 0°C and -10°C . F-values for $S(60)$ (Table 8) showed the levels chosen had insignificant effects on the measurement of $S(60)$. This was confirmed by looking at the average effects, most of which were less than 1 percent. For $m(60)$ measurements, F-value for one material-laboratory was over 5.59, and the percent effect varied randomly, with a low average effect. There appears to be little effect due to this factor.

Time for Which Beams Were Chilled Before Demolding

The beams were chilled for 20 ± 10 min in the freezer before demolding. These limits are much more relaxed than what AASHTO published later in TP1, Edition 1A. F-values for $S(60)$ (Table 8) showed that two material-laboratories had a significant effect at these levels. The percent effects showed that in four material-laboratories there was a strong negative effect, while in three material-laboratories there was a strong positive effect. These effects cancel out each other, showing an overall effect that is insignificant. These results are inconclusive at these limits. Perhaps, the more conservative limits for time in the freezer set by AASHTO in TP1 would show insignificant effects.

Time in the Test Bath

The beams were soaked for 60 ± 5 min at the test temperature before testing. These limits are the same as in AASHTO TP1. Only one material-laboratory showed F-values greater than 5.59 for this effect. The percent effects tended to be both negative (showing a maximum effect of -4.75 percent) and positive (with a maximum effect of 3.18 percent). When averaged, these effects became insignificant because they cancelled out each other (Table 8). It was concluded that the time in the test bath did not have a significant effect on $S(60)$ at the limits considered. In the measurement of $m(60)$, none of the material-laboratories showed F-values over 5.59 (Table 9). The percent effect tended to be negative, even though they averaged out to an insignificant -0.39 percent.

Load on the Beam

The levels chosen for the load on the beam had an insignificant effect on the measurement of $S(60)$. The F-values were less than 5.59 in all cases, and the average effects were less than 1 percent. This indicates insignificant effects due to varying the load within these limits. Note that

the actual (measured) load was used to calculate the $S(60)$. Similarly, there were insignificant effects due to load on the beam for the measurement of $m(60)$.

Test Temperature

The factor for the test temperature was varied $\pm 0.2^\circ\text{C}$ from the set temperature. These limits are used in AASHTO TP1 provisional specifications as well. For $S(60)$, five material-laboratories show F-values greater than 5.59. The percent effects were mostly negative and were strong. The overall average of the percent effects was -2.78 percent, which implies that the temperature had to be controlled to $\pm 0.07^\circ\text{C}$ to achieve a 1 percent effect. For $m(60)$, only one material-laboratory showed an F-value greater than 5.59. The percent effects were random and the average was less than 1 percent, indicating that this factor had no significant effect on $m(60)$. It was concluded from the ruggedness testing that the temperature should be controlled to $\pm 0.1^\circ\text{C}$ in order to minimize the effect due to the test temperature.

In summary, the ruggedness test for the bending beam rheometer indicates that the method used to make the beam has an important effect on the results. It may be necessary to measure the thickness of the beams cast in silicone rubber mold prior to testing and use this value in the test to eliminate some variation. Even though the time the samples were left at room temperature showed some effect, this effect could not be reproduced in independent experiments. In any case, the present test procedure⁽¹⁾ calls for less time than that used in the ruggedness test. This should limit the effect due to the time left at room temperature. It is the conclusion of the ruggedness testing that the temperature should be controlled to $\pm 0.1^\circ\text{C}$ to achieve acceptable control over test results.

Precision and Bias Estimates

As a result of the analysis of the ruggedness experiments, the factors such as the temperature of demolding, load on the beam, and time at room temperature were found to have insignificant effects. Hence, in the model for analysis of variance, these factors were included in the error term. The model used for analysis of variance is, therefore,

$$Z = \beta_0 + \text{LAB} + \beta_1 X_1 + \beta_2 X_2 + \beta_3 X_3 + \beta_4 X_4 + \beta_5 X_5 + e$$

where β_0 is the true, but unknown mean; β_1 through β_5 are the unknown coefficients for the factors aluminum vs. silicone rubber molds, time in freezer before demolding, time in test bath, test temperature, and the laboratory effect, respectively, and e is the random error. All the factors were assumed to be normal random variables with a mean of zero.

Table 15. Between- and within-laboratory coefficient of variation.

Material	Mean from All Labs	Between-Lab CV	Within-Lab CV
$S(60)$			
A	300	17.9	7.7
B	130	23.3	9.1
C	542	11.2	6.7
$m(60)$			
A	0.279	42.1	3.7
B	0.297	44.1	3.6
C	0.247	46.2	2.8

Table 15 lists the results of these analyses. The results showed that the within-laboratory coefficient of variation (CV) varied from 6.7 to 9.1 percent, while the between-laboratory CV

varied from 11.2 to 23.3 percent. Furthermore, it was found that increasing the $S(60)$ resulted in higher CVs for between- and within-laboratory results. The within-laboratory CV for the measurement of $m(60)$ was between 2.8 and 3.7, while the between-laboratory CV was between 42.1 and 46.2.

It must be emphasized that the within-laboratory and the between-laboratory coefficients of variation must be used with caution as these experiments were not designed to obtain this information. A formal inter-laboratory test to determine the precision and bias according to the ASTM procedures will alone determine the coefficient of variation. Another indicator for these coefficients of variation is the laboratory proficiency test conducted by the AASHTO Materials Reference Laboratory in August 1994. From a sample of 24 laboratories that made 2 measurements each, the within-laboratory and between-laboratory coefficients of variation were estimated at 4.3 percent and 10.5 percent, respectively, for $S(60)$, and 1.6 percent and 4.1 percent, respectively, for $m(60)$.

Dynamic Shear Rheometer

Analysis of Standardized Residuals

As before, we shall look at the standardized residuals to eliminate any bad data points. In the case of DSR data, each of the four measurements— G^* measurement by 8-mm parallel plate, δ measurement by 8-mm parallel plate, G^* measurement by 25-mm parallel plate, and δ measurement by 25-mm parallel plate—will be looked at separately. Figures 7 through 10 show the standardized residuals for these active variables. From these figures, one can see that there are no trends in the standardized residuals. No one lab or material consistently shows higher or lower standardized residuals. The histogram of the residuals are also shown in Figures 7 through 10. The standardized residuals are distributed around 0, with a maximum of six measurements over 2.0 and six measurements under -2.0. This indicates that the data obtained were of good quality. There is no indication of any unreasonable residuals. As a result of this residual analysis, we did not eliminate any data points.

Data Overview

In our experiment, three out of four laboratories followed the truly random sequence of experiments suggested in the procedure, while the fourth lab followed a different sequence. A repetition effect is normally included in the model to separate out any changes (environmental or other) that might have occurred between the testing of the first set of experiments and the second set of experiments. Since all the laboratories mixed the first and second repetitions randomly, this factor was taken out of the model. Tables 16 through 19 display the raw data showing the

Table 16. Complex shear modulus (in kPa) measured with 8-mm parallel plates.

	FIRST REPLICATION								SECOND REPLICATION							
	1	2	3	4	5	6	7	8	1	2	3	4	5	6	7	8
LAB I																
A	7929	8873	7120	8834	8788	7762	8192	7862	8386	9123	7708	8380	8539	8420	8285	7475
B	6284	7264	6479	7118	7013	7036	6877	6115	5873	6826	5813	6319	7298	6477	7228	4887
C	213	212	160	188	212	188	217	188	208	227	163	40225	220	189	244	215
D	37812	41741	33178	39709	42239	39762	43191	35774	37431	37558	34736	41148	41017	36154	37956	35813
LAB II																
A	12159	12553	7208	13102	11001	9518	13806	6901	9876	13966	7584	14894	12938	30534	13154	8342
B	6413	8654	5664	7696	8651	6586	9345	5276	6337	8211	5388	7247	8339	16762	6037	5640
C	264	343	167	295	277	220	437	207	238	388	154	321	321	6	415	198
D	43482	52002	32020	58885	46544	43755	1796	34567	45483	61857	38812	52275	58218	1283	54428	51
LAB III																
A	7672	11800	7148	11650	12080	8293	12150	6835	8473	12560	7783	11580	11690	8028	11670	6230
B	5512	8413	5438	11630	8480	8143	7673	5681	5857	7857	5716	8680	8417	6205	8473	5156
C	172	363	152	341	250	169	309	171	189	354	144	260	282	193	295	180
D	40000	50510	32190	51480	50130	36700	48710	31980	41930	51460	48920	51340	49110	32100	53480	32640
LAB IV																
A	7130	10600	6790	10700	12400	6770	10500	6980	6370	11100	6530	9760	12000	7660	9900	6660
B	5090	6850	5060	6170	6860	4800	7110	5340	5370	6870	4880	6100	7360	4880	7060	4560
C	248	306	182	300	318	197	340	191	208	359	182	288	311	191	291	197
D	32800	49100	30800	46400	43700	32000	38200	36200	33800	47200	33700	37500	46900	32700	43100	34500

complex shear modulus (G^*) and the phase angle (δ) measured using an 8-mm and a 25-mm parallel plate geometry, respectively. These tables list the properties for four materials (A, B, C, and D) and eight experiments (1 through 8). The eight experiments vary seven variables according to the Youden square experimental design as described in Table 30 in Appendix 1. The materials used in this study are listed in Table 2.

Table 20 shows an overall view of the data, averaging the data by the lab and the material. It is helpful to view the averaged G^* and δ (Figures 11, 13, 15, and 17) and averaged coefficient of variation (CV) (Figures 12, 14, 16, and 18) for the different laboratories and materials. The following observations can be made:

- The average G^* measured with 8-mm parallel plates showed more variability than 25-mm parallel plates. With the 25-mm parallel plates, the laboratories were very close to one another, except for material D, which showed some variation.
- The CVs for G^* (8-mm parallel plates) range from 13.0 percent to 3.7 percent, with Lab II showing the highest average CV and Lab I showing the lowest. Since the effects of the factors are subtracted in calculating this quantity, this indicates that there is considerable scatter among laboratories.

Table 17. Phase angles (in degrees) measured with 8-mm parallel plates.

	FIRST REPLICATION								SECOND REPLICATION							
	1	2	3	4	5	6	7	8	1	2	3	4	5	6	7	8
LAB I																
A	64.1	63.4	64.8	63.8	63.6	65.0	64.6	64.6	64.2	63.5	64.3	64.2	63.1	64.8	63.9	64.8
B	46.2	45.4	45.8	45.9	45.0	45.8	46.1	46.4	47.0	45.2	46.5	46.3	45.2	40.1	45.7	46.7
C	66.9	67.1	68.6	68.3	67.6	68.1	67.1	66.9	67.3	66.9	68.5	67.8	67.6	68.3	66.7	66.8
D	49.0	46.4	42.2	47.8	46.5	47.7	47.4	48.5	48.4	47.7	49.0	47.9	45.8	49.0	0.2	48.0
LAB II																
A	63.0	60.0	64.8	60.0	59.1	63.7	60.5	64.7	64.1	59.6	65.2	58.7	59.4	64.5	60.1	64.6
B	47.3	45.3	48.5	46.0	43.7	47.8	45.6	47.0	47.2	45.2	48.0	46.3	44.5	51.3	45.5	47.3
C	65.2	64.4	68.7	66.6	65.6	67.8	64.1	65.9	66.6	63.7	69.2	66.4	65.4	69.5	63.5	67.0
D	46.5	41.3	48.6	41.8	42.2	45.9	43.7	46.5	47.1	40.5	46.6	43.2	41.0	48.2	43.6	87.0
LAB III																
A	65.6	61.9	65.8	62.6	61.3	65.1	62.0	66.0	64.9	60.8	65.0	62.1	61.5	65.3	62.2	67.3
B	48.5	45.8	48.1	42.3	45.5	45.9	46.0	46.4	47.4	46.2	47.4	45.7	45.8	44.7	46.0	47.9
C	69.1	66.1	69.4	67.1	68.2	68.2	66.7	68.2	68.2	65.7	69.8	68.6	67.4	68.2	67.1	67.8
D	49.5	45.3	51.7	46.6	44.5	49.2	47.0	51.4	49.9	46.6	45.2	46.4	46.1	50.5	46.2	49.9
LAB IV																
A	64.2	59.7	64.8	59.5	58.1	63.5	60.3	64.2	65.2	59.2	64.6	60.9	57.9	63.4	59.8	64.6
B	46.5	44.5	45.8	44.6	44.1	47.0	45.0	46.2	45.5	42.7	46.9	45.1	43.5	46.0	43.9	46.6
C	64.4	63.7	67.2	65.0	65.0	66.8	63.9	65.7	65.6	63.3	67.3	65.4	65.2	66.8	64.5	65.5
D	46.5	39.9	47.5	40.5	41.1	48.0	43.2	45.3	48.0	40.8	46.6	43.6	41.1	45.2	41.2	46.3

- The CVs for G^* measurements with 25-mm parallel plates ranged from 14.4 percent to 3.1 percent, with Lab II and Lab III showing high CVs.
- The δ , on the other hand, did not vary significantly between laboratories. The ranges of δ among laboratories were within 4° for measurements with 8-mm parallel plates and within 2° for measurements with 25-mm parallel plates.
- The CVs for δ were lower than 2.0 percent for 25-mm parallel plates, and lower than 4 percent for 8-mm parallel plates, indicating that the measurement of δ is very repeatable. Also, CVs for δ were much lower than that for G^* .

Table 18. Complex modulus (in Pa) measured with 25-mm parallel plates.

	FIRST REPLICATION								SECOND REPLICATION							
	1	2	3	4	5	6	7	8	1	2	3	4	5	6	7	8
LAB I																
A	38880	46034	35455	40631	44167	5373	43817	34513	38587	43725	33556	42830	46717	37125	43259	35886
B	2159	2465	1950	2332	2393	1871	2427	1988	2206	2538	1957	2204	2454	2128	2548	1807
C	1075	1282	1058	1259	1264	1052	1215	1002	1130	1360	975	1317	1286	1067	1274	977
D	3404	4189	3262	4409	4217	3750	3940	3512	3461	4325	3400	4342	4527	3388	4132	3334
LAB II																
A	32810	63640	29700	61110	63120	31160	62480	29630	33330	52870	30100	60940	52690	31480	68110	26980
B	1840	3088	1590	2897	3060	1690	3158	1662	1669	3390	1480	3155	3215	1660	3254	1583
C	997	1808	808	1202	1595	889	1506	862	726	1410	812	1650	1723	853	1679	815
D	3020	6165	2703	5713	5408	3063	5576	2809	2998	6126	2528	6289	5691	2842	5574	4503
LAB III																
A	30610	62770	27050	59570	61340	31510	42640	29310	32800	59370	29110	54740	62910	32730	61730	28770
B	1562	2819	1387	2924	2555	1512	2998	2504	1500	2842	1491	3046	2629	1541	2952	1391
C	897	1796	870	1537	1562	834	1542	791	836	1642	871	1745	1493	806	1557	786
D	2946	6728	2818	5496	7346	3410	6648	2916	2844	6462	2776	7139	6121	3548	5976	3152
LAB IV																
A	30600	54800	27300	54000	55200	28700	52300	26500	29000	58700	27800	51900	56700	31200	65000	26000
B	1620	3210	1500	2840	2990	1750	3290	1740	1640	3140	1540	2970	3180	1690	2930	1470
C	879	1640	914	1410	1560	846	1620	810	967	1530	821	1620	1510	805	1570	855
D	2820	5320	2860	5280	5720	2810	5030	2450	2840	5730	2670	4850	5860	2740	5110	2500

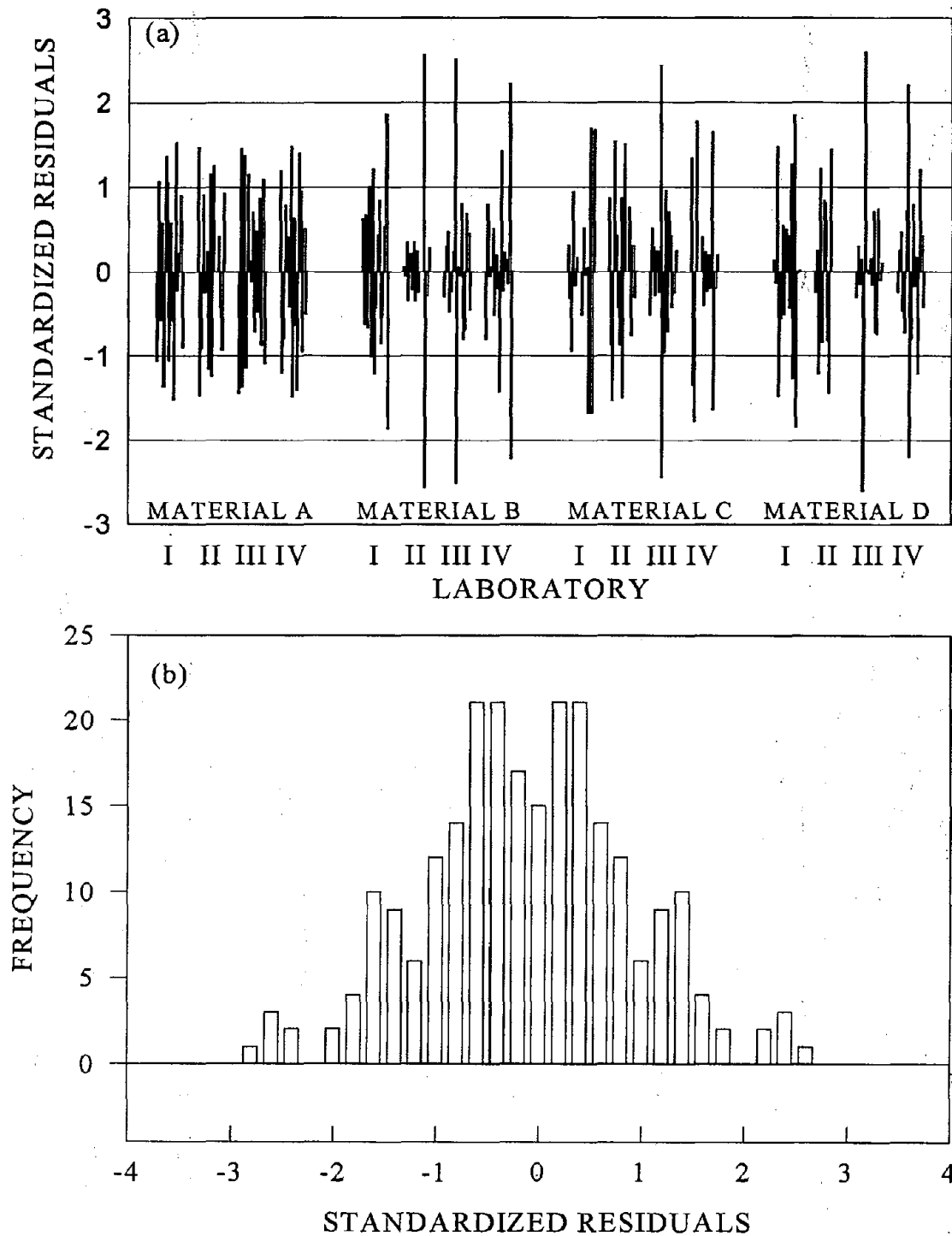


Figure 7. Standardized residuals in G^* measurements with 8-mm parallel plates: (a) grouped by material and laboratory, and (b) distribution of all standardized residuals.

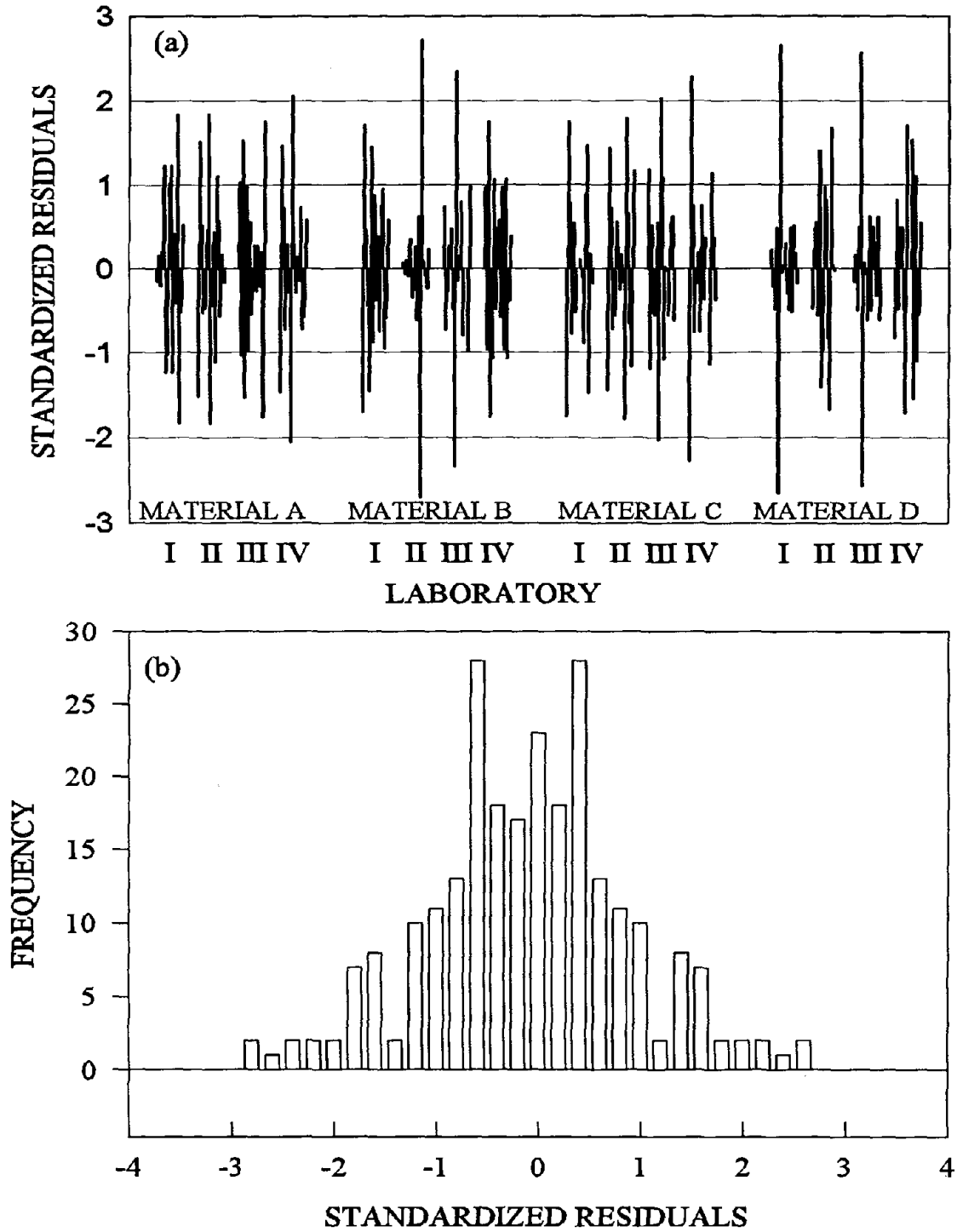


Figure 8. Standardized residuals in phase angle measurements with 8-mm parallel plates: (a) grouped by material and laboratory, and (b) distribution of all standardized residuals.

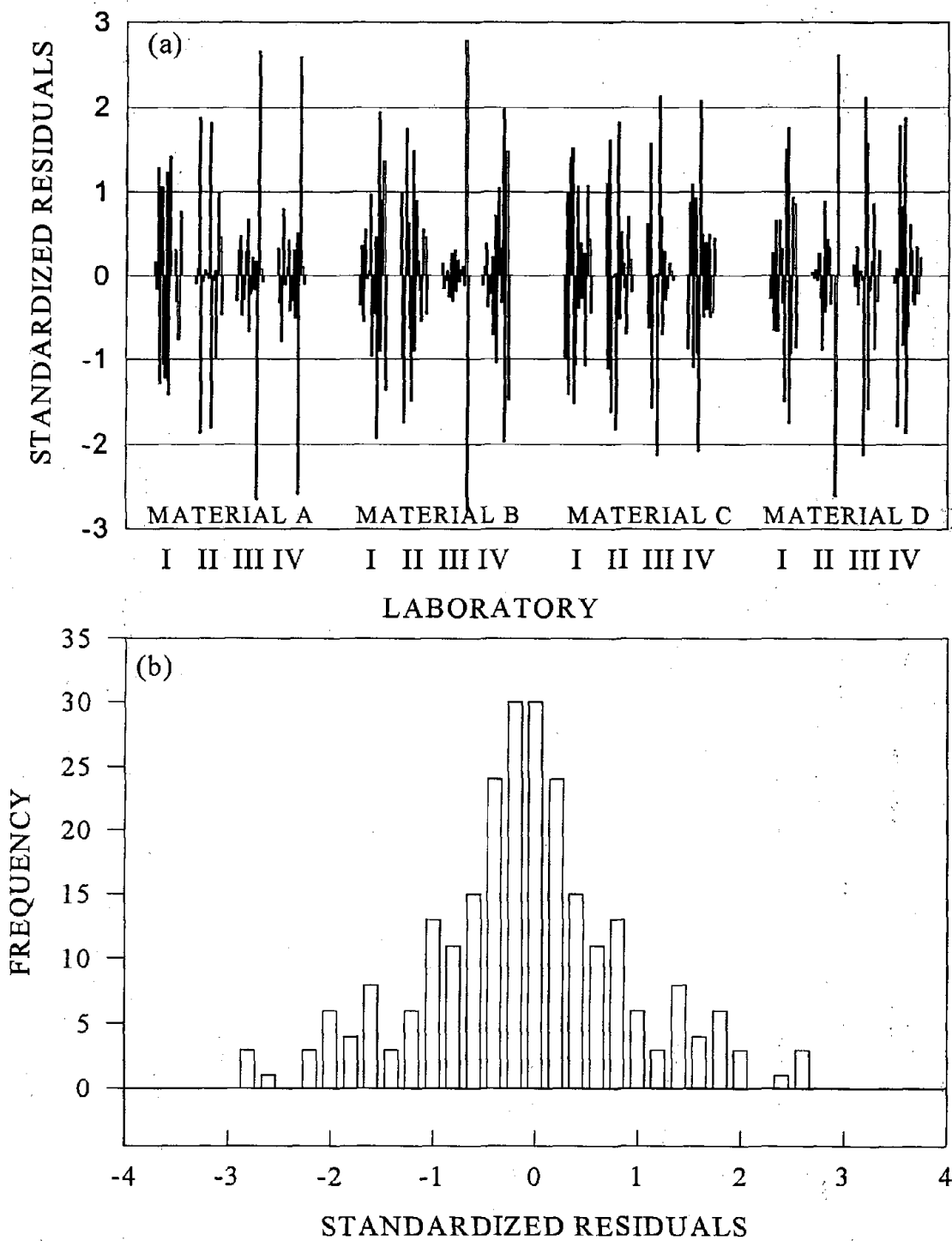


Figure 9. Standardized residuals in G^* measurements with 25-mm parallel plates: (a) grouped by material and laboratory, and (b) distribution of all standardized residuals.

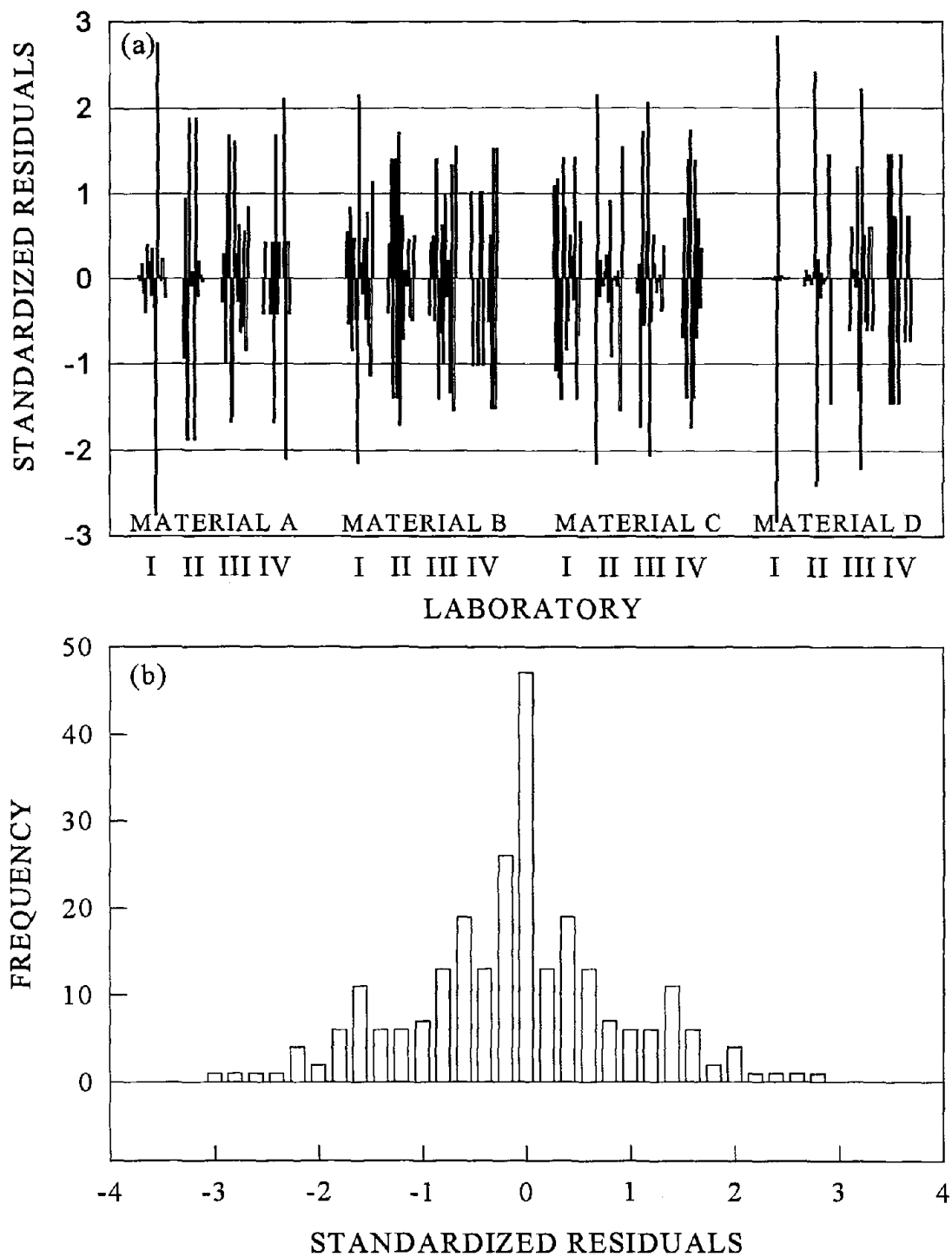


Figure 10. Standardized residuals in phase angle measurements with 25-mm parallel plates: (a) grouped by laboratory and materials, and (b) distribution of all standardized residuals.

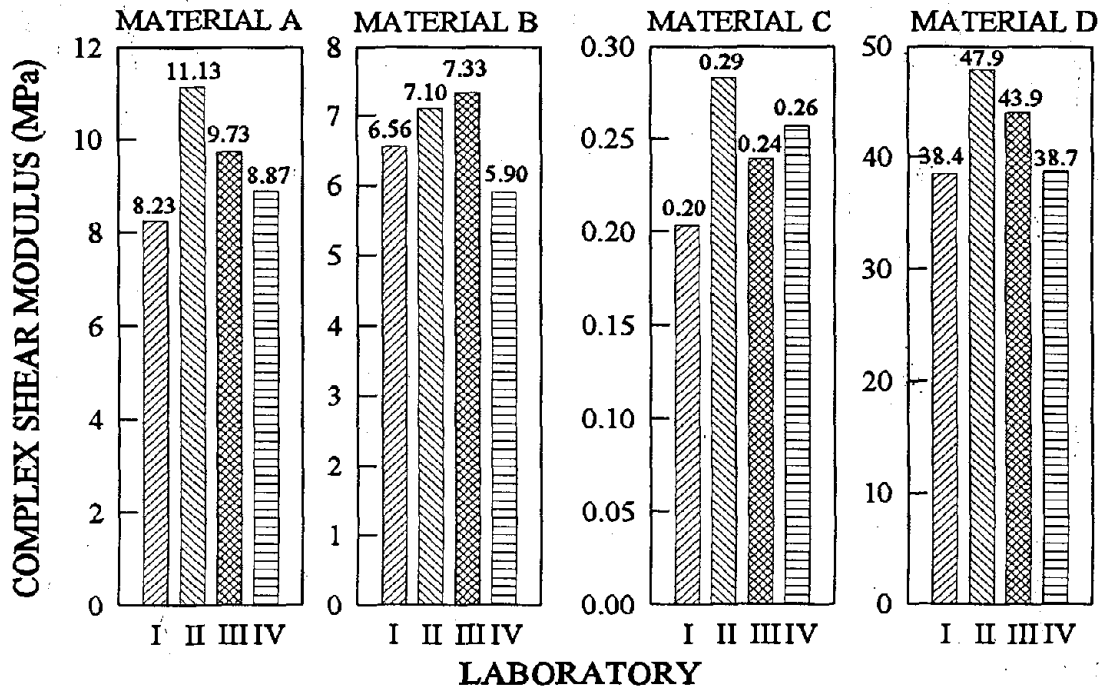


Figure 11. Complex shear modulus measurements with 8-mm parallel plates averaged by material and laboratory

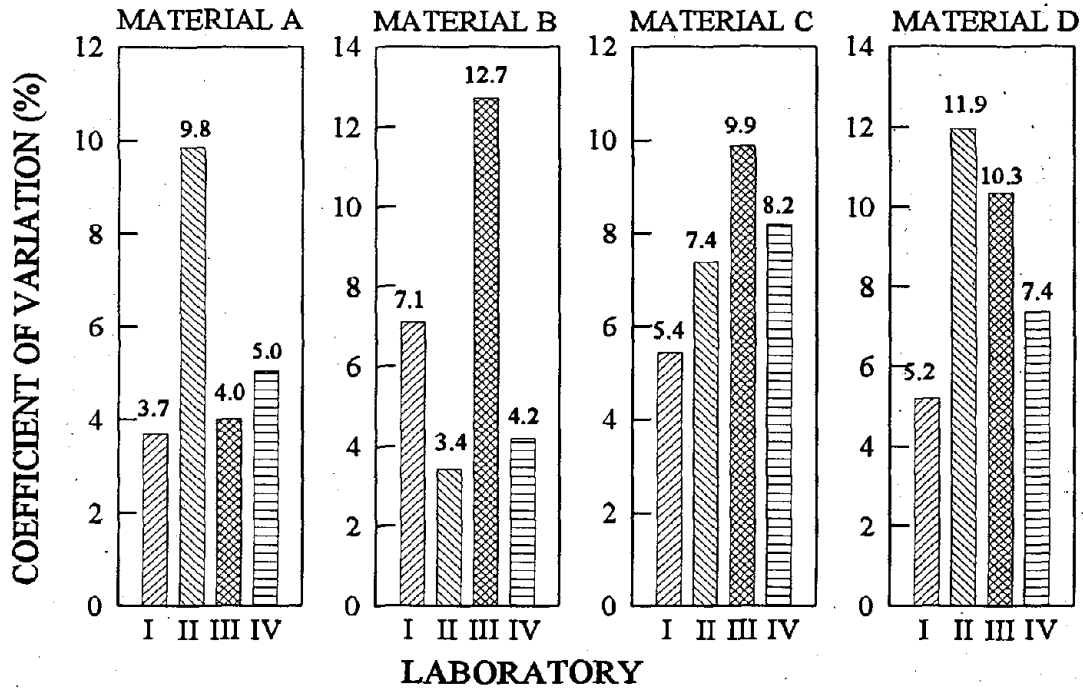


Figure 12. Coefficient of variation in G^* measurements with 8-mm parallel plates averaged by material and laboratory.

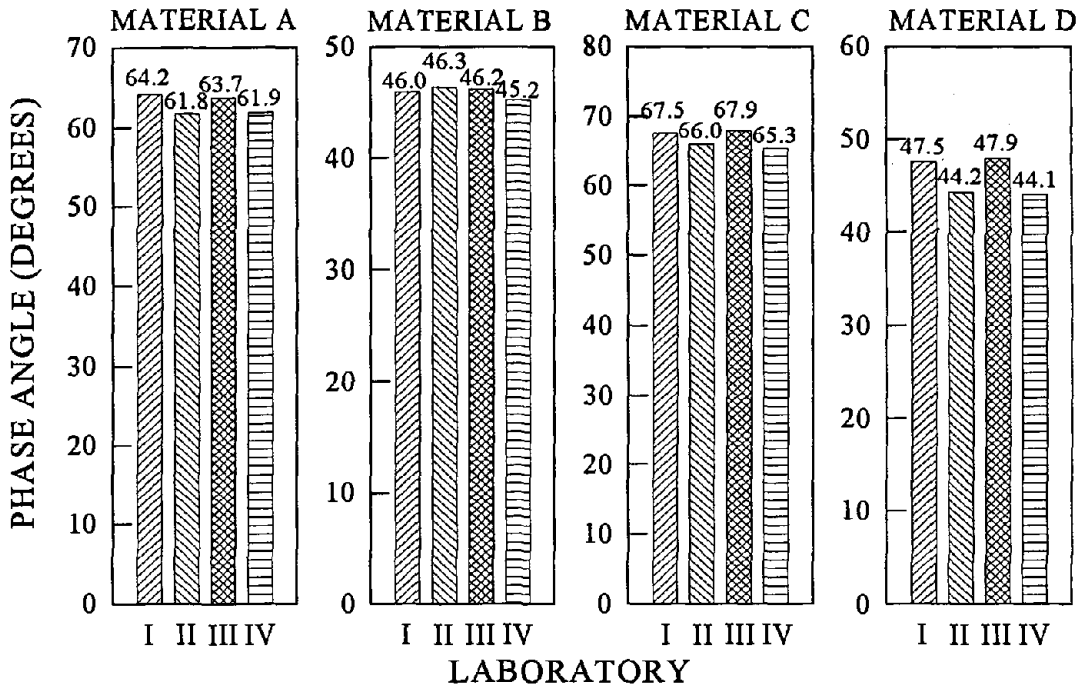


Figure 13. Phase angle measurements with 8-mm parallel plates averaged by material and laboratory.

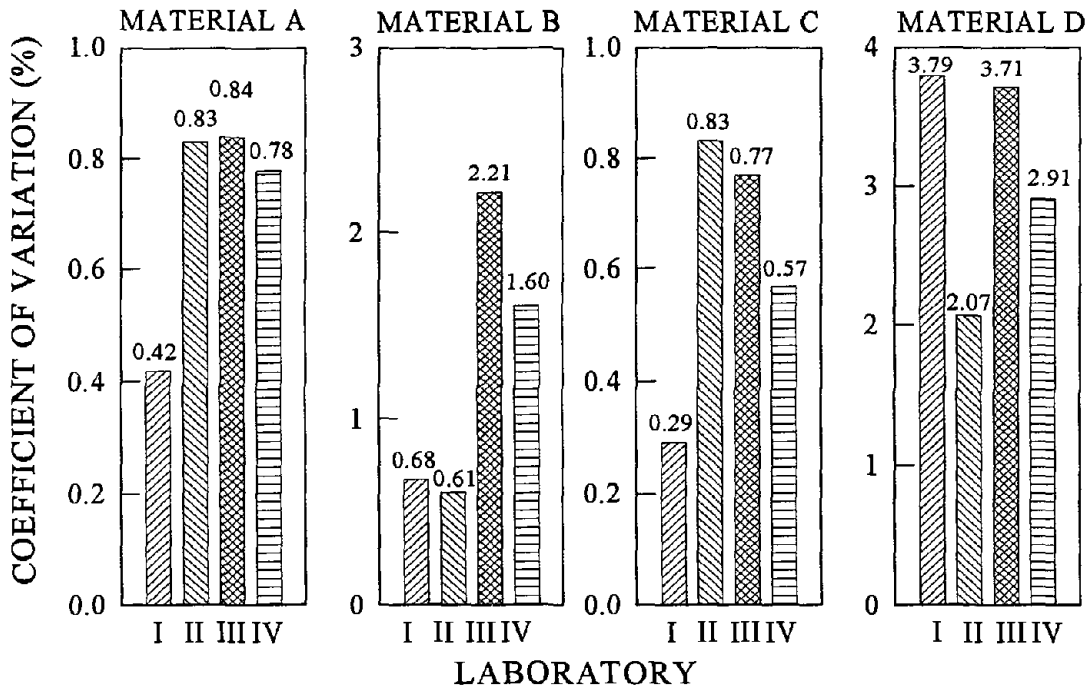


Figure 14. Coefficient of variation in phase angle measurements with 8-mm parallel plates averaged by material and laboratory.

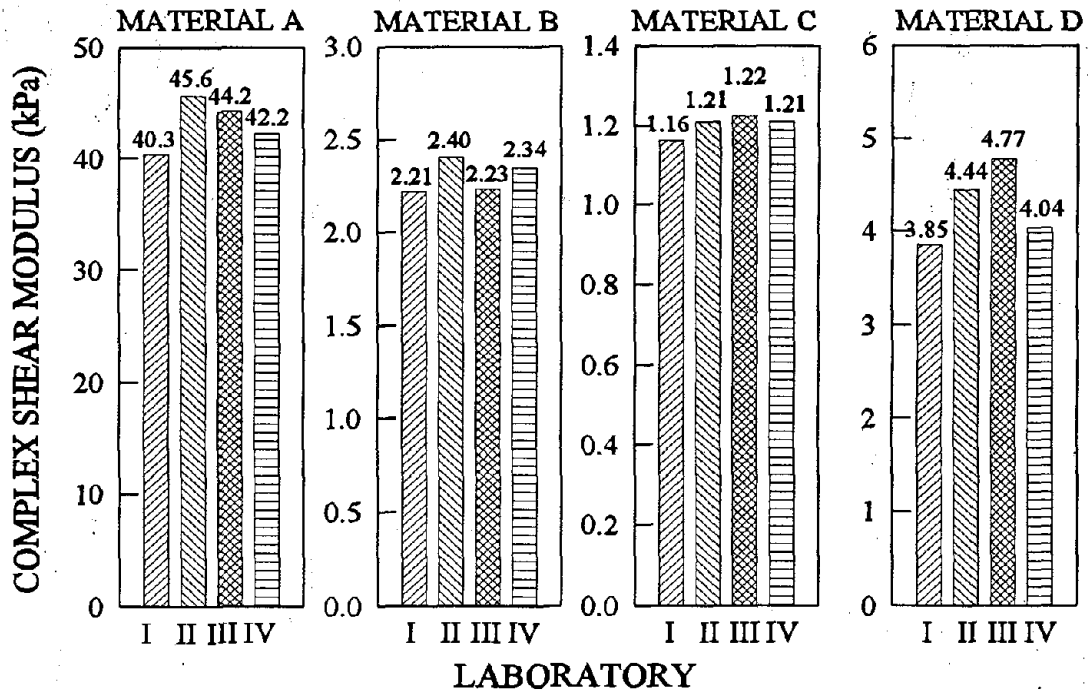


Figure 15. Complex shear modulus measurements with 25-mm parallel plates averaged by material and laboratory.

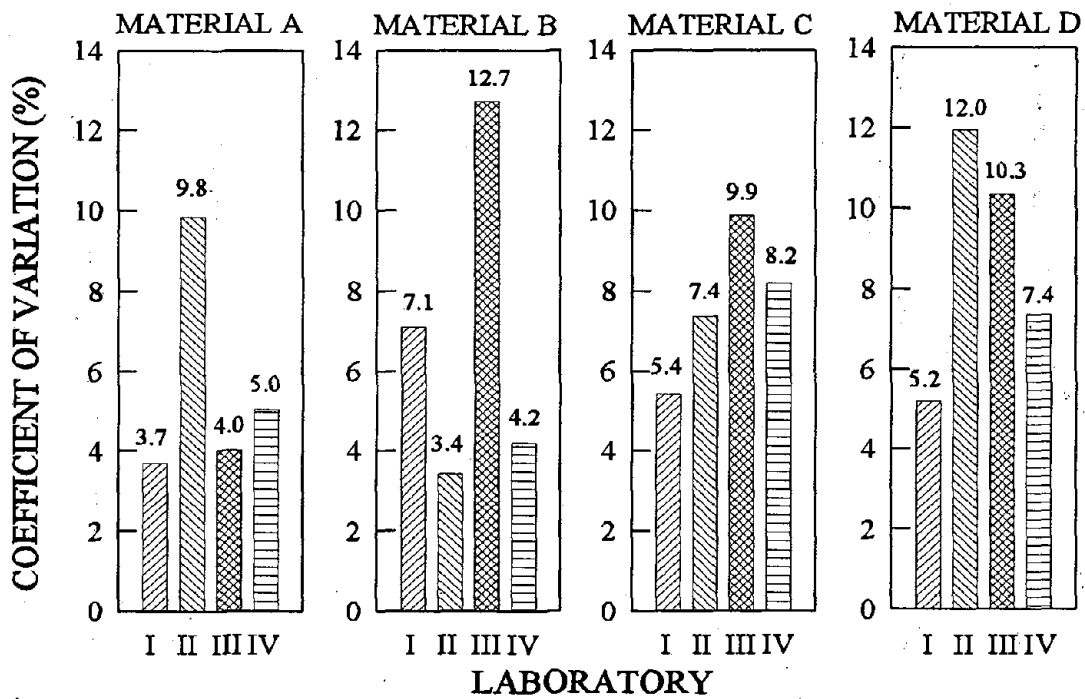


Figure 16. Coefficient of variation in G^* measurements with 25-mm parallel plates averaged by material and laboratory.

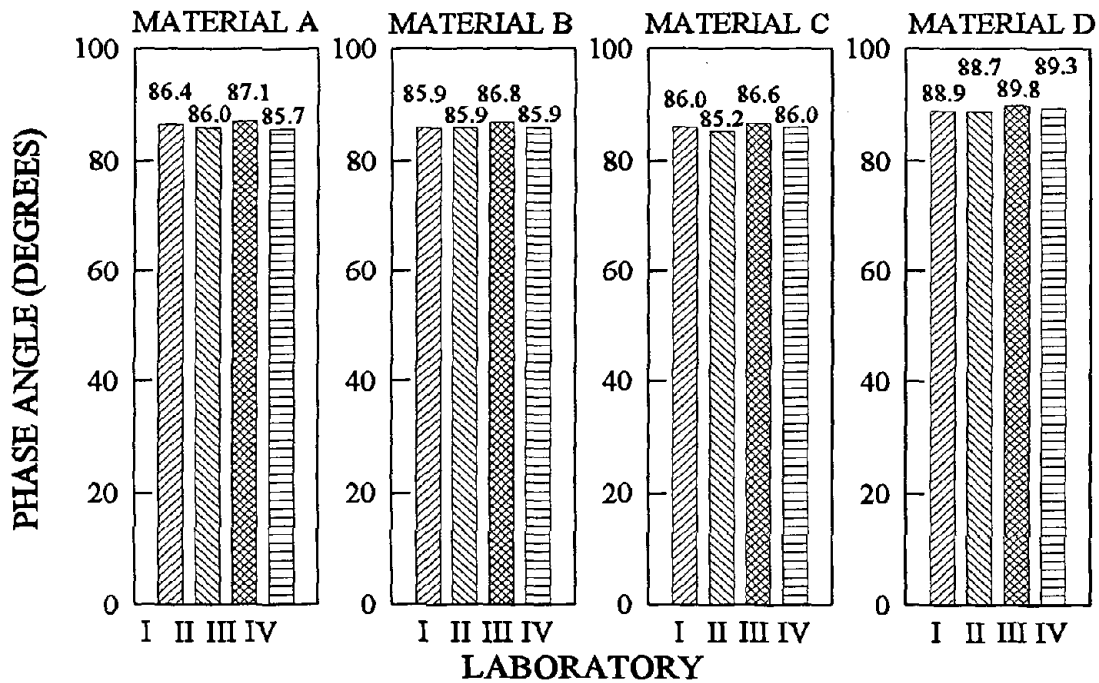


Figure 17. Phase angle measurements with 25-mm parallel plates averaged by material and laboratory.

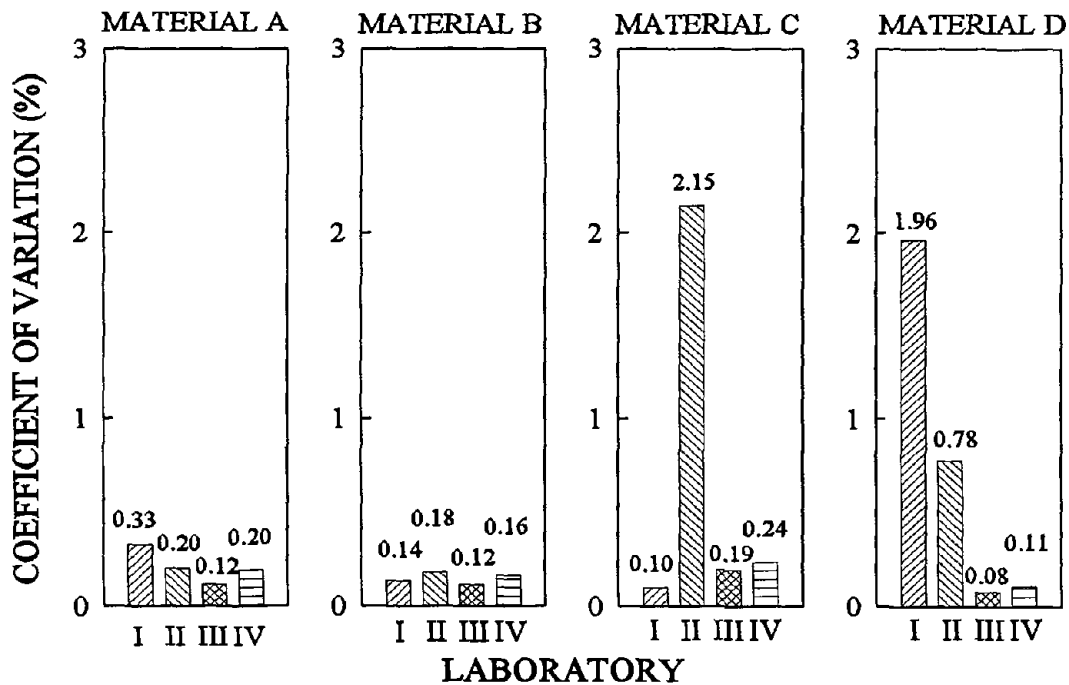


Figure 18. Coefficient of variation in phase angle measurements with 25-mm parallel plates averaged by material and laboratory.

Table 19. Phase angles (in degrees) measured with 25-mm parallel plates.

	FIRST REPLICATION								SECOND REPLICATION							
	1	2	3	4	5	6	7	8	1	2	3	4	5	6	7	8
LAB I																
A	86.6	86.3	86.6	86.5	86.4	85.6	86.4	86.7	86.6	86.2	86.8	86.5	86.2	86.7	86.4	86.6
B	86.0	85.7	86.1	85.9	85.9	86.1	85.8	86.1	85.9	85.6	86.0	70.7	85.9	86.0	85.7	86.3
C	86.1	85.8	86.1	86.0	85.9	86.1	86.0	86.2	86.0	85.6	86.2	85.9	85.9	86.1	85.8	86.3
D	89.4	89.3	89.4	89.3	82.3	89.3	89.3	89.4	89.4	89.3	89.4	89.3	89.2	89.4	89.3	89.4
LAB II																
A	86.6	85.1	86.4	85.3	85.1	86.7	85.3	86.7	86.6	85.4	86.8	85.3	85.5	86.7	85.3	86.7
B	86.2	85.4	86.6	85.9	85.6	86.2	85.4	86.4	86.3	85.1	86.3	85.5	85.4	86.2	85.3	86.5
C	81.2	85.0	86.2	86.2	85.8	86.1	85.1	82.7	86.8	85.5	86.4	85.5	83.4	86.1	85.4	86.7
D	89.0	89.0	89.4	88.8	88.9	89.4	89.1	88.2	89.1	89.1	89.5	86.4	88.7	89.3	89.1	86.8
LAB III																
A	87.2	86.7	87.6	86.8	86.8	87.3	86.8	87.3	87.2	86.8	87.4	87.0	86.7	87.2	86.8	87.4
B	87.0	86.7	87.1	86.3	86.7	87.0	86.3	87.0	87.0	86.6	86.9	86.4	86.9	87.0	86.5	87.2
C	86.9	85.9	86.7	86.6	86.4	86.9	86.3	87.1	86.9	86.3	86.8	86.1	86.5	86.9	86.4	87.1
D	89.9	89.8	89.9	90.0	89.7	89.8	89.8	89.9	89.9	89.9	89.9	89.9	89.9	89.7	89.9	89.8
LAB IV																
A	86.5	84.8	86.4	84.9	84.7	86.4	85.1	86.6	86.6	84.8	86.5	85.3	84.8	86.4	84.6	86.5
B	86.5	85.3	86.5	85.6	85.5	86.3	85.1	86.3	86.3	85.3	86.7	85.4	85.5	86.4	85.4	86.6
C	86.4	85.4	86.1	85.9	85.4	86.4	85.4	86.6	86.4	85.6	86.5	85.4	85.8	86.6	85.5	86.6
D	89.6	89.1	89.5	89.1	89.1	89.5	89.2	89.6	89.4	88.9	89.4	89.3	89.1	89.6	89.1	89.6

Ruggedness Testing Analysis

Tables 21, 22, 24, and 25 show the F-values and effects for G^* and δ for each material and each laboratory measured with both 8-mm and 25-mm parallel plates. Also, the effects are averaged by material (Tables 23 and 26) and a grand average of all the materials and laboratories are given for each effect. These tables will be referred to in the following discussions.

8-mm Parallel Plates

Tables 21 and 22 give the F-values and percent effects for the G^* and δ measurements, respectively. As in the case of BBR analysis, the effects are presented as a percentage of the mean so that they can be compared with one another.

Oven Temperature

This is the temperature the asphalt samples were heated to before they were poured onto the plates or the mold. For G^* measurement with 8-mm parallel plates, 2 of the 16 material-laboratories had F-values over 5.59. Table 21 shows the percent effects to have both negative and positive values yielding an average effect much less than 1 percent, indicating that there were no consistent effects due to this factor.

In the case of δ measurement, although four material-laboratories showed F-values greater than 5.59, the effects were extremely small and had inconsistent direction. Therefore, the limits chosen for the given temperature were acceptable.

Test Temperature

Four material-laboratories showed F-values greater than 5.59 for the G^* measurement. The effects were all negative, indicating that G^* decreased with an increase in temperature. An increase in temperature by 0.2°C decreased G^* by 2.84 percent, implying that the temperature had to be controlled to $\pm 0.07^\circ\text{C}$ in order to limit this change to 1 percent. In the case of the δ measurement, even though there were nine material-laboratories showing F-values greater than 5.59, the effects were very small, indicating that this factor had little effect on the δ measurement. Most of the percent effects were positive, indicating that δ increases with an increase in temperature. G^* was more sensitive to temperature compared to δ and this dictates the control necessary to obtain acceptable repeatability.

Equilibration Time

For the equilibration time at the test temperature, three material-laboratories showed significant F-values in the G^* measurement and three material-laboratories showed significant F-values in δ measurement. The percent effects, however, were in random directions and had an average effect of less than 1 percent in both cases. This indicated that the equilibration time within the limits chosen had little effect on the G^* and δ measurements.

Table 20. Average G^* and δ measured with 8-mm parallel plates.

	G^* (Pa)			δ (°)		
	MEAN	STD DEV	CV	MEAN	STD DEV	CV
LAB I						
A	8229775	311954	3.8	64.2	0.3	0.4
B	6556644	374775	5.7	46.0	0.3	0.6
C	202961	8762	4.3	67.5	0.2	0.3
D	38451188	183728	4.8	47.5	1.7	3.7
			4.7			1.3
LAB II						
A	3671733	362564	9.9	62.0	0.6	0.9
B	2319200	281781	12.2	46.7	0.9	1.9
C	93315	7255	7.8	66.2	0.7	1.0
D	15787692	170880	10.8	44.4	1.1	2.4
			10.1			1.6
LAB III						
A	9727625	416401	4.3	63.7	0.6	0.9
B	7333188	895545	12.2	46.2	1.1	2.3
C	238850	25022	10.5	67.9	0.6	0.8
D	43917500	449971	10.3	47.9	1.9	3.9
			9.3			2.0
LAB IV						
A	8865825	442944	5.0	61.9	0.5	0.8
B	5897500	264359	4.5	45.2	0.7	1.6
C	256813	21871	8.5	65.3	0.4	0.5
D	38662500	304554	7.9	44.1	1.4	3.1
			6.5			1.5

Table 21. F-values and percent effects for G* measurements with 8-mm parallel plates.

	LAB I				LAB II				LAB III				LAB IV			
	A	B	C	D	A	B	C	D	A	B	C	D	A	B	C	D
F-VALUES																
Preheat	0.72	0.26	5.89	1.15	1.76	14.6	1.99	0.29	1.17	0.06	1.79	3.3	4.74	2.54	0.19	0.12
Test temp	10.6	3.02	5.16	2.33	1.98	14.8	0.78	1.71	12.6	0.01	1.6	0	12.1	3.29	3.94	2.44
Eq. time	2.16	0.2	0.85	0	0.05	10.9	0.89	0.09	1.17	2.77	6.31	2.09	0.61	10.5	0.37	1.22
Sampling	0.22	1.4	21.3	0.01	1.15	7.95	33.7	0.06	0.3	4.71	6.62	0	3.56	4.65	4.13	0.97
Freq	27.3	14.1	15.5	17.9	54.4	325	162	20.7	493	34.6	132	36.5	322	211	119	56.4
Strain	0.34	2.76	0.48	0.69	0.17	14.8	6.38	0.07	4.24	0.16	2.04	0.09	1.45	0.44	0.02	0.19
Overhang	0.33	0.67	0.6	1.93	11.2	11.8	16.1	2	4.7	3.54	0.11	0.23	5.71	1.46	0.04	5.05
PERCENT EFFECTS																
Preheat	-0.8	0.9	3.5	1.4	-3.5	3.7	2.8	-1.9	-1.1	-0.7	-3.3	-4.7	2.7	1.7	-0.9	-0.6
Test temp	-3.0	-3.1	-3.3	-2.0	-3.7	-3.7	-1.7	-4.6	-3.6	-0.4	-3.1	-0.2	-4.4	-1.9	-4.1	-2.9
Eq. time	-1.4	0.8	1.3	-0.0	0.6	3.2	1.8	-1.1	1.1	-5.3	-6.2	3.7	1.0	3.4	1.2	-0.2
Sampling	0.4	-2.1	6.6	-0.1	2.8	2.7	11.4	0.9	-0.6	-6.9	6.3	-0.2	-2.4	2.3	4.2	1.8
Freq	16.1	0.0	18.9	18.4	19.3	17.2	24.9	16.0	22.3	18.7	28.3	15.6	22.6	15.3	22.3	13.8
Strain	0.5	-2.9	1.0	1.1	1.1	-3.7	-4.9	-0.9	-2.1	1.3	-3.5	-0.8	1.5	-0.7	0.3	0.8
Overhang	0.5	1.4	1.1	1.8	8.7	3.3	7.8	4.9	2.2	6.0	0.8	1.3	-3.0	-1.3	0.4	-4.1

The shaded area indicates F-values that are not significant at 95 percent confidence level.

Sampling Technique

The data for the sampling technique are not as straightforward as for the other factors. Two methods were used—in one, asphalt was poured directly into the plates, and in the other, asphalt was cast into a pellet in a silicone rubber mold and then transferred to the plates. Four material-laboratories showed significant F-values for the G* measurements and four showed significant F-values for the δ measurements. The average percent effects for G* measurements (Table 26) were significant for materials B and C, but showed opposite signs. Careful examination of Table 21 indicates that the percent effects were not consistent in direction except for material DSR-C, which showed strong positive effects. In the same manner, Table 22 indicates that material DSR-C had a consistently positive effect for δ measurements. Even though the effect is not seen for all materials, all the laboratories consistently showed an effect for the material DSR-C, indicating that this factor could be important for some materials.

In the pellet technique, the asphalt underwent additional thermal treatment as compared to the direct pour. This is because, in the pellet technique, the asphalt was frozen at less than 0°C and heated to 40°C before it was set to the test temperature. The effect of thermal history is dependent on the asphalt as evident from the greater effect of this factor on AAM-1 and thin film aged AAM-1 (DSR-B and DSR-C, respectively) as compared to AAG and thin film oven-aged AAG (DSR-D and DSR-A, respectively). Furthermore, the fact that the signs are not consistent between laboratories indicates that the thermal history of the asphalt was not consistent between laboratories. This was probably because efforts to rigorously control the thermal history were not made. As will be seen later, the effects are not so strong for DSR measurements with 25-mm parallel plates. This is due to the reduction in thermal history effect at higher temperatures due to

Table 22. F-values and percent effects for δ measurements with 8-mm parallel plates.

	LAB I				LAB II				LAB III				LAB IV			
	A	B	C	D	A	B	C	D	A	B	C	D	A	B	C	D
F-VALUES																
Preheat	4.44	1.46	5.82	0.20	0.63	30.49	7.03	1.42	0.78	0.65	1.00	0.27	10.70	0.06	1.02	0.15
Test temp	9.34	8.20	0.69	0.01	15.93	43.70	10.90	8.69	9.70	0.00	2.60	0.14	15.16	2.19	6.19	0.49
Eq. time	1.48	0.07	0.20	-0.65	3.44	0.00	0.50	16.69	1.61	5.69	7.95	0.66	0.00	0.27	0.37	1.19
Sampling	0.16	3.36	141	1.33	6.18	0.14	46.82	1.28	0.85	4.71	14.63	0.63	5.46	0.52	66.25	0.22
Freq	37.5	21.6	3.83	0.26	283	229	67	74.5	204	10.3	32.3	16.4	412	34.7	80	67
Strain	3.15	3.02	4.12	0.28	4.49	12.00	0.08	0.00	2.40	0.03	2.48	0.14	0.13	0.01	1.31	0.00
Overhang	5.26	4.93	1.37	2.71	2.77	11.46	0.51	1.09	0.01	2.62	0.08	0.44	3.69	1.29	0.11	2.19
PERCENT EFFECTS																
Preheat	0.2	-0.2	-0.2	0.4	0.0	-0.6	-0.4	-0.1	0.2	-0.4	-0.2	0.5	0.6	0.1	0.1	-0.3
Test temp	0.3	0.5	0.1	-0.1	0.6	0.7	0.5	1.4	0.7	-0.0	0.3	0.3	0.8	0.6	0.4	0.5
Eq. time	-0.1	-0.5	-0.0	-0.8	0.1	-0.3	-0.1	1.1	-0.3	1.3	0.5	-0.8	-0.0	-0.2	0.1	0.8
Sampling	-0.0	0.3	-0.9	1.1	0.2	-0.3	-1.6	0.1	0.2	1.2	-0.7	0.7	0.5	-0.3	-1.2	-0.3
Freq	-2.1	-2.6	-0.5	1.6	-3.7	-2.5	-1.8	-6.1	-3.0	-1.8	-1.1	-3.8	-4.0	-2.4	-1.3	-6.0
Strain	-0.2	0.3	-0.1	0.5	-0.4	-0.6	-0.0	-0.2	0.3	-0.1	0.3	0.4	-0.1	0.0	-0.2	0.0
Overhang	0.2	0.4	0.1	1.6	-0.4	0.5	-0.2	0.6	0.0	-0.9	0.1	0.6	0.4	0.5	-0.0	1.1

The shaded area indicates F-values that are not significant at 95 percent confidence level.

relaxation in the asphalt. More detailed study is necessary to completely understand the effect of the sampling technique.

However, it is recommended that when using the pellet technique, the asphalt need not be cooled to below 0°C, but should be left to cool to room temperature and directly transferred from the silicone rubber mold to the plate (without any additional handling).

Frequency of Measurement

The frequency had the largest effect on the measurement of both G^* and δ . For G^* , the effect of changing the frequency by ± 0.5 Hz had an 18.1 percent increase in the average G^* . If this change should be brought to 1 percent, then the frequency had to be controlled to ± 0.025 Hz. In the case of δ , the effect was in the opposite direction as expected, and the magnitude of the effect was much smaller, indicating that obtaining acceptable repeatability in the G^* measurement will ensure repeatable measurement in δ .

Table 23. Average percent effects for G^* and δ measurements with 8-mm parallel plates.

Factor	A	B	C	D	Average
COMPLEX MODULUS					
Preheat	-0.6	1.4	0.5	-1.5	-0.1
Test temp	-3.7	-2.3	-3.0	-2.4	-2.8
Eq. time	0.3	0.5	-0.4	0.6	0.3
Sampling	0.1	-1.0	7.1	0.6	1.7
Freq	20.1	12.8	23.6	15.9	18.1
Strain	0.3	-1.5	-1.8	0.0	-0.7
Overhang	2.1	2.4	2.5	1.0	2.0
PHASE ANGLE					
Preheat	0.3	-0.3	-0.2	0.1	-0.0
Test temp	0.6	0.4	0.3	0.5	0.5
Eq. time	-0.1	0.1	0.1	0.1	0.1
Sampling	0.2	0.2	-1.1	0.4	-0.1
Freq	-3.2	-2.3	-1.2	-3.5	-2.6
Strain	-0.1	-0.1	-0.0	0.2	-0.0
Overhang	0.1	0.1	-0.0	1.0	0.3

Strain

In the case of both G^* and δ , the selected limits on strain had little effect on repeatability. This is significant because the strains used were rather large (20 percent and 40 percent of the linear region). These results verify the fact that for unmodified asphalts, strains as high as 40 percent of the linear limit will not cause unacceptable error in the test results.

Overhang

Four material-laboratories showed significant F-values for G^* measurements and one material-laboratory did so for δ measurements. The effect was positive for G^* measurements in Labs I, II, and III, while Lab IV showed negative effects. When averaged by laboratory, 10 percent overhang caused 1.2, 5.5, 2.4, and -2.0 percent higher G^* measurements for Labs I, II, III, and IV, respectively.

Overhang is excess material that protrudes from the edges of the plates and is deliberately introduced to compensate for several effects. The formula for the calculation of G^* assumes that the sample between the plates is an infinite sheet, which is valid if the diameter is much greater than the thickness (the diameter-to-gap ratio is only 4, while the formula assumes that the diameter is much greater than the gap). The overhang further compensates for any deficiencies in the trimming technique. Also, any contraction of asphalt due to temperature changes is compensated by the overhang. Calculations have shown⁽⁵⁾ that in certain situations, the asphalt could contract and form a concave surface (a negative overhang). Further work is required to understand the effect of overhang. In conclusion, the limits of frequency that were used in these experiments had the greatest effect. By a linear interpolation, one can show that the frequency

Table 24. F-values and percent effects for δ measurements with 25-mm parallel plates.

	LAB I				LAB II				LAB III				LAB IV			
	A	B	C	D	A	B	C	D	A	B	C	D	A	B	C	D
F-VALUES																
Preheat	1.02	0.71	2.35	1.02	0.59	0.10	0.03	0.14	1.09	1.67	5.61	6.77	1.09	0.81	0.55	1.67
Test temp	2.83	4.29	5.56	1.03	0.01	5.43	0.36	3.57	6.93	6.19	0.08	4.13	1.80	0.81	0.00	1.67
Eq. time	0.53	2.58	0.00	0.97	0.50	0.01	0.25	4.56	0.25	0.12	0.02	0.00	0.56	0.29	1.52	0.60
Sampling	0.17	4.46	0.89	1.09	0.05	2.97	0.96	0.13	1.93	0.04	0.02	0.00	0.02	3.90	0.06	0.07
Freq	1.0	13.5	41.3	1.2	246.6	121.9	0.0	0.4	111.9	88.4	49.2	1.6	369.8	233.1	78.6	72.6
Strain	0.75	4.46	3.78	1.03	0.13	2.65	1.01	3.50	0.20	0.42	3.58	1.56	1.80	1.58	1.35	1.67
Overhang	0.38	0.00	0.28	1.04	0.03	0.15	0.01	0.06	0.48	17.05	0.01	0.37	1.09	1.58	0.00	1.67
PERCENT EFFECTS																
Preheat	-0.1	0.0	0.0	-0.5	0.0	-0.0	-0.1	-0.1	-0.0	0.0	0.1	-0.1	-0.1	-0.0	0.0	0.0
Test temp	0.1	0.1	0.1	0.5	0.0	0.1	0.3	-0.4	0.1	-0.1	0.0	0.0	0.1	0.0	0.0	0.0
Eq. time	0.1	-0.1	0.0	-0.5	-0.0	0.0	-0.3	0.4	-0.0	0.0	-0.0	-0.0	-0.0	0.0	-0.1	-0.0
Sampling	0.0	-0.1	-0.0	-0.5	-0.0	-0.1	-0.5	-0.1	-0.0	-0.0	0.0	0.0	0.0	-0.1	-0.0	-0.0
Freq	-0.3	-0.4	-0.5	-1.8	-0.8	-0.5	-0.0	-0.1	-0.3	-0.3	-0.3	0.0	728.5	-0.6	-0.5	-0.2
Strain	0.1	0.1	0.0	-0.5	0.0	0.1	-0.5	-0.6	-0.0	0.0	0.1	0.0	0.1	0.1	0.1	0.0
Overhang	-0.1	-0.0	-0.0	0.5	-0.0	-0.0	0.0	0.0	-0.0	-0.1	0.0	0.0	0.1	-0.1	0.0	0.0

The shaded area indicates F-values that are not significant at 95 percent confidence level.

Table 25. F-values and percent effects for G* measurements with 25-mm parallel plates.

	LAB I				LAB II				LAB III				LAB IV			
	A	B	C	D	A	B	C	D	A	B	C	D	A	B	C	D
F-VALUES																
Preheat	1.56	0.27	4.24	0.00	0.01	0.12	0.54	0.00	0.03	0.20	8.90	0.76	0.29	1.26	0.52	0.05
Test temp	28.4	7.13	7.92	2.53	0.24	2.90	0.92	0.04	4.10	2.35	0.36	1.28	1.03	3.32	0.17	22.5
Eq. time	0.03	4.14	0.07	2.40	0.80	0.08	0.26	4.79	0.27	1.77	1.23	0.39	0.76	0.05	1.30	3.58
Sampling	0.10	5.14	0.06	2.92	0.35	3.36	0.15	1.91	0.29	1.72	0.21	0.20	0.53	1.26	1.82	2.32
Freq	127	77.2	152	126	218	606	70	145	121	76.4	500	157	255	506	381	1064
Strain	0.19	0.82	0.03	1.97	0.30	0.22	0.08	1.02	0.42	0.25	0.97	0.03	1.31	1.35	0.22	0.01
Overhang	0.17	0.74	1.39	0.01	4.05	0.27	0.23	0.22	0.50	0.14	0.04	0.02	0.49	0.01	0.07	6.28
PERCENT EFFECTS																
Preheat	0.5	-0.6	-1.7	0.0	0.2	0.5	2.6	-0.1	-0.7	1.4	-4.2	2.5	1.1	1.5	-1.1	-0.2
Test temp	-3.5	-2.8	-2.4	-1.5	1.1	-2.2	-3.4	0.5	-5.8	4.9	-0.8	-3.3	-2.1	-2.5	-0.6	-4.8
Eq. time	1.0	2.2	-0.2	-1.5	2.0	0.4	1.8	-5.7	-1.5	-4.2	-1.6	-1.8	1.8	-0.3	1.7	1.9
Sampling	1.1	2.4	0.2	-1.6	1.3	2.3	1.4	3.6	-1.6	4.2	0.7	-1.3	1.5	1.5	2.0	-1.5
Freq	31.0	31.0	34.4	35.6	32.8	31.4	30.1	31.1	31.6	27.7	31.6	36.0	32.8	30.9	28.7	32.8
Strain	0.3	-1.0	0.1	1.3	-1.2	-0.6	-1.0	2.6	1.9	1.6	-1.4	-0.5	-2.4	-1.6	-0.7	0.1
Overhang	0.3	0.9	1.0	0.1	4.5	0.7	-1.7	-1.2	-2.0	1.2	-0.3	-0.4	1.4	-0.1	0.4	-2.5

The shaded area indicates F-values that are not significant at 95 percent confidence level.

needs to be controlled to 0.025 Hz for repeatable measurements. The temperature of measurement had a large effect and should therefore be controlled to $\pm 0.1^\circ\text{C}$. The overhang had a definite effect even though it is unclear how one would eliminate this. The sampling technique had a definite effect, possibly due to the unnatural thermal history to which the pellets were subjected.

25-mm Parallel Plate

Oven Temperature

One material-laboratory had F-values higher than 5.59 for G* measurements, while two had significant F-values for δ measurements. Oven temperature has inconsistent effects (Tables 24 and 25) on G* measurements and negligible effects on δ measurements. The average effect is well within 1 percent for both G* and δ measurements. This indicates that the oven temperature does not have any significant effects on the G* and δ measurements.

Test Temperature

Four material-laboratories showed significant F-values for G* measurements, while two showed

Table 26. Average percent effects for G* and δ measurements with 25-mm parallel plates.

	A	B	C	D	Average
COMPLEX MODULUS					
Preheat	0.3	0.7	-1.1	0.5	0.1
Test temp	-2.6	-0.7	-1.8	-2.3	-1.8
Eq. time	0.8	-0.5	0.4	-1.8	-0.3
Sampling	0.6	2.6	1.1	-0.2	1.0
Freq	32.1	30.3	31.2	33.9	31.8
Strain	-0.3	-0.4	-0.7	0.9	-0.2
Overhang	1.1	0.7	-0.2	-1.0	0.1
PHASE ANGLE					
Preheat	-0.0	0.0	0.0	-0.1	-0.0
Test temp	0.1	0.0	0.1	0.1	0.1
Eq. time	-0.0	-0.0	-0.1	-0.0	-0.0
Sampling	-0.0	-0.1	-0.1	-0.1	-0.1
Freq	181.8	-0.5	-0.4	-0.5	45.1
Strain	0.0	0.1	-0.1	-0.3	-0.1
Overhang	-0.0	-0.0	0.0	0.1	0.0

significant F-values for δ measurements. The test temperature had a consistently negative effect on G^* measurements and an insignificant positive effect on δ measurements. The average temperature effect for G^* is 1.82 percent, indicating that the temperature has to be controlled to $\pm 0.1^\circ\text{C}$ to have less than 1 percent effect on G^* measurements.

Equilibration Time and Sampling

Table 24 showed that the F-values for all the material-laboratories for both G^* and δ measurements were below 5.59, indicating that for the equilibration times chosen, there is no significant effect. The effects are random and do not show consistent behavior, either in magnitude or in direction. This is true for sampling technique as well.

Frequency

Frequency is the factor that showed a large effect for the levels chosen. On the average, frequency had a 32 percent effect on G^* measurements. This indicates that the frequency should be controlled to ± 0.015 Hz or ± 0.1 rad/s to achieve acceptable control.

Strain and Overhang

The levels used for this factor do not cause any significant variation in the measurement of either G^* or δ .

In conclusion, the procedure appears more repeatable for 25-mm parallel plates than for 8-mm parallel plates. The sampling technique and overhang, which showed definite effects in 8-mm plates, were insignificant here. The frequency control should be better for 25-mm than for 8-mm plates, and the temperature had slightly less effect for 25-mm plates.

Precision and Bias Estimates

As a result of the analysis of the ruggedness experiments, the factors—such as oven temperature and strain—were found to have insignificant effects. Hence, in the model for analysis of variance, these factors were included in the error term. The model used for analysis of variance is, therefore,

Table 27. Between- and within-laboratory coefficient of variation for G^* and δ measurements.

	Mean from All Labs	Standard Deviation (Lab)	Between- Lab CV	Within - Lab CV
Complex Modulus (kPa) 8-mm Parallel Plate				
A	9463	2060	21.8	8.4
B	6710	1111	16.6	10.2
C	245	54	22.0	10.5
D	41948	7220	17.2	9.1
Phase Angles ($^\circ$) 8-mm Parallel Plate				
A	62.9	2.0	3.2	0.9
B	46.0	1.0	2.2	2.1
C	66.7	2.0	3.1	0.9
D	46.0	3.4	7.4	3.0
Complex Modulus (Pa) 25-mm Parallel Plate				
A	42553	5506	12.9	12.5
B	2296	149	6.5	7.8
C	1201	40	3.3	7.7
D	4274	707	16.5	9.2
Phase Angles ($^\circ$) 25-mm Parallel Plate				
A	86.3	1.1	1.2	0.3
B	86.1	0.8	0.9	0.2
C	86.0	0.9	1.1	0.9
D	89.2	0.8	0.9	1.1

$$Z = \beta_0 + \text{LAB} + \beta_1 X_1 + \beta_2 X_2 + \beta_3 X_3 + \beta_4 X_4 + \beta_5 X_5 + e$$

where β_0 is the true but unknown mean; β_1 through β_5 are the unknown coefficients for the factors test temperature, equilibration time, sampling, frequency, and overhang; LAB is the laboratory effect; and e is the random error. All the factors were assumed to be normal random variables with a mean of zero.

Table 27 lists the results from these analyses separately for the G^* and δ measurements for 8-mm and 25-mm parallel plate geometries. The within-laboratory and between-laboratory CVs for G^* measurements with 8-mm parallel plates tend to be higher than for 25-mm parallel plates. The CVs for phase angle measurements were much lower than for G^* measurements. The between-laboratory CVs for G^* measurements have a maximum CV of 22 percent.

APPENDIX 1. TESTING PROCEDURES

Ruggedness testing is a process to refine a test procedure prior to conducting an inter-laboratory study to determine the precision and bias. Needless to say, testing procedures are needed for each test before ruggedness testing can be started. At the time when the testing started (September 1992), a set of procedures developed in the Strategic Highway Research Program (SHRP) were available. These were inadequate for ruggedness testing and therefore a workable set of procedures had to be developed.

Considerable effort was directed toward developing workable procedures for these tests. An initial set of procedures was developed at FHWA and distributed to the participating laboratories and other knowledgeable organizations, such as the American Association of State Highway and Transportation Officials (AASHTO), SHRP, and Asphalt Materials Reference Library (AMRL). Their suggestions and recommendations were incorporated into the procedures. A meeting of the participating laboratories and interested organizations was held in November 1992 to refine the procedures, select the factors that were most likely to affect the repeatability and were therefore to be included in the testing, and to select the materials to be used in each test. These factors and materials agreed upon were incorporated into the procedures and the final version was written. These procedures are given in this section as Version 2.2 (Final).

RUGGEDNESS TESTING OF SHRP SPECIFICATION TESTS

VERSION 2.2 (FINAL)

Introduction

The SHRP specification for performance grading of asphalt cements requires asphalts to be tested by three new methods. These methods, along with the parameters they measure, are listed as follows:

1. Dynamic shear rheometer to measure the complex modulus and the loss angle for the asphalts for a range of temperatures at 10 rad/s frequency. The reported parameters are: (a) $G^*/\sin(\delta)$ in the temperature range 52 to 70°C on original asphalts, (b) $G^*/\sin(\delta)$ in the temperature range 52 to 70°C on TFO residues, and $G^*\sin(\delta)$ in the temperature range 7 to 34°C on TFO-PAV² residues.
2. Bending beam rheometer to measure the creep stiffness and the slope of log creep stiffness versus log time curve at 8, 15, 30, 60, 120, and 240 s loading time on original and TFO-PAV residues at a range of temperatures (-36 to 0°C).

² TFO-PAV indicates that the binder was aged in rolling thin film oven followed by pressure aging vessel.

3. Direct tension to measure the stress at failure and the strain at failure for a range of temperatures (-36 to 0°C) at 1-mm/min strain rate for TFO-PAV aged asphalts. (Failure is defined as the point of maximum stress in a brittle failure mode.)

Some of the tests described above need asphalt samples that have been aged by a pressure aging vessel (PAV) using a specific procedure. Since the proposed aging procedure using a pressure aging vessel has not been evaluated, this method also needs to be tested according to ruggedness procedure.

The ruggedness test is a screening program that detects the sources of variation in a test method. In the procedure described in ASTM C1067 (Conducting a ruggedness or screening program for test methods for construction materials), a few laboratories introduce known variations in pertinent variables related to testing techniques and environment in order to judge the magnitude of their effect on the test results. This information is used to determine the controls necessary for these variables in the test method.

The ruggedness testing will be conducted for four test procedures—dynamic shear rheometer, bending beam rheometer, direct tension tester, and pressure aging vessel. The ruggedness testing procedures for each of these tests are considered separately.

The four laboratories participating in this study are the following—Pennsylvania Transportation Institute at Pennsylvania State University, State College, PA; National Center for Asphalt Technology at Auburn University, Auburn, AL; Federal Highway Administration, Office of Engineering and Highway Operations Research and Development, Materials Division, HNR-30; and Federal Highway Administration, Office of Technology Applications, HTA-21.

The selection of seven critical variables in each test technique were made after the November 1992 meeting with the representatives from participating laboratories, followed by discussions.

Samples

The selection of samples for the ruggedness testing was also made during the meeting on November 12, 1992. Four materials each for the dynamic shear rheometry and pressure aging procedures, and three materials each for the bending beam rheometry and direct tension (DT) measurement procedures were selected. Each material was appropriately aged and distributed into separate containers for each test. The uniformity of each batch of containers was tested by measuring the complex shear modulus of a sample of eight containers selected at random. The coefficient of variation³ in the complex shear modulus at 50°C has been less than 5 percent in each of the batches.

Each participating laboratory will receive the following samples, along with these instructions—four materials in seventy-two 30-mL containers each for DSR, four materials in thirty-six 120-mL containers each for PAV, three materials in thirty-six 30-mL containers each for BBR, and three materials in thirty-six 30-mL containers each for DT. Each container has a five-digit serial number that must be recorded with each measurement.

³ Coefficient of variation= 100*standard deviation/mean

Pre-Testing Requirements

Calibration: Prior to conducting tests, each laboratory will calibrate the equipment for the tests according to the instructions in this section.

Temperature Calibration

The temperature calibration is very important for each of the tests as the properties measured are affected by small changes in temperature. Therefore, great care should be taken to calibrate the temperature-measuring instruments according to the procedures given below.

DSR: The temperature of the asphalt between the plates has to be measured accurately. For this purpose, it is necessary to calibrate the offset that exists in an instrument between the asphalt and the temperature-measuring device. For this purpose, a thermistor embedded in a silicone rubber tablet having the same dimensions as the asphalt sample will be available from the Cannon Instrument Company. The calibration of the thermistor should be checked using a constant temperature water-ice mixture and a calibrated ASTM mercury-in-glass thermometer, such as ASTM 89C. A schematic diagram of the silicone rubber probe is shown in Figure 19.

BBR: A mercury-in-glass thermometer, such as the ASTM 89C mentioned above, can be used. This thermometer should be placed so that the bulb is near the temperature probe in the BBR bath. The difference between the thermometer and the temperature probe should be measured and the offset used in reporting and setting the correct temperature.

DT: A complete immersion thermometer, such as the ASTM 62C, should be used for this purpose. The thermometer should be hung adjacent to the sample inside the controlled-environment chamber such that the temperature can be read through the glass window. Any offset between the thermometer and the measured temperature should be recorded and used in setting and reporting the correct temperature.

PAV: The temperature probe in the PAV can be removed from the lid and calibrated in an ice-water bath in a manner similar to calibrating the thermistor for DSR. Any offset between the thermometer and the measured temperature should be used in setting and reporting the correct temperature.

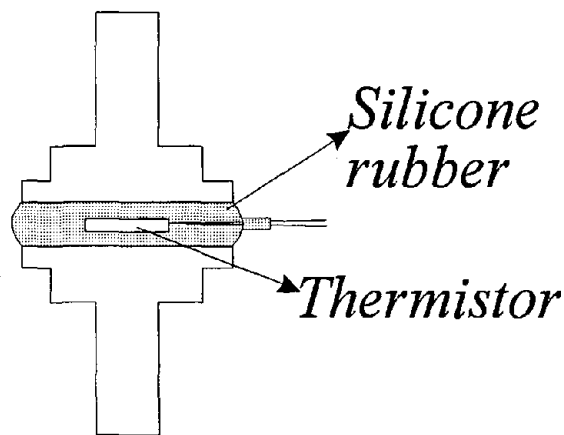


Figure 19. The thermistor embedded in silicone rubber for DSR temperature calibration.

Pressure Calibration

The pressure gauge in the PAV should be calibrated for these tests. The gauges can be sent to FHWA for calibration.

Operator Precision

It is very important that the repeatability of the measurement by the operator running the ruggedness tests be documented prior to the running of these tests. For this purpose, the procedures given in the later sections can be followed for any one set of variables.

The material used should be a thin film or rolling thin film aged sample. For this purpose, 100 g of (any) PAV-aged asphalt should be homogenized in a 240-mL container and distributed to ten 30-mL containers. The specific aging procedure used is not critical for checking the uniformity, but care should be taken that the asphalt in all ten 30-mL containers is uniform. Perform the following experiments:

1. Measure the complex modulus and $\tan(\delta)$ at 10°C and 10 rad/s for eight samples (8-mm parallel plates).
2. Measure the complex shear modulus and phase tangent at 60°C and 10 rad/s for eight samples (25-mm parallel plates).
3. Measure the creep stiffness and m -value at 60 s loading time for eight samples.

Report these numbers to the authors prior to conducting the tests.

Sources for Molds

The molds (two sizes each for 8-mm and 25-mm parallel plates) to make small pellets of asphalts for DSR testing will be supplied to the participants by Dr. David A. Anderson of Pennsylvania Transportation Institute. The silicone rubber molds for making BBR specimens can be obtained from Harold Keller at Bi-Co Machine & Tool Co., P.O. Box 5, Phillipsburg, PA 16866, Tel: (814) 342-0198, Fax: (814) 342-5377.

Note

The ruggedness testing of the direct tension has been temporarily held back until the procedure can be thoroughly checked. Efforts are being made by the Materials Division of the Office of Engineering and Highway Operations Research and Development at FHWA to improve the procedure so that consistent repeatability can be obtained with tolerable coefficient of variation. The samples for this test are being sent out to the laboratories with the hope that the procedure will be ready by the time the laboratories complete the other ruggedness tests.

1. BENDING BEAM RHEOMETER

The bending beam rheometer (BBR) is used to measure the flexural creep stiffness of asphalt at temperatures between -36 and 0°C after loading times of 8, 15, 30, 60, 120, and 240 s. This test is performed on the original and TFO-PAV residues. The stiffness and the slope of log stiffness versus log time curve at 60 s (*m*-value) is reported.

1.1 SCOPE OF THE STUDY

This study is intended to detect and reduce the sources of variation in the determination of flexural creep stiffness and slope of stiffness versus log time curve at 60 s by the bending beam rheometer in asphalt cement samples. The test samples are provided in 30-mL containers, one for each measurement. The study does not cover the aspects related to the thermal history of asphalts prior to the distribution in 30-mL containers.

1.2 INSTRUMENTATION AND ACCESSORIES

A bending beam rheometer or an apparatus capable of applying a constant load on an asphalt beam in three-point flexural testing, maintained accurately at the test temperature, is required. The deflection of the beam should be continuously monitored with time and recorded using a suitable recording device. For each test, the deflection of the bar with time is recorded for 240 s, and the required parameters are calculated from this data.

1.2.1 SPECIMEN MOLDS

The aluminum specimen molds consist of five rectangular aluminum bars with three plastic strips secured by O-rings. The dimensions of the components and their assembly are illustrated in Figure 20. A silicone rubber mold with aluminum supports is also used to make specimens as shown in Figure 21.

1.2.2 THREE-POINT FLEXURAL TESTING

The beam is tested in three-point flexure. The schematic diagram for this setup is shown in Figure 22. The dimensions shown in Figure 22 have to be measured to a tolerance of 0.1 mm.

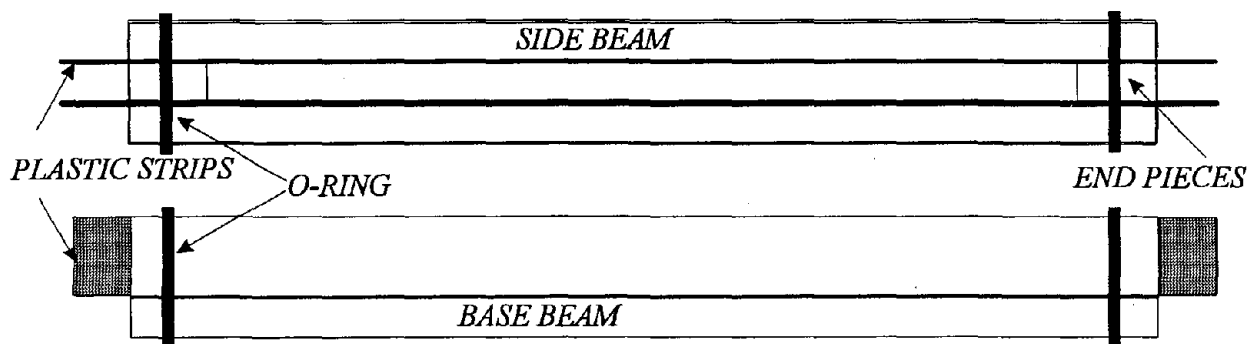


Figure 20. Schematic diagram of an aluminum mold.

The whole apparatus is immersed in a cold bath, the temperature of which has to be maintained at the test temperature within $\pm 0.1^\circ\text{C}$. At the beginning of the experiment, a constant load is applied and the deflection of the specimen is measured and recorded continuously as a function of time.

The flexural creep stiffness can be calculated from the deflection by the following formula:

$$S(t) = \frac{PL^3}{4bh^3\delta(t)} \quad (2)$$

where $S(t)$ is the time-dependent creep stiffness, P is the constant load, L is the span length (Figure 22), b is the width of the beam, h is the depth of the beam, and $\delta(t)$ is the time-dependent deflection.

Report the creep stiffness and the m -value (slope of the log creep stiffness versus the log time curve) at 8, 15, 30, 60, 120, and 240 s loading time.

1.3 VARIABLES THAT AFFECT THE MEASUREMENT

The variables that affect the measurement are as follows:

1. **MOLDS:** Aluminum molds were developed first, followed by silicone molds. Both these techniques have their advantages and disadvantages. These two techniques for making specimens are selected as a variable. The aluminum mold and the silicone rubber mold are illustrated in Figures 20 and 21, respectively.

THERMAL HISTORY: The thermal history of the asphalt is very critical and has to be controlled. The consistency of thermal history for samples prepared by various operators in various labs can be achieved by following certain criteria in several steps. These criteria are addressed as variables as follows:

2. The time the specimen is left in the mold at room temperature (before trimming) after the asphalt is poured into the mold (20 min and 5 h).

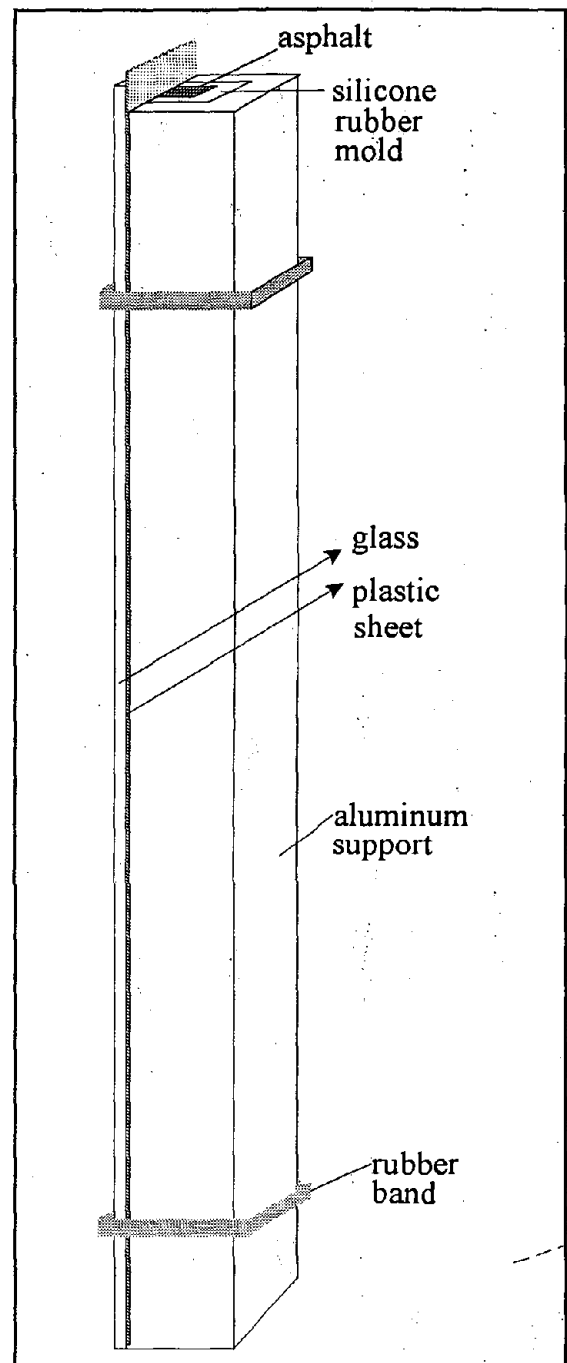


Figure 21. Schematic diagram of a silicone rubber mold.

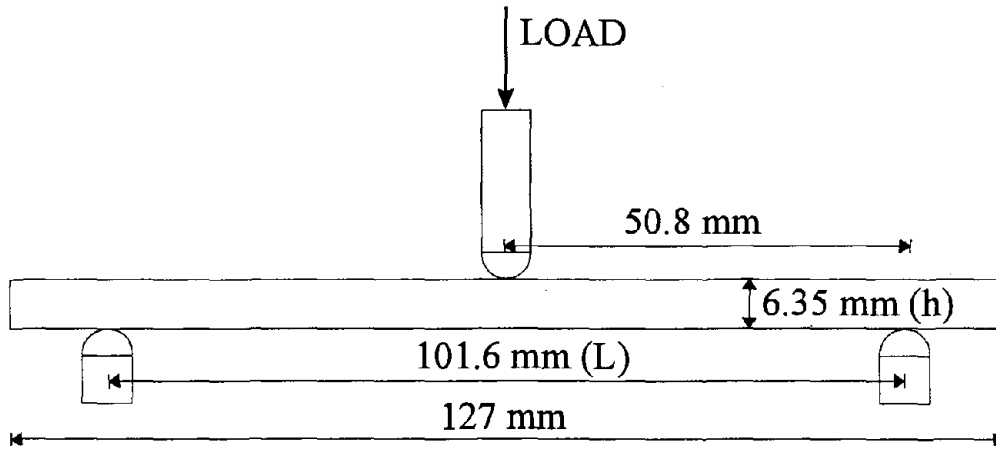


Figure 22. Three-point flexural testing setup for measuring the low-temperature properties of asphalt.

3. The temperature at which the specimen in the mold is chilled before demolding (0 and -10°C).

4. The time the specimen in the mold is chilled before demolding (10 min and 30 min).

5. The time the specimen is equilibrated at the test temperature before testing (55 and 65 min, ±1 min in each case).

TESTING PARAMETERS:

6. Load applied (95 and 105 g).

7. Temperature of the test bath ($T \pm 0.2^\circ\text{C}$).

1.4 SAMPLES

Three materials will be provided in twenty 30-mL containers (per material) for testing the

Table 28. Fractional factorial design for BBR ruggedness testing.

Variable	Determination Number							
	1	2	3	4	5	6	7	8
A or a	a	a	a	a	A	A	A	A
B or b	b	b	B	B	b	b	B	B
C or c	C	c	C	c	C	c	C	c
D or d	D	D	d	d	d	d	D	D
E or e	e	E	e	E	E	e	E	e
F or f	F	f	f	F	F	f	f	F
G or g	G	g	g	G	g	G	G	g

- a= Aluminum molds for making the specimens
- A= Silicone rubber molds for making the specimen
- b= 20 min, time left at room temperature before trimming
- B= 300 min, time left at room temperature before trimming
- c= 0°C, temperature of freezer for demolding
- C= -10°C, temperature of freezer for demolding
- d= 10 min in the freezer before demolding
- D= 30 min in the freezer before demolding
- e= 55 min, soak at the test temperature
- E= 65 min, soak at the test temperature
- f= 95 g, load on the beam
- F= 105 g, load on the beam
- g= $T - 0.2^\circ\text{C}$, test temperature
- G= $T + 0.2^\circ\text{C}$, test temperature

procedures for the bending beam rheometer. This would mean that 60 containers will be distributed to each laboratory for testing the procedure for the bending beam rheometer. Each container will have a label indicating the following:

1. Identity of the laboratory organizing the ruggedness tests.
2. The test and the material. For instance, BBR-A indicates that the specimen is material A provided for the ruggedness testing of the bending beam rheometer test.
3. A five-digit serial number, which must be kept track of and reported with the results.

1.5 REPORT

Three materials with eight experiments each and two repetitions indicate 48 measurements. Each of these measurements have to be randomized to avoid any systematic errors. Table 29 gives the random order of analyses and a table that should be used to report the data. Besides these data, the deflection-time curves for each test should be submitted on an 88.9-mm (3.5-in) diskette in ASCII format. The test number is just a counter provided to aid in the performance of the test. The serial number, however, is the number on the container. This must be reported in the space provided, for it will be useful in interpreting data. The experimental conditions are abbreviated by a code that designates the material, the determination number (from Table 28), and the repetition. For instance, B-5-2 indicates that the material being tested is B, the determination number is 5 (A,b,C,d,E,F,g), and it is the second repetition.

1.6 PROCEDURES FOR BENDING BEAM RHEOMETER

1.6.1 CALIBRATION PROCEDURES

Follow the procedures recommended by the manufacturer of the BBR to calibrate and check the performance of the instrument. Perform the temperature calibration according to the procedure given in the introduction document.

1.6.2 TEST PROCEDURE

The flexural creep stiffness of asphalt at low temperatures is found to be very dependent on the thermal history. From the time the specimens are poured into the molds to the time of testing, all temperatures and time intervals specified should be strictly followed to avoid variation in results.

1.6.3 PREPARE MOLDS (factor a/A)

ALUMINUM MOLDS: Cover one face of the two side beams and the base beam with a tacking material to hold the plastic strips used as release material. A commercial petroleum jelly that retains the tackiness at the pouring temperature and does not become excessively stiff at low temperatures is recommended. The layer of grease applied should be sufficient to hold the plastic and the metal in intimate contact and should therefore be uniform and thin.

Table 29. Recommended sequence of experiments for BBR ruggedness testing.

Test No.	Ser. No.	Exp. Conditions	Creep Stiffness (MPa)					<i>m</i> -value				
			8	16	32	64	128	8	16	32	64	128
1		B-7-2										
2		C-7-1										
3		A-2-1										
4		C-4-1										
5		C-3-1										
6		C-2-2										
7		B-8-1										
8		C-5-1										
9		B-3-1										
10		A-4-2										
11		B-6-1										
12		B-2-2										
13		B-5-2										
14		B-1-1										
15		B-4-2										
16		C-1-2										
17		B-7-1										
18		B-6-2										
19		A-5-1										
20		A-1-1										
21		B-5-1										
22		B-4-1										
23		C-6-1										
24		C-3-2										
25		B-1-2										
26		A-5-2										
27		A-7-1										
28		A-3-2										
29		A-3-1										
30		B-3-2										
31		C-5-2										
32		A-6-1										
33		C-8-1										
34		C-2-1										
35		A-8-1										
36		A-2-2										
37		A-8-2										
38		A-4-1										
39		C-8-2										
40		C-7-2										
41		A-6-2										
42		B-8-2										
43		A-7-2										
44		B-2-1										
45		C-1-1										
46		A-2-1										
47		C-4-2										
48		C-6-2										

Cover the greased beams with the plastic (Mylar) sheets and press to remove all air bubbles from between the mold and the plastic sheets. Since it has been found that plastic sheets, once used, develop folds and other defects that result in the formation of defects in the test beam, it is strongly recommended that a new set of plastic strips be used each time.

The plastic strips can be cut from the plastic sheets used to make transparencies. The dimensions of the cut sheets should be very carefully controlled, since irregular sheets can affect the quality of the beam.

Cover one end of each end piece with a thin layer of a thin paste made by mixing glycerine and talcum powder (50:50 ratio by weight). When assembled, the coated side forms the inside of the mold. Place the end pieces at the edge of the base plates on the face covered with the plastic sheet and then place the two side beams with their covered sides facing inward. Secure the assembled mold with O-rings as shown in Figure 20.

Once the mold is assembled, inspect the mold for any air bubbles and for any detachment of the plastic strips from the metal beams. To ensure good contact between the plastic strips and the metal beam, a clean metal beam 6.35 mm (0.25 in) thick is inserted into the mold between the side beams and is moved back and forth using a sliding motion. The longer length of the side plastic sheets enables pulling from both ends after the assembly of the mold to ensure a good contact between the plastic sheets and the side beams. At this stage, the inside of the mold is covered with plastic sheets on three sides and with the talcum powder/glycerine mixture at the ends.

SILICONE RUBBER MOLDS: Clean the silicone rubber molds of any dust or asphalt that remains. Place the silicone rubber mold in an aluminum housing with a plastic sheet between the mold and the aluminum housing. Cover the mold with a second plastic sheet and a glass plate. Secure the plate to the aluminum support with clips. (Figure 20 illustrates the assembled mold.) The assembled mold should contain, in the order of assembly, the aluminum housing, a plastic sheet, the silicone rubber mold, a second plastic sheet, and the glass cover plate. The entire assembly is held in place with spring clamps. Preheat this assembly at 135°C.

1.6.4 HEAT THE ASPHALT SAMPLE

Heat the asphalt sample provided in the 30-mL container (with the lid on, but not closed tight) in an oven preheated to 150°C. Hold the sample in the oven for 20 min. Remove the sample from the oven and stir the asphalt gently with a spatula to ensure homogeneity. The stirring should not introduce any air bubbles in the asphalt.

1.6.5 FILL THE MOLD WITH THE ASPHALT

ALUMINUM MOLDS: Pour the asphalt into the mold in a steady stream, starting from one end of the mold to the other, filling the mold in one pass. Pouring the beam in layers through several passes should be avoided, since it may result in air gaps or bubbles entrapped in the specimen. The mold should be slightly overfilled with asphalt so that it

can be trimmed after the asphalt cools. Overfilling also ensures square edges and corners and a beam with uniform width. After pouring the specimen, the filled mold can be left at room temperature for the specified period (factor b/B) to cool down.

SILICONE RUBBER MOLDS: In the case of silicone rubber molds, remove the heated mold assembly and place the mold assembly in an upright position on a laboratory bench. Immediately fill the mold with hot binder by pouring a continuous stream of binder into the cavity until the binder is flush with the top surface of the mold.

1.6.6 TRIM THE SPECIMEN IN THE ALUMINUM MOLD

ALUMINUM MOLDS: A hot knife or heated spatula is used to trim the upper face of the specimen and make it level with the top of the mold. Any excess asphalt on the side beam should be carefully cleaned with the hot knife or any other sharp edge. Trimming the specimen and cleaning the top edge is very important as it ensures a crack-free release of the beam from the mold. After trimming, the specimen is left in the mold for the specified time (factor b/B) for the specimen to reach thermal equilibrium.

SILICONE RUBBER MOLDS: No trimming is necessary for the bar made in the silicone rubber mold.

1.6.7 DEMOLD THE SPECIMEN

Place the asphalt and the mold in a freezer maintained at the specified temperature (factor c/C) for the specified time (factor d/D). Remove the specimen from the freezer, demold the specimen, and place the specimen in the testing bath at the test temperature (factor g/G). The demolded specimen should be left in the test bath for the specified period of time (factor e/E) for it to equilibrate.

1.6.8 LOAD THE SPECIMEN AND CONDUCT THE TEST

The specimen should be handled carefully with tongs and loaded on the two supports in the test frame. The loading shaft should just touch the beam at zero load. Keep the beam on the two supports ready to go. When the specified time (factor e/E) is elapsed, start the test. Apply the specified load (factor f/F) and record the deflection of the beam as a function of time (every second).

2. DYNAMIC SHEAR RHEOMETER

The dynamic shear rheometer (DSR) is used to test the original asphalt, the TFO-aged asphalt, and the TFO-PAV-aged asphalts. The original and the TFO-aged asphalts are tested in the temperature range of 52 to 70°C, while the TFO-PAV-aged asphalt is tested from 7 to 34°C. In all cases, the complex modulus (G^*) and the phase angle (δ) are the measured parameters.

2.1 SCOPE OF THE STUDY

This study is intended to detect and reduce the sources of variation in the determination of complex shear modulus and loss angle by dynamic shear rheometry of asphalt cement samples. The test samples are provided in 30-mL containers, one for each measurement. The study does not cover the aspects related to the thermal history of asphalts prior to the distribution to 30-mL containers.

2.2 INSTRUMENTATION AND ACCESSORIES

A dynamic shear rheometer with the capability for accurate control of frequency, temperature, strain, and gap between plates is needed. The accessories needed are 8-mm and 25-mm diameter parallel plates.

2.3 VARIABLES THAT AFFECT THE MEASUREMENT

The variables that affect the measurement are as follows (the \pm indicates the upper and lower limits specified for the variable):

- A. Temperature to which the asphalt is heated ($135\pm 5^\circ\text{C}$).
- B. Set temperature ($60\pm 0.2^\circ\text{C}$ for the 25-mm parallel plate and $10\pm 0.2^\circ\text{C}$ for the 8-mm parallel plate).
- C. Time of soak at the test (DSR) temperature (15 ± 5 min after the test temperature $\pm 0.2^\circ\text{C}$ has been reached).
- D. The method of introducing binder sample onto the parallel plates (pouring hot binder directly onto the plates or transferring a cast pellet of the binder to the plates).
- E. Frequency (1.35 and 1.65 Hz).
- F. Strain (10 and 20 percent for 25-mm parallel plate and 0.5 and 1.5 percent for 8-mm parallel plate).
- G. The gap between the parallel plates at the final trimming of asphalt in the parallel plate (0.1 mm and 0.2 mm over the gap setting). This essentially quantifies the extent of the overhang at the edge of the parallel plates and quantifies the contribution of the end effects.

2.4 SAMPLES

Four materials will be provided in thirty-six 30-mL containers (per material) for testing the procedures for dynamic shear rheometer. This would mean that 144 containers will be distributed to each laboratory for the dynamic shear rheometer test. Each container will have a label indicating the following:

- 1. The laboratory organizing the ruggedness tests.
- 2. The test and the material. For instance, DSR-A indicates that the specimen is material A provided for the ruggedness testing of the dynamic shear rheometer test.

3. A five-digit serial number, which must be kept track of and reported with the results.

2.5 REPORTING

The data that will be used for statistical analyses are one value of G^* and $\tan(\delta)$ for each experiment. The data should also include the serial number of the container used in the study. Table 31 gives the format needed for reporting the results.

2.6 RANDOMIZATION

In order to eliminate any bias, each laboratory is required to truly randomize the order of the experiments. Table 31 includes the required order of experiments.

Conditions are described by the format sample-test-repetition, where there are four asphalt samples, eight sets of test conditions (from Table 30), and two repetitions. This series of experiments has to be repeated at 10°C (8-mm diameter plates) and at 60°C (25-mm plates).

The test number is just a counter provided to aid in the performance of the test. The serial number, however, is the number on the container. This must be reported in the space provided, for it will be useful in interpreting data. The experimental conditions are abbreviated by a code that designates the material, the determination number (from Table 30), and the repetition. For instance, B-5-2 indicates that the material being tested is B, the determination number is 5 (A,b,C,d,E,F,g), and it is the second repetition.

2.7 TESTING PROCEDURES

- 2.7.1 Calibrate the torque measurement transducer according to the procedure recommended by the instrument manufacturer.

Table 30. Fractional factorial design for DSR ruggedness testing.

Variable	Determination Number							
	1	2	3	4	5	6	7	8
A or a	a	a	a	a	A	A	A	A
B or b	b	b	B	B	b	b	B	B
C or c	C	c	C	c	C	c	C	c
D or d	D	D	d	d	d	d	D	D
E or e	e	E	e	E	E	e	E	e
F or f	F	f	f	F	F	f	f	F
G or g	G	g	g	G	g	G	G	g

a= 130°C, the lower level of asphalt temperature

A= 140°C, the higher level of asphalt temperature

b= 59.8°C (for 25-mm plate) or 14.8°C (for 8-mm plate)

B= 60.2°C (for 25-mm plate) or 15.2°C (for 8-mm plate)

c= 10 min, lower soak time at test temperature

C= 20 min, higher soak time at test temperature

d= Pouring hot binder onto the plate

D= Introducing the binder as a cast pellet

e= 1.35 Hz, lower level frequency

E= 1.65 Hz, higher level frequency

f= 10% or 0.5% strain for 25- or 8-mm plate, respectively

F= 20% or 1.5% strain for 25- or 8-mm plate, respectively

g= 5% over the set gap, lower level

G= 10% over the set gap, higher level

- 2.7.2 Calibrate the temperature-measuring device according to the procedure explained in the introduction document.
- 2.7.3 Load the parallel plates in the instrument. Set the temperature to the test temperature. Allow the chamber to equilibrate for 2 min after the test temperature ($\pm 1^\circ\text{C}$) is reached. Zero the micrometer. Now, set the temperature to 40°C .
- 2.7.4 Select a 30-mL container of asphalt of a specific material provided at random and note its serial number. Heat the container at the specified temperature (factor a/A) for 20 min. Remove the container and gently stir the asphalt with a spatula (taking care not to entrap air bubbles) to homogenize the sample.

Table 31. Recommended sequence of experiments for DSR ruggedness testing.

Test No.	Exp. Conditions	AT 10°C			AT 60°C		
		Ser. No.	G*	tan(δ)	Ser. No.	G*	tan(δ)
1	A-7-2						
2	B-7-2						
3	C-7-2						
4	D-7-2						
5	A-2-1						
6	B-2-1						
7	C-2-1						
8	D-2-1						
9	A-4-1						
10	B-4-1						
11	C-4-1						
12	D-4-1						
13	A-2-2						
14	B-2-2						
15	C-2-2						
16	D-2-2						
17	A-8-1						
18	B-8-1						
19	C-8-1						
20	D-8-1						
21	A-5-1						
22	B-5-1						
23	C-5-1						
24	D-5-1						
25	A-3-1						
26	B-3-1						
27	C-3-1						
28	D-3-1						
29	A-4-2						
30	B-4-2						
31	C-4-2						
32	D-4-2						
33	A-6-1						
34	B-6-1						
35	C-6-1						
36	D-6-1						
37	A-5-2						
38	B-5-2						
39	C-5-2						
40	D-5-2						
41	A-1-1						
42	B-1-1						
43	C-1-1						
44	D-1-1						
45	A-1-2						
46	B-1-2						
47	C-1-2						
48	D-1-2						
49	A-7-1						
50	B-7-1						
51	C-7-1						
52	D-7-1						
53	A-6-2						
54	B-6-2						
55	C-6-2						
56	D-6-2						
57	A-3-2						
58	B-3-2						
59	C-3-2						
60	D-3-2						
61	A-8-2						
62	B-8-2						
63	C-8-2						
64	D-8-2						

- 2.7.5 **Binder Pellets:** For making pellets of binder material, pour the asphalt into the silicone rubber mold in such a way that there are no bubbles entrapped (prior practice with other asphalts will be helpful and is highly recommended). Allow the asphalt to cool to room temperature for 15 min. Chill the mold in the freezer at -5°C for 10 min and demold by flexing the silicone rubber mold. Place the pellet at the center of the parallel plate. Proceed to step 2.7.7.
- 2.7.6 **Pouring Technique:** Remove one of the parallel plates, pour the asphalt onto the center of the plate with the spatula until the amount of material covering the plate (2 to 3 mm thick) reaches a distance 2 mm from the perimeter. Load the plate in the rheometer when the asphalt is stiff to resist flowing when inverted.
- 2.7.7 Lower the upper plate to squeeze the asphalt against the lower plate. Set the gap at the specified value (factor g/G):
- Factor g for 8-mm plate: Trim at 2.1 mm.
 - Factor G for 8-mm plate: Trim at 2.2 mm.
 - Factor g for 25-mm plate: Trim at 1.05 mm.
 - Factor G for 25-mm plate: Trim at 1.1 mm.
- 2.7.8 For the sample prepared by the pouring technique, trim the excess asphalt using a heated tool with a straight edge. Trimming might be needed more than once before the desired gap is achieved if excess asphalt has been poured on the plate. The final trimming should be performed at the specified value (factor g/G). After finishing the trimming, close the door of the controlled-environment chamber and set the temperature to the desired value (factor b/B).
- For the specimen prepared by the pellet technique, no trimming is necessary. (In step 2.7.3, the temperature was set at 40°C .) After this temperature is reached, set the gap to the final value (2.0 mm and 1.0 mm for 8- and 25-mm parallel plates, respectively). And let the sample equilibrate for 10 min. Now set the temperature to the test temperature (factor b/B).
- 2.7.9 Condition the sample at the test temperature for the specified time (factor c/C) after the sample has reached the test temperature (within $\pm 0.2^{\circ}\text{C}$).
- 2.7.10 Select the specified strain amplitude (factor f/F) for testing. Condition the specimen before measurement by applying the selected strain (factor f/F) for 10 cycles at the selected frequency (factor e/E) before starting the measurement (dynamic conditioning).
- 2.7.11 Report the values of the complex modulus G^* and the phase angle in Table 30.

3. PRESSURE AGING VESSEL

The pressure aging vessel (PAV) treatment is a method to oxidatively age asphalt binders to simulate long-term pavement field aging. The aging is accomplished by heating asphalt samples at temperatures between 90 and 110°C for 20 h at 2.07 MPa (300 lbf/in²) air pressure. The specification requires PAV aging of TFO residues to obtain aged asphalts on which flexural creep, dynamic rheological, and tensile strength measurements are conducted.

3.1 SCOPE OF THE STUDY

This study is intended to detect and reduce the sources of variation in the oxidative aging procedure with a pressure aging vessel. Four asphalt samples are provided in 30-mL containers. The study examines the effect of variations when following a standard procedure for aging the asphalt samples on the rheological properties of the residues. The rheological properties at both the high temperatures (60°C) and low temperatures (10°C) are measured by a dynamic shear rheometer over a frequency range of 1 to 100 rad/s.

3.2 INSTRUMENTATION AND ACCESSORIES

A pressure vessel capable of controlling pressure to ± 13.79 kPa (2 lbf/in²) and temperature to $\pm 0.2^\circ\text{C}$ is required. The vessel should be capable of withstanding oxidative (air) atmospheres at 100°C and 2.07 MPa (300 lbf/in²) pressures. Also required are thin film oven pans as specified in the test ASTM D1754 and a dynamic shear rheometer to evaluate the complex shear modulus and loss tangent at temperatures of 10°C and 60°C, scanning from a frequency of 1 to 100 rad/s (0.1 to 10 Hz). Additionally, the means to measure the temperature inside the vessel during operation by the insertion of a platinum resistance thermometer and a temperature indicator should be added to the equipment. Furthermore, an external pressure gauge (apart from the one provided with the regulator) that reads in the interval of 13.79 kPa (2 lbf/in²) is required.⁴

3.3 VARIABLES THAT AFFECT THE MEASUREMENT

The variables that affect the measurement are as follows (the \pm indicates the upper and lower limits specified for the variable):

1. Thickness of asphalt film, controlled by the quantity of asphalt put in the pan, 50 \pm 2 g.
2. Temperature of the vessel, 100 \pm 0.2°C.
3. Pressure of the vessel, 2.07 \pm 0.14 MPa (300 \pm 20 lbf/in²).
4. Time in the PAV, 20 \pm 1 h.
5. Temperature at which the vessel is pressurized, 90 and 100°C.
6. Time left in pans after PAV aging, but before distributing to containers, 2 and 96 h.
7. Maximum instantaneous pressure release rate, 69 and 138 kPa/min (10 and 20 lbf/in²-min).

⁴ Available from Ashcroft.

3.4 SAMPLES

Four materials will be provided in eighteen 120-mL containers (per material) for testing the procedures for the pressure aging vessel. This would mean that 72 containers will be distributed to each laboratory for the pressure aging vessel test. Each container will have a label indicating the following:

1. The laboratory organizing the ruggedness tests.
2. The test and the material. For instance, PAV-A indicates that the specimen is material A provided for the ruggedness testing of the procedure for the pressure aging vessel.
3. A five-digit serial number that is printed on the containers, which must be kept track of and reported with the results.

The aging procedure by PAV is described in a later section, followed by the exact procedure for evaluating the degree of aging by DSR.

The effect of each of these seven parameters on the degree of aging can be evaluated in eight experiments with two replications, using a fractional factorial experimental design. Such an experimental design is described in Table 32. The high and low

values for these parameters are also listed in Table 32. The eighteen 120-mL containers per material provided should therefore suffice for a total of 16 experiments/material.

3.5 REPORT

Four materials with eight experiments each and two repetitions indicate 64 measurements. For each of these measurements, one TFO pan should be aged in the PAV and evaluated using the DSR and the raw data reported. Each of these measurements has to be randomized to avoid any systematic errors. Table 33 gives the random order of analyses and a table that should be used to

Table 32. Fractional factorial design for PAV ruggedness testing.

Variable	Determination Number							
	1	2	3	4	5	6	7	8
A or a	a	a	a	a	A	A	A	A
B or b	b	b	B	B	b	b	B	B
C or c	C	c	C	c	C	c	C	c
D or d	D	D	d	d	d	d	D	D
E or e	e	E	e	E	E	e	E	e
F or f	F	f	f	F	F	f	f	F
G or g	G	g	g	G	g	G	G	g

- a= 48 g to obtain lower thickness of asphalt film
- A= 52 g to obtain higher thickness of asphalt film
- b= 98°C, lower temperature of PAV
- B= 102°C, higher temperature of PAV
- c= 19 h, shorter time in the PAV
- C= 21 h, longer time in the PAV
- d= 1.93 MPa (280 lbf/in²), lower air pressure of the PAV
- D= 2.21 MPa (320 lbf/in²), higher air pressure of the PAV
- e= 90°C lower temperature at which the PAV is pressurized
- E= 100°C higher temperature at which the PAV is pressurized
- f= 2 h, the time asphalt is left in pans after PAV
- F= 168 h, the time asphalt is left in the pans after PAV
- g= 69 kPa/min (10 lbf/in²), slower pressure release rate
- G= 138 kPa/min (20 lbf/in²), faster pressure release rate

report data. Besides these data, the raw data for each test should be provided on an 88.9-mm (3.5-in) diskette in ASCII format.

The test number is just a counter provided to aid in the performance of the test. The serial number, however, is the number on the container. This must be reported in the space provided, for it will be useful in interpreting data. The experimental conditions are abbreviated by a code that designates the material, the determination number (from Table 32), and the repetition. For instance, B-5-2 indicates that the material being tested is B, the determination number is 5 (A,b,C,d,E,F,g), and it is the second repetition.

Table 33. Recommended sequence of experiments for PAV ruggedness testing.

Test No.	Exp. Conditions	Ser. No.	BEFORE PAV				AFTER PAV				
			10°C		60°C		10°C		60°C		
			G*	δ	G*	δ	G*	δ	G*	δ	
1	A-7-2										
2	B-7-2										
3	C-7-2										
4	D-7-2										
5	A-2-1										
6	B-2-1										
7	C-2-1										
8	D-2-1										
9	A-4-1										
10	B-4-1										
11	C-4-1										
12	D-4-1										
13	A-2-2										
14	B-2-2										
15	C-2-2										
16	D-2-2										
17	A-8-1										
18	B-8-1										
19	C-8-1										
20	D-8-1										
21	A-5-1										
22	B-5-1										
23	C-5-1										
24	D-5-1										
25	A-3-1										
26	B-3-1										
27	C-3-1										
28	D-3-1										
29	A-4-2										
30	B-4-2										
31	C-4-2										
32	D-4-2										

Test No.	Exp. Conditions	Ser. No.	BEFORE PAV				AFTER PAV				
			10°C		60°C		10°C		60°C		
			G*	δ	G*	δ	G*	δ	G*	δ	
33	A-6-1										
34	B-6-1										
35	C-6-1										
36	D-6-1										
37	A-5-2										
38	B-5-2										
39	C-5-2										
40	D-5-2										
41	A-1-1										
42	B-1-1										
43	C-1-1										
44	D-1-1										
45	A-1-2										
46	B-1-2										
47	C-1-2										
48	D-1-2										
49	A-7-1										
50	B-7-1										
51	C-7-1										
52	D-7-1										
53	A-6-2										
54	B-6-2										
55	C-6-2										
56	D-6-2										
57	A-3-2										
58	B-3-2										
59	C-3-2										
60	D-3-2										
61	A-8-2										
62	B-8-2										
63	C-8-2										
64	D-8-2										

3.6 OPERATOR TIME REQUIRED

The aging studies should be done on 4 materials and 8 experimental conditions, with 2 repetitions each, thereby totaling 64 experiments. Each experiment needs 20 h of PAV aging. Fortunately, preliminary experiments have shown that different asphalts can be aged at the same time. Therefore, all four materials can be aged at the same time. Thus, it would take eight experiments with two repetitions for this procedure. At the rate of four PAV runs/week, 4 weeks will be needed to perform this task.

3.7 EXPERIMENTAL PROCEDURE

3.7.1 **CALIBRATION:** At the outset, the temperature measurement has to be calibrated according to the procedures outlined in the introduction. The pressure gauge will be calibrated by the FHWA at AMRL.

3.7.2 The samples have been provided in 120-mL containers, containing approximately 75 g of asphalt each. Pick one container and a set of experimental conditions as specified in Table 33. Note the serial number of the container on the table before proceeding any further.

3.7.3 HEAT THE CONTAINER OF ASPHALT

Heat the container of asphalt in an oven at 135°C for 30 min. Remove the container and stir the asphalt with a spatula and place it back in the oven for further heating for 15 min. Pour the specified amount (factor a/A) into one TFO (thin film oven) pan. Pour two 30-mL containers for DSR measurements and label the containers with the serial number. Leave the pans at room temperature for the specified period of time (factor f/F).

Repeat the above procedure for the other three materials with the same experimental conditions. In other words, if the experiment being conducted is A-4-2, perform B-4-2, C-4-2, and D-4-2 simultaneously.

3.7.4 LOAD THE TFO RESIDUE INTO THE PRESSURE AGING VESSEL

Preheat the PAV oven along with the panrack to the specified temperature (factor b/B) for at least 2 h before the test. Load the four pans onto the preheated rack, making sure that the position of each material is clearly marked. Load the panrack into the PAV and set the PAV in the oven. When the temperature inside the PAV reaches the pressurization temperature (factor e/E), bring the pressure to the test pressure (factor d/D). Leave the pans in the vessel for the specified period of time (factor c/C), starting at the time when the temperature inside the vessel reaches 98°C.

3.7.5 DEPRESSURIZE AND REMOVE THE PAN FROM THE PAV

After the specified time for aging (factor c/C) is completed, release the air at the specified rate (factor g/G). Remove the pans from the PAV and allow them to cool for 15 min. Transfer the pans to an oven maintained at 150±5°C and heat them for 30 min. Pour the contents of each TFO pan into three 30-mL containers without scraping.

3.7.6 MEASURE THE COMPLEX MODULUS AND LOSS TANGENT BY DYNAMIC SHEAR RHEOMETER (DSR)

Measure the complex modulus and loss tangent at 10°C with an 8-mm parallel plate, and at 60°C with a 25-mm parallel plate geometry, over a frequency range from 1 to 100 rad/s with five logarithmically evenly spaced points following the procedure given in Appendix 1. Report the results on hardcopy, as well as on an IBM-compatible 88.9-mm (3.5-in) diskette in ASCII format. Also, measure the complex modulus and the loss tangent at 10 and 60°C for 10 asphalts chosen randomly from the containers set apart in instruction 3.7.3.

3.8 DSR MEASUREMENTS FOR PAV SAMPLES

- 3.8.1 **CALIBRATION:** At the outset, the instrument should be calibrated according to the manufacturer's specifications. In particular, the temperature control has to be calibrated according to the procedure described in the introduction.
- 3.8.2 Load the appropriate parallel plate (8 mm for measurement at 10°C and 25 mm for 60°C) and zero the plates at the test temperatures. Heat the asphalt sample in the 30-mL container in an oven preheated to 135±5°C (150°C for samples after PAV) for 20 min.
- 3.8.3 Remove one of the plates from the rheometer. After the specified time, remove the 30-mL container from the oven, stir the contents, and pour the appropriate amount onto the parallel plate with an appropriate method until the plate is covered with a smooth, circular specimen of asphalt about 2 to 3 mm thick, reaching to within 1 to 2 mm of the edge of the plate.
- 3.8.4 Mount the plate back in the rheometer. In the case of 8-mm plates, the temperature should be set at 40°C during the sample loading. Lower the upper plate until the gap is 2.2 mm for 8-mm plates and 1.1 mm for 25-mm plates. Trim the edge of the specimen flush with the edge of the upper plate. The trimming procedure should take less than 2 min. Close the oven, proceed to the next step.
- 3.8.5 Next, lower the gap to 2.0 mm for 8-mm plates and 1.0 mm for 25-mm plates. In the case of 8-mm plates, let the sample equilibrate at 40°C for 5 min and set the temperature to 10°C. After 20 min (since the temperature was set at 10°C or 60°C), the sample is ready to be tested.
- 3.8.6 Tests should be run over two decades of frequency from 1 to 100 rad/s, using five logarithmically evenly spaced points per decade (1.0000, 1.5849, 2.5119, 3.9811, 6.3096, 10.0000, 15.8489, 25.1189, 39.8107, 63.0957, 100.0000). Report the frequency, G^* , G' , G'' , and $\tan(\delta)$.

APPENDIX 2. CHANGES TO PROCEDURES

As the test procedures were one of the earliest versions written and were constantly evolving, certain modifications and changes were made after version 2.2 of the specifications were sent out. These were made in the form of memoranda as necessary. In the following section, a summary of these memoranda is presented to accurately describe the procedures used in conducting these tests.

Bending Beam Rheometer

The temperatures at which the ruggedness testing was performed were based on studying a range of stiffness values from 150 MPa to 600 MPa. This range was obtained by changing the temperatures at which the BBR testing should be performed. This was communicated to the participants on July 27, 1993. The use of ethanol as the fluid medium in the baths was required of all laboratories for uniformity.

It was recognized that true randomization was difficult for BBR ruggedness testing experiments. This was primarily because of the time it took to equilibrate at each temperature. Therefore, it was suggested that experiments be divided into two groups according to temperature. This would place experiments 1, 4, 6, and 7 and experiments 2, 3, 5, and 8 into separate groups. Each group of four experiments, along with their repeats (a total of eight), would be run in a day.

Factor b/B in the procedures was mentioned in steps 1.6.5 and 1.6.6 in an ambiguous manner and was clarified. In step 1.6.5, the beams should be trimmed 45 min after the specimen was poured. In the case of the silicone rubber mold, since there was no trimming involved, the total time the mold was allowed to cool down was 45 min + factor b/B . Also, for BBR-A and BBR-B samples, the asphalt does not become fluid enough to pour into the molds when heated to 150°C. Therefore, it was required that the asphalts be heated to 160°C.

A plastic sheet was initially used to separate the asphalt from the glass in the silicone rubber mold (instruction 1.6.3 of Appendix 1). These plastic sheets deformed when asphalts were heated to 160°C, leading to imperfections in the beam. Therefore, 3-mm-thick silicone rubber sheets were supplied to all the participating laboratories and were used instead.

Dynamic Shear Rheometer

Following the same reasoning as for the bending beam rheometer, the ruggedness of the test at various stiffness levels was tested. The stiffness levels chosen were the specification level (2.2 kPa), and 1.5 decades above (69.57 kPa) and 1.5 decades below (69.57 Pa) for 25-mm parallel plates. For 8-mm parallel plates, the stiffness levels were 5 MPa, and $5 \pm 10^{1.5}$ MPa (158 and 0.16 MPa). This was performed by varying the test temperature.

The strain values previously selected in version 2.2 of the procedures were independent of the asphalt and temperature. For example, if the high and low values selected (10 and 20 percent strains) were within 10 percent of the linear strain limit⁵ (as with DSR-D at 55°C), the ruggedness testing may not detect any significant effects due to strain. However, if the high and low values selected were within 90 percent of the linear strain limit, the testing may detect significant effects due to strain. In order to address this, initially (June 1993) strain limits were chosen so that 60 percent and 90 percent of the linear strain limit were taken as the low and high values (factors f and F) for the specified asphalt at the specified temperature. Later (September 1993), it was found that the stress control rheometers could not achieve the high strains and, therefore, 10 percent and 20 percent of the linear strain limit were chosen. The temperatures and strains used for DSR ruggedness testing are summarized in Table 34. The table gives the value of the temperature of measurement (T). The factor b will then be T-0.2°C, while factor B will be T+0.2°C.

Initially, casting a pellet with the silicone rubber mold was thought to eliminate the need for trimming as a precise amount of material can be transferred. This is reflected in instruction 2.7.7 in Appendix 1. This was changed as this induced significant error in the measurement and the sample was trimmed for all of the tests.

Table 34. Temperatures and strains to perform DSR ruggedness testing.

ASPHALT	25-mm PARALLEL PLATE			8-mm PARALLEL PLATE		
	TEMP (°C)	STRAIN HIGH (%)	STRAIN LOW (%)	TEMP (°C)	STRAIN HIGH (%)	STRAIN LOW (%)
DSR-A	45	12.0	6.0	20	0.8	0.4
DSR-B	60	27.0	13.5	15	0.4	0.2
DSR-C	70	38.0	19.0	35	1.2	0.6
DSR-D	55	21.9	43.8	10	0.4	0.2

Pressure Aging Vessel

Several clarifications were issued to the pressure aging vessel (PAV) procedures. The repetitions were to be performed in separate runs. This was because the repetitions were done to check reproducibility and to obtain an estimate of error for the aging procedure. Table 33 was changed to reflect only DSR measurements after PAV. Since the asphalts were homogenized after the short-term aging, before being distributed to the laboratories, the measurements before PAV should be equivalent. The modified table is given as Table 35.

⁵ The linear strain limit is defined as the strain at which G* decreases to 95 percent of its value at the lowest measurable strains.

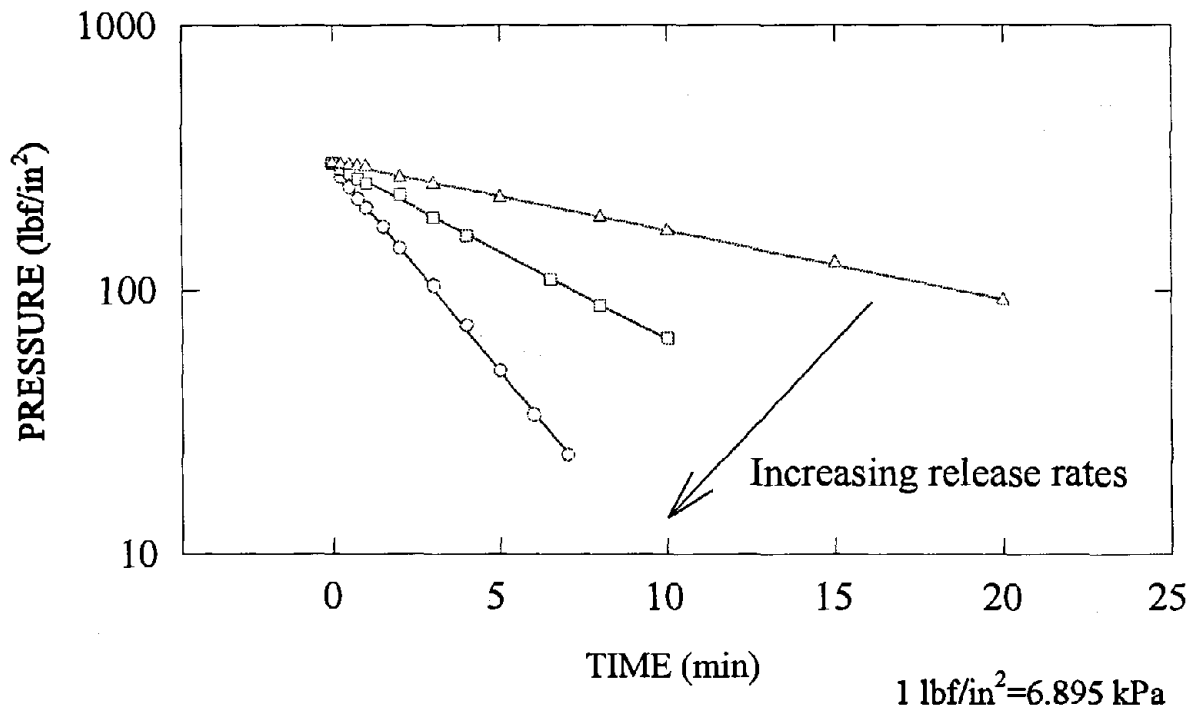


Figure 23. Pressure in a PAV as a function of time when released at different valve settings.

Pressure Release Rate

A procedure to control and quantify the rate of pressure release was described, including a method to calibrate the metering valves. An example was also included to illustrate the procedure. To precisely control the pressure release rate, a metering valve was installed in each PAV. The metering valve was then calibrated according to the following procedure.

Calibration

When the instantaneous pressure is plotted in the logarithmic scale as a function of time, a linear equation can be fit through the data points. This equation relates the instantaneous pressure (P) to the initial pressure (P_0), a rate constant (k), and time (t), according to the following equation:

$$\log(P) = -kt + \log(P_0) \quad (3)$$

When the vessel is pressurized to 2.07 MPa (300 lbf/in²) and the instantaneous pressure is recorded at three settings (0.5, 0.75, 1.00) of the metering valve during release, three values of rate constant can be obtained. When these rate constants are plotted as a function of the

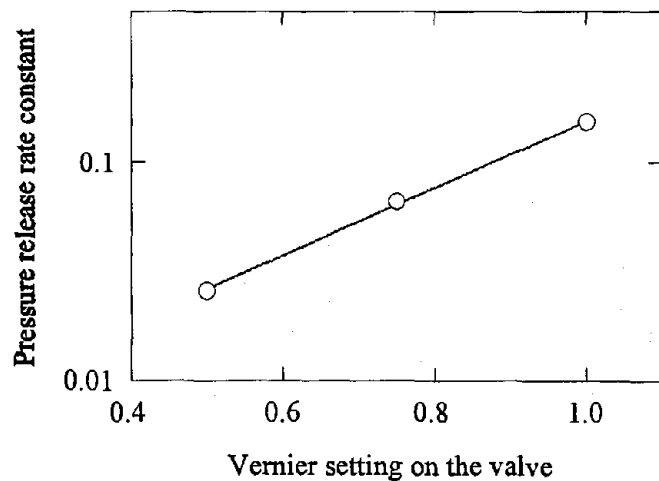


Figure 24. Relationship between pressure release rate constant and the vernier setting on the valve.

metering valve (vernier) settings, an equation can be fit through the data points in a log-linear scale as shown below:

$$\log(k) = m\Theta + C \quad (4)$$

where m and C are the slope and the intercept, respectively. From this equation, it is possible to find the vernier setting to obtain the desired k -values. The parameters m and C are characteristics for each instrument and should be determined experimentally. A plot illustrating equation 4 is shown in Figure 24.

Table 35. Modified sequence of experiments for PAV ruggedness testing.

Test No.	Exp. Conditions	Ser. No.	AFTER PAV			
			10°C		60°C	
			G*	tan(δ)	G*	tan(δ)
1	A-7-2					
2	B-7-2					
3	C-7-2					
4	D-7-2					
5	A-2-1					
6	B-2-1					
7	C-2-1					
8	D-2-1					
9	A-4-1					
10	B-4-1					
11	C-4-1					
12	D-4-1					
13	A-2-2					
14	B-2-2					
15	C-2-2					
16	D-2-2					
17	A-8-1					
18	B-8-1					
19	C-8-1					
20	D-8-1					
21	A-5-1					
22	B-5-1					
23	C-5-1					
24	D-5-1					
25	A-3-1					
26	B-3-1					
27	C-3-1					
28	D-3-1					
29	A-4-2					
30	B-4-2					
31	C-4-2					
32	D-4-2					

Test No.	Exp. Conditions	Ser. No.	AFTER PAV			
			10°C		60°C	
			G*	tan(δ)	G*	tan(δ)
33	A-6-1					
34	B-6-1					
35	C-6-1					
36	D-6-1					
37	A-5-2					
38	B-5-2					
39	C-5-2					
40	D-5-2					
41	A-1-1					
42	B-1-1					
43	C-1-1					
44	D-1-1					
45	A-1-2					
46	B-1-2					
47	C-1-2					
48	D-1-2					
49	A-7-1					
50	B-7-1					
51	C-7-1					
52	D-7-1					
53	A-6-2					
54	B-6-2					
55	C-6-2					
56	D-6-2					
57	A-3-2					
58	B-3-2					
59	C-3-2					
60	D-3-2					
61	A-8-2					
62	B-8-2					
63	C-8-2					
64	D-8-2					

In our example, the equation relating the release rate and the vernier setting is given by:

$$\log(k) = -2.36103 + 1.5563 \Theta \quad (5)$$

with an R^2 value of 0.9996.

The time it takes for the pressure to decrease from 2.07 MPa (300 lbf/in²) to 20.7 kPa (3 lbf/in²) is given by $t=2/k$. For $\Theta=0.5$, $t=77$ min; for $\Theta=0.75$, $t=30$ min; and for $\Theta=1.0$, $t=12.95$ min. Another important factor to consider is the instantaneous pressure release rates at any given pressure. The instantaneous pressure release rate is given by the following expression:

$$\frac{dP}{dt} = kP \quad (6)$$

These rates indicate that a reasonable total time of 13 min will imply an initial release of 0.32 MPa/min (46.35 lbf/in²-min). For the valve with a constant opening, a constant pressure release rate with variable pressure head cannot be achieved. One has to utilize fairly expensive valves or pressure controllers to achieve a constant pressure release rate.

Table 36. Instantaneous release rates at different pressures.

Pressure [†] MPa	Vernier setting (Θ)		
	0.50	0.75	1.00
2.07 (300)	7.73	19.71	46.35
1.38 (200)	5.15	13.14	30.90
0.69 (100)	2.58	6.57	15.45

[†]The numbers in parentheses are in lbf/in².

One compromise is to have three settings during the pressure release, such that the instantaneous pressure release rate does not exceed a limit. If Θ is set at 0.57 at 2.07 MPa (300 lbf/in²), then at 0.68 at 1.38 MPa (200 lbf/in²), and finally at 0.87 at 0.69 MPa (100 lbf/in²), then the total time for release will be 26.5 min and the instantaneous pressure release rate will not exceed 68.95 kPa/min (10 lbf/in²-min).

Using such a method, one can control the maximum instantaneous pressure release rate to 68.95 and 137.9 kPa/min (10 and 20 lbf/in²-min) when the k-values shown in Tables 35 and 36 are used. Using equation 5, one will have to calculate the vernier settings in the valve that would achieve these k-values.

Other clarifications to the procedure included the following:

Factor b/B: The temperature of the vessel is 98 and 102°C.

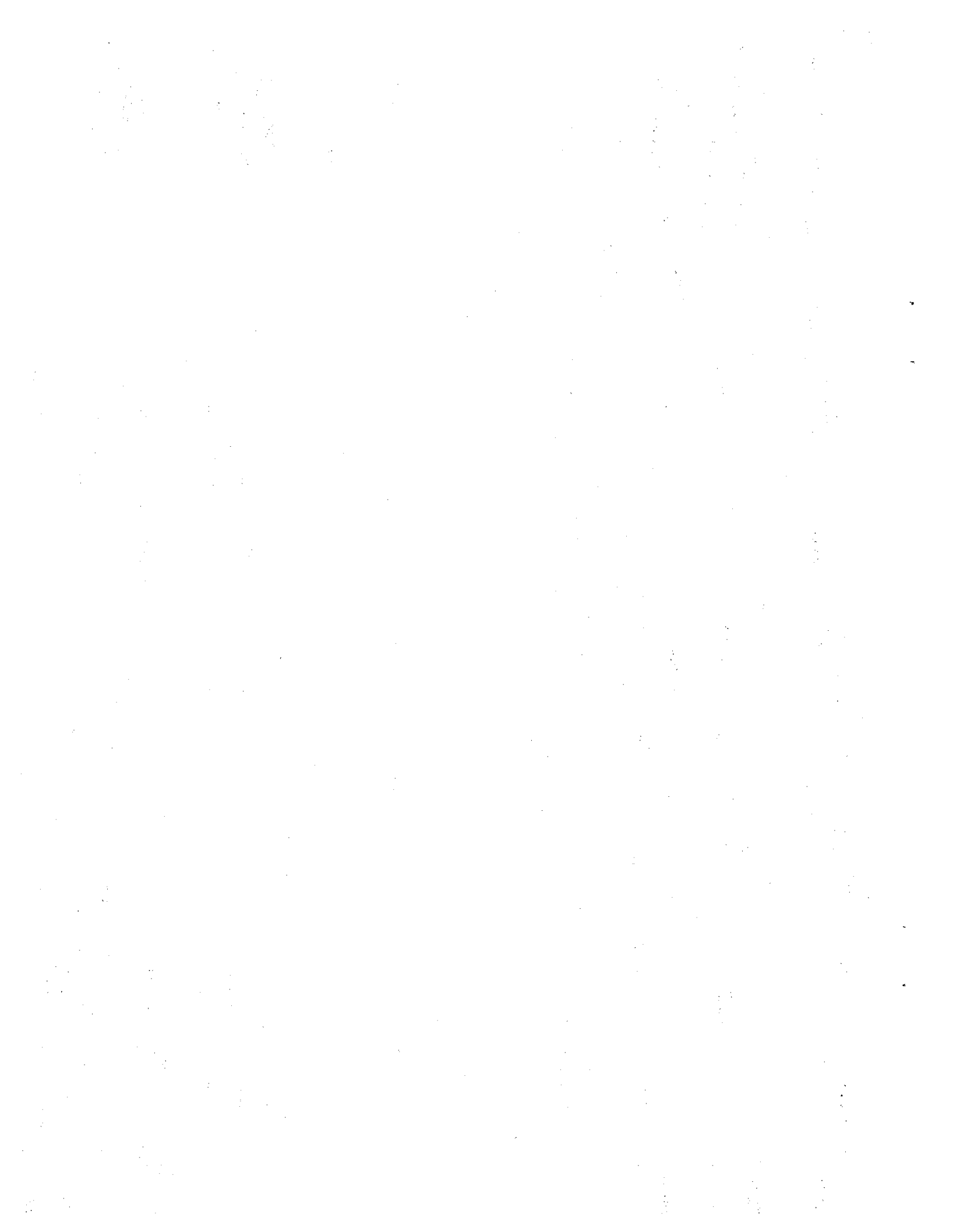
Factor d/D: The pressure of the vessel is 280 and 320 lbf/in².

Factor f/F: Time asphalt is left in pan after PAV. After factor f/F, the asphalt should be heated in the pan.

Table 37. Calibration of the pressure release valve.

Pressure [†] MPa	Factor g		Factor G	
	k	Θ	k	Θ
2.07 (300)	-0.0333		-0.0667	
1.38 (200)	-0.0500		-0.1000	
0.69 (100)	-0.1000		-0.2000	

[†]The numbers in parentheses are in lbf/in².



REFERENCES

1. "Standard Test Method for Determining the Rheological Properties of Asphalt Binder Using a Bending Beam Rheometer," AASHTO Designation TP1, Edition 1A, 1993.
2. "Standard Test for Measuring the Rheological Properties of Asphalt Binder Using a Dynamic Shear Rheometer," AASHTO Designation TP5, Edition 1A, 1993.
3. "Conducting a Ruggedness or Screening Program for Test Methods for Construction Materials," ASTM C1067 (1987).
4. Dah-Yinn Lee, B.V. Enustun and S.S. Kim, "Asphalt Cement Characterization by Thermomechanical Analysis," *Materials Characterization by Thermomechanical Analysis*, A.T. Riga and C.M. Neag, Eds., American Society for Testing and Materials, Philadelphia, 1991, pp. 176-190.
5. N. Shashidhar, Unpublished results, 1993.

